Molecular Imaging of Dopaminergic Neurotransmission in Subclinical Paranoia

Rami Hamati

Thesis submitted to the University of Ottawa
in partial fulfilment of the requirements for the degree of
Doctorate in Philosophy in Neuroscience

Department of Cellular and Molecular Medicine
Faculty of Medicine
University of Ottawa

Acknowledgements

First and foremost, I would like to thank Lauri Tuominen; For taking me in when I had little background in neuroimaging; For teaching me PET and fMRI; For teaching me how to code; For teaching me how to fish (figuratively not literally); For constantly teaching me new methods and ways of thinking; For teaching me to be okay with myself. I would also like to deeply thank Clifford Cassidy; For teaching me neuromelanin-sensitive MRI; For showing me what it takes to push an innovation to the clinic; For endearing me with his passion for neuroscience; For his advice, both academic and personal; For his academic presence, as his departure from Ottawa has been felt deeply. And to both of you for treating me as a colleague and an equal. I could not have asked for better supervisors.

I would like to thank Zachary Kaminsky, Natalia Jaworska, Jennifer Phillips, Reggie Taylor, Katie Dinelle, Owen Clarkin, Pierre Blier, Mostafa El Mansari, Matthew Holahan, Michael Hildebrand and John Stead for their part in raising me as a neuroscientist in the past 12 years. It really takes a whole village.

I would like to thank my many lab mates, past and present: Rami Al Haddad, Zacharie Saint-Georges, Nour Kanaa, Cecelia Shvetz, Reihaneh Forouhandehpour, Ahmad Sibahi, Bianca Chidiac, Krysta Boutin-Miller, Vanessa Zayed and Michael Chidiebere Iro. A special thanks to Patricia Burhunduli for her support, both academic and personal, throughout our Master's and PhD studies. You are an inspiration and a blessing to this world, a true friend.

To Areebah Ahmed, my heart. I have no doubt you will be a great neuroscientist one day.

To my friends, for keeping me grounded. To Anthony Ianni, who could have become a neuroscientist but wisely became a real estate agent instead.

To my family: Issa Hamati, Samia Abou Assi & Julie Hamati. Without your unwavering love and support I would not be a fraction of what I am today.

Table of Contents

List of Abbreviations

APS: Attenuated Psychotic Symptoms

BLIPS: Brief Limited Intermittent Psychotic Episodes

BS: Basic Symptoms

CHR-P: Clinical High-Risk state for Psychosis

CS: Conditioned Stimulus

FEP: First Episode Psychosis

fMRI: functional Magnetic Resonance Imaging

NM-MRI: Neuromelanin-sensitive Magnetic Resonance Imaging

PANSS: Positive and Negative Syndrome Scale

PET: Positron Emission Tomography

SCR: Skin Conductance Recordings

SN/VTA: Substantia Nigra/Ventral Tegmental Area

US: Unconditioned Stimulus

Abstract

Elevated dopamine system function in the striatum is a hallmark of psychotic illness. However, the extent to which genetic risk factors contribute to striatal hyperdopaminergia remains largely unexplored. Here, we examined dopaminergic correlates of psychosis risk in those with and without a first-degree relative with psychosis. In the first study, we examined neuromelanin-sensitive magnetic resonance imaging (NM-MRI), which is a proxy of dopamine released over the lifespan and has been shown to be associated with positive symptoms in psychosis. We show that despite lack of a group difference in NM-MRI between those with and without a first-degree relative with psychosis, frequency of subclinical paranoid thought is associated with elevated NM-MRI in the dorsomedial substantia nigra and ventral tegmental area complex. In the second study, we examined task-based dopamine release in the same population using simultaneous [^{11}C]raclopride positron emission tomography (PET) and functional MRI (fMRI) during fear conditioning. First, we confirmed the validity of the PET/fMRI experiment to capture dopamine release during the fear conditioning task. We show that fear conditioning elicits dopamine release in the dorsoposterior striatum of humans, which for the first time, confirms fear-elicited dopamine release in the analogous rodent tail of the striatum. We then compared dopamine release during fear conditioning in those with and without a first-degree relative with psychosis. We report that dopamine release is blunted in the dorsoposterior striatum in those with a first-degree relative. Finally, we report that lack of dopamine release in the dorsoposterior striatum is associated with increased frequency of subclinical paranoid thought. We also show that poor recall of the CS+ is associated with increased frequency of subclinical paranoid thought. For the first time, our findings suggest a lack of adaptive dopamine release is associated with subclinical positive symptomatology. Altogether, these two studies demonstrate that a static measure of dopamine released over the lifespan may be associated with paranoid thought, but that this increased release may not be occurring at relevant times and that a lack of adaptive dopamine release may be also contributing to paranoia, a prominent positive symptom in psychosis.

1. Introduction to Schizophrenia

1.1 Conception, and symptoms of schizophrenia

The word “Schizophrenia” was first mentioned over 100 years ago by Professor Paul Eugen Bleuler. In Bleuler’s conception, splitting (greek root of “to split”; *schizen)* of the mental faculties (greek root of “soul, spirit or mind”; *phren*) was the most defining feature of the disease (Fusar-Poli & Politi, 2008). Although our understanding of schizophrenia has greatly developed since that time, the core concept captured by this term remains. Now, schizophrenia is understood to be a multi-faceted neurodevelopmental disorder with diverse presentations of psychotic (positive), negative and cognitive symptoms (**Box 1;** (Howes et al., 2024)).

Box 1. DSM-5 diagnostic criteria for schizophrenia (Carter, 2014)**.**

A. Two or more of:
- Delusions
- Hallucinations
- Disorganized speech
- Grossly disorganized or catatonic behaviour
- Negative symptoms, such as diminished emotional expression, avolition and anhedonia.

B. Marked functional impairment, including interpersonal, academic and occupational.
C. Continuous disturbance for at least 6 months, including 1 month of list A symptoms and can include a prodromal or residual period.
D. Mood disorder excluded as a primary diagnosis.
E. Symptoms not caused by physiological effects of a substance or another medical condition.
F. In the context of autism spectrum disorder or communication issues, prominent delusions or hallucinations must be present to make a diagnosis.

1.2 Measurement and classification of symptoms in schizophrenia

Early attempts to measure schizophrenia symptoms, such as the brief psychiatric rating scale, captured various facets of the disorder (Overall & Gorham, 1962). However, a comprehensive assessment categorizing symptoms into positive, negative, and general psychopathological domains was lacking until the development of the Positive and Negative Syndrome Scale (PANSS) (Kay et al., 1987). The PANSS, a 30-item, 7-point rating instrument, defines positive symptoms as productive features (e.g., delusions, hallucinations), negative symptoms as deficit features (e.g., blunted affect, anhedonia), and general psychopathological symptoms as a parallel measure of severity (e.g., poor attention) (Kay et al., 1987). Others further classified these 30-items into positive, negative, disorganized/cognitive, hostility/excitement and anxiety/depression factors (Marder et al., 1997). Nevertheless, it is the distinct identification of positive and negative symptoms, along with severity ratings, that made the PANSS the gold-standard in measuring response to antipsychotic medications.

1.3 Trajectory of symptoms in schizophrenia

Schizophrenia is increasingly seen as a neurodevelopmental disorder with a prepsychotic phase characterized by attenuated symptoms beyond just positive ones. This clinical high-risk state for psychosis (CHR-P) is analogous to chest pain, potentially leading to psychosis or other mental disorders. Criteria include asymptomatic genetic risk, basic symptoms ([BS]; depressive, anxious, negative or cognitive), attenuated psychotic symptoms (APS), brief limited intermittent psychotic episodes (BLIPS), and first episode psychosis (FEP). These criteria manifest at different levels across premorbid, CHR-P, and early psychosis phases, as shown in **Figure 1** (Fusar-Poli et al., 2013; Iyer et al., 2008; Phillips et al., 2005).

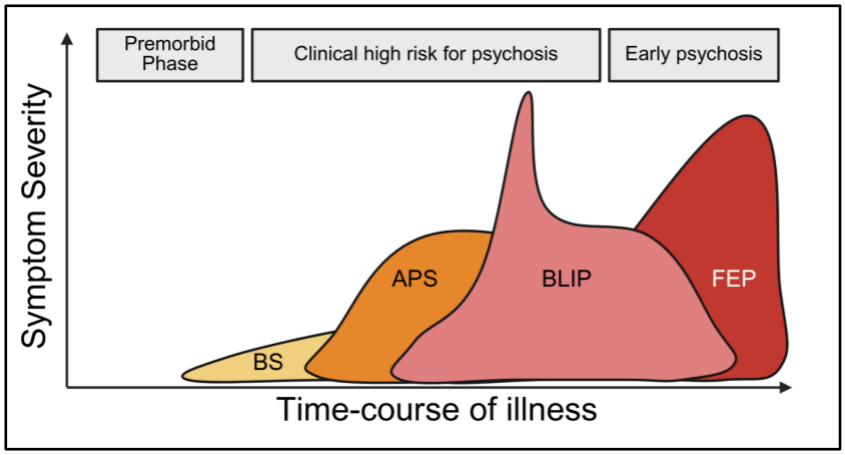

Figure 1. Time-course of illness progression from premorbid phase to full-blown psychosis. Adapted from (Fusar-Poli et al., 2013) with modifications from (Fusar-Poli, 2017).

When referring to early psychosis, it is important to note that this usually means the emergence of delusions and hallucinations, two criteria of schizophrenia that are typically grouped together into what we now know as positive symptoms. Really, it is the continuation of these positive symptoms for more than six months that qualifies an individual for a schizophrenia diagnosis. Interestingly, the two main positive symptoms also present at different points within the time-course of illness. In a landmark study examining CHR-P and FEP individuals, several observations on the emergence and stability of delusions and hallucinations can be made. Individuals are 3-8 times more likely to report delusions as a first symptom before hallucinations and are more stable only falling in severity after hallucination onset (Mourgues-Codern et al., 2025). Furthermore, it is the preoccupation with and distress towards delusions that differentiate patients from those who simply hold unusual beliefs, and it is these dimensions of severity, rather than conviction (strength of the belief) that improve with antipsychotic treatment (Sisti et al., 2012; So et al., 2014). Thus, these observations poise the frequency and distress dimensions of delusions as particularly important targets in the prevention and treatment of schizophrenia.

1.4 Epidemiology and burden of schizophrenia

Comprehensive global epidemiological reviews to date report a rather stable incidence (0.017-0.018%) and prevalence (0.29-0.39%) of schizophrenia and psychosis (Jongsma et al., 2019; Moreno-Küstner et al., 2018; Solmi et al., 2023). In Canada (2019), these estimates translate to approximately 6,400 new cases and 110,000 current cases (Government of Canada, 2019). Despite lower prevalence compared to other mental disorders, schizophrenia imposes a significant socioeconomic burden, ranking highest among 354 diseases at an estimated $2.2 billion in Canada ([$20 000 x 110 000]) (GBD 2017 Disease and Injury Incidence and Prevalence Collaborators, 2018; Stewart et al., 2022). With only 14-21% of individuals recovering, a substantial proportion continues to strain society (Hansen et al., 2023; Robinson et al., 2004). This limited recovery may stem from antipsychotic medications primarily targeting positive symptoms, rather than negative or general psychopathological symptoms (Tandon, 2011).

1.5 Treatment of schizophrenia and psychosis

The discovery that chlorpromazine alleviated hallucinations and delusions provided the first evidence for the antipsychotic effect of medication (Winkelman, 1954). Since then, while antipsychotic drug classes have evolved, the primary pharmacodynamic target, the dopamine D_2 receptor, has remained largely unchanged. These medications are effective on positive symptoms, but not negative, or cognitive symptoms, reinforcing dopamine as the key factor in psychosis specifically (Citrome, 2015; Fabiano et al., 2025; Feber et al., 2025; Osugo et al., 2022; Seeman & Lee, 1974). Given its prominent role in the treatment of psychosis, the dopamine system will be the central focus of this thesis.

2. The dopamine system

2.1 Dopaminergic nuclei

Dopamine synthesizing and releasing neurons are concentrated in several nuclei of the brain (Dahlstroem & Fuxe, 1964). These nuclei are denoted A8 to A17 and reflect their location based on the anterior distance, in *mm*, from the interaural line of the skull (A0). In the most basic classification system, A8, 9 and 10 neurons are proximally close and reside in the midbrain (German & Manaye, 1993). Further rostral, A11-17 neurons reside in and around the hypothalamic areas and extend anteriorly to the olfactory bulb (Goldsmith et al., 1990). The former, A8-10 neurons, have been studied most extensively in regards to neuropsychiatric disorders. Although demarcated as individual nuclei, A8 (retrorubral field), A9 (substantia nigra) and A10 (ventral tegmental area) dopamine neurons comprise a single network with no clear structural landmarks. Instead, these neurons can be more clearly classified based on differences in receptor expression within dorsal and ventral ‘tiers’ as well as projection sites (Haber et al., 1995; Zahm & Trimble, 2008). Thus, the

neuroanatomical location of A8-10 dopamine neurons confer likelihoods, but not absolutes, in terms of projections to target sites and *vis-a-vis*, functional involvement. Nevertheless, A8-17 nuclei project to discrete regions in the brain.

2.2 Dopaminergic tracts

There are nine main tracts arising from A8-17 dopaminergic nuclei summarized in **Table 1** below. In order, these correspond to the mesostriatal, mesocortical, tubero-infundibular, diencephalospinal, incertohypothalamic, periventricular, suprachiasmatic/supraoptic, olfactory and retinal tracts (Albanese et al., 1986; Björklund & Dunnett, 2007; Hamati et al., 2024). The main focus of the current thesis will be dopamine neurons in tract 1. This is because two of the methods used are neuromelanin-sensitive MRI (NM-MRI) and [^{11}C]raclopride positron emission tomography. NM-MRI is a proxy for dopaminergic neurons of A8,9 and 10 nuclei (**see section 4.1**) and [^{11}C]raclopride positron emission tomography (PET) is a proxy for D_2 receptors, which can only be reliably imaged in the striatum (**see section 4.2**).

Table 1. Dopaminergic tracts according to their innervation targets

Tract #	Cell group(s)	System	Main Target	References
1	A8,9,10	Retrorubral field, substantia nigra, ventral tegmental area (midbrain)	Striatum	Rodent: (German & Manaye, 1993) Primate: (François et al., 1999)
2	A8,9,10	Midbrain	Cortex	Rodent: (Lindvall et al., 1978) Primate: (Björklund et al., 1978)
3	A12,14	Arcuate and periventricular hypothalamus	Pituitary gland	Primate: (Goldsmith et al., 1990)
4	A11	Paraventricular hypothalamus	Spinal cord	Primate: (Goldsmith et al., 1990; Holstege et al., 1996)
5	A13	Zona incerta	Hypothalamus, Thalamus, lateral septum	Primate: (Goldsmith et al., 1990; Sánchez-González et al., 2005)
6	A11,14	Periaqueductal and periventricular gray	Thalamus, Hypothalamus	Primate: (Goldsmith et al., 1990; Sánchez-González et al., 2005)
7	A15	Suprachiasmatic nucleus and supraoptic nucleus	Supraoptic nucleus, Thalamus	Primate: (Goldsmith et al., 1990; Sánchez-González et al., 2005)
8	A16	Olfactory bulb	Olfactory glomeruli	Primate: (Loopuijt & Sebens, 1990)
9	A17	Inner nuclear layer of retina	Inner and outer plexiform layers	Primate: (Frederick et al., 1982)

2.3 Dopamine synthesis, release and reuptake

Dopaminergic neurons are identified through the proteins that they express: enzymes, receptors and transporters dedicated to dopamine synthesis, regulation, and reuptake. Tyrosine hydroxylase is one of the earliest markers that was used to identify dopamine neurons. Tyrosine hydroxylase is the first enzyme involved in the synthesis of dopamine, converting tyrosine to L-DOPA. L-DOPA is then converted to dopamine via aromatic acid decarboxylase. It is then loaded into synaptic vesicles by the vesicular monoamine transporter 2. These dopamine-loaded vesicles are docked at active zones located on varicosities (i.e. the pre-synaptic site is atypical, not located on axonal boutons). Release occurs via calcium-evoked exocytosis, mediated by SNARE proteins that drive vesicle fusion. The active zone is already primed with many of these vesicles, known as a readily releasable pool, and so dopamine axons release dopamine with a high probability. In addition, dopamine can can also be released somatodendritically, which can activate D_2 receptor mediated inhibition of those dopamine neurons (autoinhibition) via inhibitory currents mediated by G protein-activated inward rectifier K+ (GIRK) channels. Another way to reduce dopaminergic activity is through reuptake of dopamine, mediated by the dopamine transporter (DAT). Once back in the cell, dopamine is either repackaged into vesicles, broken down via monoamine oxidase or enters the neuromelanin-synthesis pathway (**see section 4.1)** (Liu et al., 2021; Martel & Gatti McArthur, 2020; Wengler, Trujillo, et al., 2024).

DAT, together with the activity of dopamine neurons, are responsible for maintaining tonic and phasic dopamine levels. Dopamine neurons can switch between silent, tonic firing and burst firing states. Of the spontaneously active neurons (~50-98%), some display an intrinsic pacemaker function and fire regularly (2-10 Hz). This regular firing produces scattered, short-lived dopamine transients (a few milliseconds) to maintain steady-state (‘tonic’) dopamine levels in the striatum. Importantly, baseline dopamine levels estimated at 2-20 nM are below the activation threshold of most dopamine receptors. These clock-like dopamine neurons can transition into a burst firing state likely via glutamatergic inputs. Synchronous firing of dopamine neurons firing *in bursts* produces phasic dopamine levels estimated at 100 µM - 1 mM. A burst is a high frequency spike train (>10 Hz, interspike interval < 0.08 s) that is thought to prolong the dwell time of dopamine, whereas the synchronous activity of these bursting neurons overwhelm DAT and produce dopamine levels above the activation threshold. In summary, DAT activity and dopamine neuron activities (tonic, phasic) determine the level and the dwell time of dopamine in the striatum. Release sites that are further than one micrometre are not likely to bind and activate dopamine receptors, and thus dopamine that is released from active sites form a small spatially specific activation zone (Grace, 2008, 2016; Grace et al., 2007; Grace & Bunney, 1983; Liu et al., 2021).

Table 2. Two modes of dopamine release, adapted from (Grace 2008); with modifications from (Grace, 2008, 2016; Grace et al., 2007; Grace & Bunney, 1983; Liu et al., 2021).

Tonic Dopamine	Phasic Dopamine
- Would influence large ensembles of striatal neurons through extended extrasynaptic binding - Potentially mediated by increased proportion of spontaneously active dopamine neurons - Likely not detectable by raclopride displacement	- Large dopamine concentration increase within the synapse, mediated by synchronized burst firing - Rapid reuptake via dopamine transporter restricts activity synaptically - Can be detected by raclopride displacement

2.4 Dopaminergic receptors

The striatum, densely innervated by A8,9 and 10 neurons, contains the highest concentration of dopamine receptors. These G protein-coupled receptors (GPCRs) are classified into D1-class (D_1 and D_5) and D2-class (D_2, D_3, and D_4) receptors. D1-class receptors are 'excitatory' receptors (K_d = 1 uM; low-affinity state), primarily coupled to G_S, which stimulate adenylate cyclase and increase cAMP levels. In contrast, D2-class receptors are 'inhibitory' receptors (K_d = 25 nM; high-affinity state), primarily coupled to $G_{i/o}$, which inhibit adenylate cyclase and decrease cAMP levels. D_2 receptors have a 40-fold higher affinity for dopamine than D_1 receptors, leading to the idea that D_2 receptors are tonically active and D_1 receptors are phasically active (Liu et al. 2021; Martel and Gatti McArthur 2020; Kawahata et al. 2024). However, rapid inhibitory currents from $G_{i/o}$ coupled GIRK channels during tonic and phasic firing challenge the idea that D_2 receptors are only activated with tonic dopamine release (Lalive et al. 2014; Beckstead et al. 2004). A small (%5) but important population of neurons co-express D_1 and D_2 receptors (Bonnavion et al. 2024). The co-localization of D_1 and D_2 receptors in striatal neurons further complicates their interaction with dopamine, with D_1 receptor manipulations potentially shifting the affinity-state of D_2 receptors (Seeman et al. 2005).

2.5 Functional relevance of tonic and phasic release to striatal dopamine pathways

To reconcile the fact that dopamine is released from varicosities (with no real post-synaptic site) but still produce precise learning signals, the domain-overlap model was proposed. This proposed model of signaling combines two models of signalling (volume transmission and synaptic transmission). Thus, sparse, spontaneous release and dopamine receptor binding produces a steady state (tonic levels) to regulate homeostatic functions, while synchronous phasic activity (phasic levels), combined with the differential distribution of dopamine receptors may allow for specific pathway recruitment (Liu et al., 2021).

2.5.1 Tonic release and homeostatic functions

Tonic dopamine refers to “baseline” dopamine that operates on a long timescale such as tens of seconds or minutes. Tonic dopamine serves two important functions, acting as both a homeostatic set point that calibrates the entire system and a gain control mechanism that modulates the ability of phasic dopamine to guide behavior. As a homeostatic signal, the continuous, low-level presence of dopamine prevents the maladaptive upregulation of dopamine synthesis and receptors, a compensatory change that would otherwise lead to a state of supersensitivity. This constant background tone establishes the baseline sensitivity of the system, ensuring it remains poised to respond dynamically to transient, high-concentration phasic signals without becoming unstable (Grace, 1991). Simultaneously, this tonic level acts as a gain control by maintaining partial occupancy of high-affinity receptors and biases learning strategies. A lower tonic level increases the gain, promoting exploitation of learned behaviors, while a higher tonic level reduces the gain, making choices more stochastic and favoring exploration (Ellwood et al., 2017; Guthrie et al., 2009; Pinto & Uchida, 2023).

2.5.2 Phasic release and striatal dopamine pathway recruitment

Phasic dopamine refers to shorter timescale dopamine (seconds or less), elicited by external stimuli, and serves as a teaching signal to reinforce behaviour. Modulation of striatal circuits in a D1-class ‘go’ pathway and a D2-class ‘no-go’ pathway has been useful in describing action selection (Kravitz & Kreitzer, 2012). D1-class activation, rise in cAMP, and protein kinase A (PKA)-mediated phosphorylation of glutamatergic receptors increase the excitability of striatal neurons to facilitate motor behaviour. Whereas D2-class activation, decrease in cAMP, and GIRK channel opening decrease the excitability of striatal neurons, which typically inhibit motor behaviour. Thus, phasic dopamine release in the striatum is classically thought to promote movement, via activation D1-class receptors on striatal neurons that ‘Go’, and at the same time, via activation of D2-class receptors, which inhibit tonically active striatal neurons that ‘No-Go’ (i.e. inhibiting the inhibitor). More contemporary views suggest both pathways are coactivated in a center-surround fashion to facilitate the selected action (center) and inhibit the competing actions (surround) (Cui et al., 2013; Li & Jin, 2023). In terms of value-based decision making, rather than a motor control view, inactivation of D1-class receptors selectively impairs value-dependent action selection and inactivation of D2-class receptors impairs value learning, respectively (Kwak & Jung, 2019).

3. Dopamine hypotheses of schizophrenia

3.1 Dopamine excess hypothesis

The dopamine excess hypothesis was originally proposed by Carlsson, Meltzer, Stahl, and Snyder (Carlsson, 1988; Meltzer & Stahl, 1976; Snyder, 1976).

Snyder (1976) first emphasizes the important role for dopamine in the central nervous system by illustrating the importance of dopamine in developing therapeutics for Parkinson's disease. Then, he states that amphetamine-induced psychosis may be the best model of schizophrenia, since individuals with either disorder present similarly and often confuse clinicians (Bell, 1973). Another line of evidence comes from the study of phenothiazines, which show antipsychotic effects (Winkelman, 1954). The phenothiazines, such as chlorpromazine, were found to produce animal behaviour similar to that of reserpine, which deplete dopamine stores (Carlsson & Lindqvist, 1963). It was only later that chlorpromazine was shown to reverse the effects of amphetamine on dopaminergic neurons, and binds to the dopamine receptor site (Aghajanian & Bunney, 1973; Seeman & Lee, 1974). In parallel, clinicians were administering several dopamine modulating compounds, namely Alpha-methyl-para-tyrosine (AMPT), which reduces dopamine synthesis as a tyrosine hydroxylase inhibitor, L-DOPA, the rate-limiting precursor to dopamine synthesis, and amphetamines, which release dopamine and of course, analogues of chlorpromazine, butyrophenones (like haloperidol) and eventually other D_2 receptor antagonists and partial agonists, in patients with schizophrenia.

3.1.1 Pharmacological studies supporting dopamine excess

In general, AMPT did not produce an antipsychotic effect on its own, but did reduce the dose of a D_2 receptor antagonist needed to produce an antipsychotic effect (Carlsson et al., 1973; Charalampous & Brown, 1967; Gershon et al., 1967; Magelund et al., 1979; Nasrallah et al., 1977; Suker et al., 2023; Wålinder et al., 1976; Wolkin et al., 1994). Whereas, L-DOPA and amphetamines, which promote dopamine synthesis and release, increase psychotic symptoms in schizophrenia (Angrist, Sathananthan, & Gershon, 1973; Angrist, Sathananthan, Gershon, et al., 1973; Davis & Janowsky, 1973; Janowsky et al., 1973; Yaryura-Tobias & Diamond, 1971). More recently, a meta-analysis reported that the psychosis incidence rate in Parkinson's disease patients taking L-DOPA was 35%, much higher than the psychosis incidence in the general population (Alsharaeh et al., 2024). Furthermore, the incidence of psychosis was 58% when patients were prescribed more than 558 mg of L-DOPA versus 33% in those prescribed less than 558 mg. In a case-control study using electronic health records, those with a past-month prescription of amphetamines were twice as likely to be hospitalized for psychosis, increasing to five-fold for higher dose prescriptions (Moran et al., 2024). Finally, a joint network meta-analysis of randomized-controlled trials and real-world effectiveness of all current D_2 receptor antagonist medications found that they were effective in treating schizophrenia (Efthimiou et al., 2024), Altogether, these data suggest pro-dopaminergic compounds produce psychosis and exacerbate positive symptoms in schizophrenia, whereas dopamine blocking medications improve them (**Table 3**).

Table 3. Administration of dopamine depleting and pro-dopaminergic compounds in schizophrenia.

Compound	Mechanism of action	Effect	Study
Chlorpromazine	D_2 receptor antagonist	Antipsychotic effect	(Winkelman, 1954)
Alpha-methyl-para-tyrosine (AMPT)	Tyrosine hydroxylase inhibitor	No antipsychotic effect	(Charalampous & Brown, 1967; Gershon et al., 1967; Wolkin et al., 1994)
D_2 receptor antagonist + AMPT	D_2 receptor antagonist +Tyrosine hydroxylase inhibitor	Antipsychotic effect	(Carlsson et al., 1973; Magelund et al., 1979; Nasrallah et al., 1977; Suker et al., 2023; Wålinder et al., 1976)
Dopamine precursor	L-DOPA	Psychotic effect	(Alsharaeh et al., 2024; Angrist, Sathananthan, & Gershon, 1973; Angrist, Sathananthan, Gershon, et al., 1973; Jaskiw & Popli, 2004; Yaryura-Tobias & Diamond, 1971)
Methylphenidate, Amphetamine, Methamphetamine	Dopamine releaser	Psychotic effect	(Davis & Janowsky, 1973; Janowsky et al., 1973; Moran et al., 2024)

3.1.2 Neuroimaging studies supporting dopamine excess

Neuroimaging studies provide further evidence for the dopamine excess hypothesis in schizophrenia, utilising techniques like single photon emission computed tomography (SPECT), PET and NM-MRI to investigate dopaminergic markers *in-vivo* in humans. Studies using [^{18}F]DOPA PET, which target aromatic acid decarboxylase (AADC), consistently show elevated dopamine synthesis capacity that is associated with positive symptoms of schizophrenia (Brugger et al., 2020; Howes et al., 2011, 2013; Jauhar et al., 2017, 2019, 2025; Lindström et al., 1999). DAT imaging with ligands such as [^{11}C]PE2I, [^{18}F]CFT, [^{123}]FP-CIT (Arakawa et al., 2009; Brugger et al., 2020; Laakso et al., 2000, 2001; Lavalaye et al., 2001) or $D_{2/3}$ receptor imaging with ligands such as [^{123}I]IBZM SPECT, [^{76}Br]bromospiperone SPECT, [^{11}C]N-methylspiperone PET, and [^{11}C]raclopride PET generally do not show elevated dopamine or association with positive symptoms on their own (Brugger et al., 2020; Farde et al., 1990; Hietala et al., 1994; Martinot et al., 1990; Nordström et al., 1995; Pérez et al., 2003; Wong et al., 1986). However, when combined with AMPT using a pre-post design, studies reveal increased synaptic dopamine levels via increases in $D_{2/3}$ receptor availability and are associated with positive symptoms (Abi-Dargham et al., 2000; Brugger et al., 2020; Caravaggio et al., 2015). Similarly, studies using $D_{2/3}$ receptor ligands (like [^{123}I]IBZM SPECT,

[^{11}C]NPA, [^{11}C]raclopride, [^{11}C]-(+)-PHNO) in conjunction with amphetamine or stress also demonstrate increased dopamine release via decreases in $D_{2/3}$ receptor availability, which are linked to positive symptoms (Abi-Dargham et al., 1998; Bertolino et al., 2000; Breier et al., 1997; Brugger et al., 2020; Frankle et al., 2018; Laruelle et al., 1996; Mizrahi et al., 2012; Pogarell et al., 2012; Tseng et al., 2018). Importantly, these SPECT/PET studies observe increased dopamine synthesis capacity, release capacity, and synaptic dopamine levels in the dorsal striatum (caudate and putamen), rather than ventral striatum (nucleus accumbens) (McCutcheon et al., 2019). Finally, NM-MRI, which measures neuromelanin levels in A8, 9, and 10 nuclei, is also elevated in schizophrenia, which is a proxy of long-term dopamine levels over the lifespan. Some of these studies show an association with positive symptoms as well (Cassidy et al., 2019; Ueno et al., 2022; Vano et al., 2024; Wengler, Seth C. Baker, et al., 2024; Wieland et al., 2021). In summary, several molecular neuroimaging techniques provide evidence for increased dopamine in schizophrenia (**Table 4**).

Table 4. Various PET radioligands in the investigation of dopamine abnormalities in schizophrenia.

Imaging Modality	Molecular Target	Elevated dopamine?	Associated with +ve symptoms?	Reference
[^{18}F]-DOPA PET	Aromatic Acid Decarboxylase	Yes	Yes	(Howes et al., 2011, 2013; Jauhar et al., 2017, 2019, 2025; Lindström et al., 1999)
[^{123}1]IBZM SPECT, [^{76}Br]bromospiperone, [^{11}C]N-methylspiperone, [^{11}C]raclopride PET	$D_{2/3}$ receptors	No	No	(Farde et al., 1990; Hietala et al., 1994; Martinot et al., 1990; Nordström et al., 1995; Pérez et al., 2003; Wong et al., 1986)
[^{123}1]IBZM SPECT, [^{11}C]raclopride PET + AMPT	Synaptic dopamine levels via change in $D_{2/3}$	Yes	Yes	(Abi-Dargham et al., 2000; Caravaggio et al., 2015)
[^{123}1]IBZM SPECT, [^{11}C]NPA, [^{11}C]raclopride PET, [^{11}C]-(+)-PHNO, + Amphetamine or Stress	Dopamine release via change in $D_{2/3}$	Yes	Yes	(Abi-Dargham et al., 1998; Bertolino et al., 2000; Breier et al., 1997; Frankle et al., 2018; Laruelle et al., 1996; Mizrahi et al., 2012; Pogarell et al., 2012; Tseng et al., 2018)
[11C]PE2I, [18F]CFT, [123I]FP-CIT	DAT	No	No	(Arakawa et al., 2009; Laakso et al., 2000, 2001; Lavalaye et al., 2001)
NM-MRI	A8, 9, 10 neuromelanin levels	Yes	Yes	(Cassidy et al., 2019; Ueno et al., 2022; Vano et al., 2024; Wengler, Seth C. Baker, et al., 2024; Wieland et al., 2021)

Note: *Previous D_1 receptor ligands did not produce consistent results (Guo et al., 2003).*

3.2 Dopamine imbalance hypothesis

3.2.1 Pharmacological studies supporting dopamine imbalance

Early on, researchers recognized that dopamine excess explained the emergence of positive symptoms, but failed to account for negative or cognitive symptoms of schizophrenia. This is partly due to reported improvements in negative symptoms when administering L-DOPA to individuals with schizophrenia. When systematically reviewed, L-DOPA administration led to a modest, but significant improvement of negative symptoms in schizophrenia, whereas symptomatic worsening occurred in roughly 20% of patients (Gerlach & Lühdorf, 1975; Inanaga et al., 1972, 1975; Jaskiw & Popli, 2004; Kay & Opler, 1985; Kumar et al., 2025). This and other observations, led to the development of dopamine receptor partial agonists for the treatment of negative and cognitive symptoms. Dopamine receptor partial agonists would increase dopamine-related signaling in brain areas where there is presumably less dopamine but still reduce dopamine-related signaling in brain areas where there is presumably more dopamine (Carlsson & Carlsson, 2006; Kikuchi et al., 2021). Studies evaluating the effectiveness of these newer medications on negative and cognitive symptoms are mixed. When compared to placebo, dopamine receptor partial agonists are effective in all symptom subdomains (Osugo et al., 2022). However, a network meta-analysis evaluating cognitive symptoms suggest no current dopaminergic antipsychotics are effective, but avoiding first-generation (dopamine receptor antagonist) medications may be warranted (Feber et al., 2025). Indeed, administration of dopamine receptor antagonists but not partial agonists, to healthy humans for seven days also produces negative symptoms (Osugo et al., 2025). Overall, pharmacological evidence suggests augmentation of dopamine signaling may also improve symptoms of schizophrenia (**Table 5**).

Table 5. Administration of pro-dopaminergic compounds alone or with antipsychotic treatment.

Compound	Mechanism of action	Effect	Study
Dopamine precursor	L-DOPA	Reduction in negative symptoms	(Gerlach & Lühdorf, 1975; Inanaga et al., 1972, 1975; Jaskiw & Popli, 2004; Kay & Opler, 1985; Kumar et al., 2025)
D_2 receptor antagonist + amphetamine	D_2 receptor antagonist + dopamine releaser	Reduction in negative symptoms	(Cesarec & Nyman, 1985)
D_2 receptor partial agonist or prodopaminergic drug	D_2 receptor partial agonist or prodopaminergic drug	Reduction in all symptoms	(Osugo et al., 2022)
D_2 receptor antagonist or partial agonist	D_2 receptor antagonist or partial agonist	No reduction in cognitive symptoms	(Feber et al., 2025; Osugo et al., 2025)

3.2.2 Neuroimaging studies supporting dopamine imbalance

Relative to neuroimaging studies examining dopaminergic excess, there are few studies looking at decreased dopamine release in schizophrenia. The reasons for this are mainly methodological; dopamine decreases are thought to be regionalized cortically but dopamine receptors are expressed in relatively lower quantities in extrastriatal areas and so produce unreliable measurements (Alakurtti et al., 2015; Slifstein et al., 2010). However, very high affinity tracers such as [^{11}C]FLB457 supposedly measure $D_{2/3}$ receptor availability in the cortex more reliably relative to [^{11}C]raclopride. In these studies, both amphetamine and a working memory task elicit less dopamine release in those with schizophrenia (Frankle et al., 2022; Rao et al., 2019; Slifstein et al., 2015). In summary, these studies provide empirical evidence for a lack of dopamine release cortically. Clearly, the story is much more complicated than a disorder of dopamine excess.

3.3 Aberrant salience hypothesis: promises and pitfalls

The aberrant salience hypothesis was postulated as a framework combining observations from neurobiology, pharmacology and phenomenology, providing a link between dopamine and schizophrenia (Kapur, 2003). The hypothesis states that dopamine excess in the ventral striatum drives the inappropriate assignment of salience to neutral stimuli, providing grounds for inappropriate associative learning and ultimately, the formation of delusions. When taking antipsychotics, individuals “do not primarily change thoughts or ideas; instead, they provide a neurochemical milieu wherein new aberrant saliences are less likely to form and previously aberrant saliences are more likely to extinguish.” (Kapur, 2003). Since then several variations of this proposal have emerged (Corlett et al., 2009; Corlett & Fraser, 2025; Howes & Kapur, 2009; Kapur et al., 2005; Maia & Frank, 2017; Millard et al., 2022; Winton-Brown et al., 2014).

3.4 Evolving Models: Bayesian, Chaotic, and Prediction Error Hypotheses

3.4.1 Bayesian uncertainty hypothesis

The Bayesian uncertainty hypothesis suggests that our world experience is shaped between prior experience (top-down processing) and current sensory input (bottom-up processing). The prediction error is essentially a mismatch between these two systems, which functions to increase the accuracy of prediction in the future (minimizing prediction error). The excitatory neurotransmitter glutamate is thought to compute the prediction error. On the other hand, neuromodulatory neurotransmitters like dopamine are thought to modulate this system by signalling the level of confidence or uncertainty about those prediction errors. For example, dopamine may increase or decrease the influence of a particular prediction error to update a belief (Corlett et al., 2009). It is thought that hallucinations and delusions

arise from differential imbalances of prior experience and sensory input. For example, aberrant bottom-up signaling forces a compensatory change in belief (delusion). Whereas, aberrant top-down signalling forces perception in the absence of strong sensory input (hallucination).

3.4.2 Chaotic dopamine hypothesis

Maia and Frank (2017) argue that schizophrenia arises from a combination of diminished phasic dopamine responses to relevant stimuli and increased spontaneous (tonic) dopamine release. Each of these disturbances contribute to a specific symptom domain (positive, negative) and explain a wide range of experimental findings. Reduced phasic responding to relevant stimuli help to explain negative symptoms: reduced learning from rewards, blunted activation of the ventral striatum, midbrain and other regions for reward prediction error. On the other hand, increased spontaneous dopamine release helps to explain positive symptoms: aberrant learning about neutral cues, increased activation of the ventral striatum, midbrain and other regions, and possibly erroneous prediction errors during neutral cues (Maia & Frank, 2017).

3.4.3 Prediction error hypothesis

Millard et al., (2022) propose a new framework where the dopamine prediction error, a signal that indicates a mismatch between expectation and reality, is interpreted differently by distinct, imbalanced brain circuits that converge in the ventral striatum. The core of the hypothesis is a differential weighting of inputs to the ventral striatum. On one hand, there exists an overweighted circuit involving input from the orbitofrontal cortex (which modulates neutral cues). On the other hand, there are underweighted circuits involving input from the prelimbic cortex (reduces salience of irrelevant cues) and lateral hypothalamus (increases salience of reward-predicting information). This imbalance causes the dopamine signal to be misconstrued: meaningless connections form and meaningful connections are not reinforced, leading to positive and negative symptoms of schizophrenia (Millard et al., 2022).

3.5 Dopamine hypothesis of schizophrenia: a way forward?

Instead of summarizing the support garnered for the salience misattribution hypothesis thus far, we will examine the most recent rebuttal of this hypothesis (Corlett & Fraser, 2025). In short, the aberrant salience hypothesis makes three critical predictions that have not held up to empirical scrutiny. First, studies using tasks designed to measure incentive salience (AKA ‘wanting’), such as the salience attribution task, have failed to show that individuals with schizophrenia have more salience misattribution than healthy controls. While some correlations exist within patient groups, the data does not support the idea that aberrant salience causes delusions. Second, the idea that salience misattribution is solely arising out of dysregulated dopamine function in the ventral striatum. Indeed, as summarized

above (**section 2.1.2**), excess dopamine synthesis capacity is more prominent in the associative and sensorimotor striatal areas relative to the ventral striatum. Third, there is a conflation of incentive salience and general salience. For example, unexpected events are salient and grab our attention because they signal a need to learn but do not necessarily motivate us to perform an action. The narrowing of scope has perhaps, unintentionally, guided researchers to focus on reward-based tasks which do not necessarily capture the larger idea of salience misattribution. However, the largest problem to date is a lack of empirical data. Although preclinical evidence suggests an imbalance between tonic and phasic dopamine neurotransmission, this remains an open question due to the time scale and other limitations of fMRI and PET imaging (Winton-Brown et al., 2014). By combining the molecular specificity of PET and the temporal resolution of fMRI, we may be able to investigate tonic and phasic dopamine signalling in humans. In the next section, we will examine the molecular imaging methodologies used in the current thesis before providing the rationale for the studies.

4. In-vivo measurement of the dopamine system in humans

4.1 Neuromelanin-sensitive MRI (NM-MRI)

Neuromelanin is a dark pigment that is responsible for the black color of the substantia nigra and locus coeruleus. Neuromelanin accumulates in healthy aging as a by-product of catecholaminergic metabolism. This pigment is lost only during cell death, and thus serves as a direct marker of dopaminergic neurodegeneration in Parkinson's disease (Sulzer et al., 2018). However, evaluating differences in neuromelanin accumulation in the absence of neurodegeneration, may serve as an important tool for understanding neuropsychiatric disease (Cassidy et al., 2019; Wengler, Trujillo, et al., 2024). Dopamine that is not repackaged into vesicles or broken down by monoamine oxidase, is left within the cytosol and enters the neuromelanin-synthesis pathway. In this pathway, dopamine-quinones form via several alternative biochemical cascades. The first being spontaneous auto-oxidation, the second being metal-dependent oxidation (i.e. copper) and the third, enzymatically, via tyrosinase (albeit at low levels) or ubiquitous enzymes such as prostaglandin H synthase (Hastings 1995; Greggio et al. 2005; Ikemoto et al. 1998; Snyder and Friedman 1998). Regardless, the resulting quinones are toxic and are quickly autophagocytosed. As they are retroactively transported back to the soma, these autophagosomes mature, polymerize and sequester iron, proteins and fats. It is the high iron content and resulting paramagnetic quality of these neuromelanin organelles that allow us to exploit neuromelanin accumulation in MRI sequences (Filimontseva et al., 2025; Wengler, Trujillo, et al., 2024; Zucca et al., 2014). One such sequence that is used in the current thesis is the 2D gradient recalled echo with magnetization transfer pulse (2D-GRE-MT) sequence. This sequence shows high reliability and is thought to be sensitive, but not specific, to neuromelanin, with

contributions from the free-water content of larger cells (Trujillo et al., 2023; Wengler et al., 2020; Wengler, Trujillo, et al., 2024).

Finally, NM-MRI is typically analyzed using a contrast-to-noise (CNR) ratio using the following formula, where for every voxel (v) (**equation 1**):

$$1.\ CNR_V = (I_V - mode(I)_{RR}) \div mode(I)_{RR}$$

Where signal intensity (I) within the region of interest (SN/VTA) is compared to a nearby reference region (RR - crus cerberi) (Cassidy et al., 2019) (**figure 2**). Because NM-MRI is a proxy of dopamine release over the lifespan, it reflects the cumulative release of tonic and phasic dopamine.

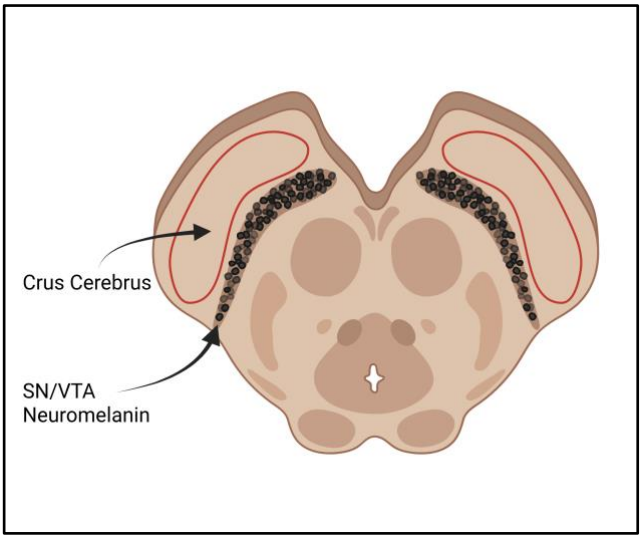

Figure 2. A cross-section of the midbrain showing that neuromelanin accumulates in the SN/VTA complex but is absent from the crus cerebri.

4.2 [^{11}C]raclopride PET to measure endogenous dopamine release

4.2.1 - Radioligand synthesis and detection

Isotopes, such as ^{11}C, are synthesized using a cyclotron to radiolabel ligands like raclopride (a selective $D_{2/3}$ antagonist), enabling the examination of the dopaminergic system (Farde et al., 1986; Hall et al., 1988; Köhler et al., 1985). In the cyclotron, highly pressurized N_2 gas mixed with O_2 gas (0.1-0.5% of the total volume) is irradiated with a beam of moderate-energy protons (~16.5 MeV). This highly efficient process produces [^{11}C]O_2 for use in subsequent radiochemistry with raclopride. Typically, through a series of chemical reactions, ^{11}C is transferred from carbon dioxide to the methyl group on raclopride (Lu et al., 2024). [^{11}C]raclopride has a half-life of 20.4 minutes because ^{11}C undergoes a phenomenon called β+ (positron) decay. During β+ decay, a proton in the unstable ^{11}C nucleus becomes a neutron. Thus, unstable ^{11}C is converted to stable ^{11}B along with the emission of a

positron and a neutrino. The positron will travel slightly (~ 1 mm) before annihilating with an electron, producing two photons with an energy of 511-keV each that travel in opposite directions. Passing through tissue and hardware, these photons are detected by a ring of PET detector crystals placed around the participants head. The annihilation is counted as a coincidence only when the photons are detected simultaneously. The coincidence can be considered a *true coincidence* if the photons arise from a single decay event and the line of response is within the field of view (FOV) of the PET detectors. In some cases, one photon of the pair can hit and deflect at an angle, but are still detected simultaneously. This sometimes results in a line of response outside of the FOV of the detectors. In this case, the event is easily considered scattered. In other cases, two photons arising from different decay events are detected simultaneously but the line of response may still reside within the FOV, and the event is considered random. Finally, a *true coincidence* may not be detected because of attenuation, which refers to the loss of true events due to scatter and/or absorption (i.e. the skull) (Turkington, 2001). There are complex reconstruction algorithms such as the 3D-OP-OSEM point spread function currently used to assign coincidences to particular voxels of the brain, as well as remove scattered and random events (Varrone et al., 2009). There are also other algorithms used to correct for attenuation, in our case, the pseudoCT method (Izquierdo-Garcia et al., 2014).

4.2.2 - Radioligand kinetic modelling

After reconstruction and attenuation correction, a reliable, time-binned [^{11}C]raclopride image is produced. Then, the mean radioactivity within a voxel or region of interest (ROI) is extracted for each bin, known as a time activity curve (TAC). These TACs can be used to quantify the binding potential relative to the non-displacement compartment (BP_{ND}). BP_{ND} refers to the ratio at equilibrium of specifically bound radioligand to that of nondisplaceable radioligand in tissue. BP_{ND} is typically reported when using reference tissue models, as it compares the concentration of radioligand in receptor-rich to receptor-free regions (Innis et al., 2007). In the current thesis, multireference tissue model 2 (MRTM2) is used to estimate the BP_{ND} of $D_{2/3}$ receptors in the striatum relative to the cerebellum (Ichise et al., 2003). Here, we use the cerebellum as the reference region because there are about 10 times fewer $D_{2/3}$ receptors, and whatever signal that is captured is not displaceable by other $D_{2/3}$ receptor binding molecules such as butaclamol (Köhler et al., 1985). Under the assumption that the signal in the cerebellum is not displaceable, then the full kinetic modelling can be described as (**equation 2**; **figure 3**):

$$2.1\ BP_{ND} = \frac{[\frac{K1}{k2}(1+\frac{k3}{k4})] - \frac{K1}{k2}}{\frac{K1}{k2}}$$

$$2.2\ BP_{ND} = \frac{[\frac{K1}{k2} + (\frac{K1}{k2} \times \frac{k3}{k4})] - \frac{K1}{k2}}{\frac{K1}{k2}}$$

$$2.3\ BP_{ND} = \frac{\frac{K1k3}{k2k4}}{\frac{K1}{k2}}$$

$$2.4\ BP_{ND} = \frac{k3}{k4}$$

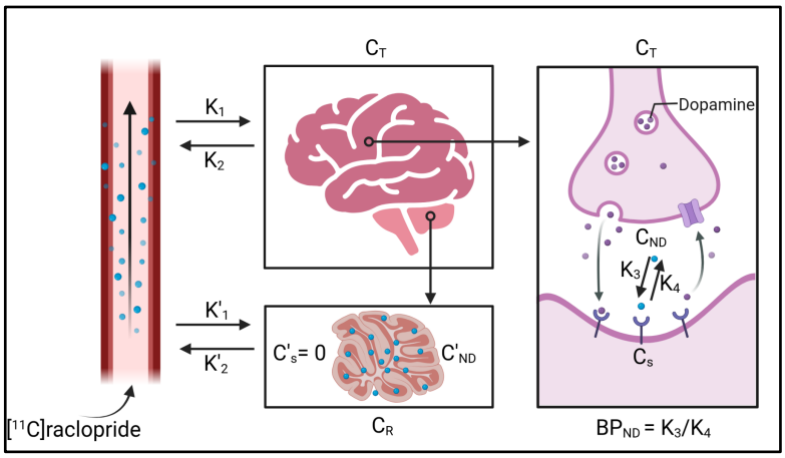

Figure 3. Depiction of a two-compartment model (MRTM2) to estimate BP_{ND}. [^{11}C]raclopride is injected and enters the target (the brain, C_T) with a kinetic constant K_1 and leaves with a kinetic constant of k_2. Using a reference region (cerebellum, C_R) where the specific binding ($C_{S\ (CER)}$) = 0 and the non-displaceable binding is equal to the non-displaceable of the target region ($C_{ND\ (CER)} = C_{ND\ (STRIATUM)}$), then the BP_{ND} can be estimated with kinetic constants k_3 / k_4. The BP_{ND} is essentially a ratio of the target TAC over the reference TAC, which is the concentration of target protein in the specifically bound compartment, relative to the reference concentration. Adapted from (Matheson, 2018) with modifications.

However, this metric is taken one step further when quantifying dopamine neurotransmission using [^{11}C]raclopride, which is sensitive to endogenous dopamine release. In this case, a challenge scan (during or directly after a drug or task) is preceded by a baseline scan. The baseline normalized difference between the scans serves as an index of dopamine release as confirmed by microdialysis (Laruelle, 2000), where (**equation 3**):

$$3.\ \%\Delta BP_{ND} = [\frac{(BP_{ND}task - BP_{ND}baseline)}{BP_{ND}baseline}] \times 100$$

Importantly, basic investigations of tonic and phasic dopamine (**section 2.3**) suggest any change observed in $\%\Delta BP_{ND}$ is due to phasic dopamine release. This has been tested in a simultaneous PET and microdialysis study in monkeys. On average, there was a -10.5% ΔBP_{ND} change corresponding to +460% dopamine concentration ([DA]; nmol/liter) after 0.2 mg/kg amphetamine and -21.3% ΔBP_{ND} change corresponding to +1365% [DA] after 0.4 mg/kg amphetamine (Breier et al., 1997). By calculating the slope, we see that there is roughly 84% Δ[DA] per $\%\Delta BP_{ND}$. Taking the lower and higher bounds of the range, we can see that the slope varies from about 19% to 136% per $\%\Delta BP_{ND}$.

4.2.3 - Measuring dopamine release during fear conditioning

Fear conditioning, a classical learning task, involves pairing a neutral stimulus (NS) with an unconditioned stimulus (US). Over a series of pairings, the initial NS may elicit a fear response (CS+) in the absence of the US. This initial pairing phase is termed fear acquisition. Fear acquisition was chosen to study phasic dopamine release due to its reliable elicitation of release and observed deficits in CHR-P and schizophrenia patients (Hamati et al., 2024; Quarmley et al., 2019; Tuominen et al., 2022). Rodent studies using microdialysis show approximately 100% (~5% theoretical ΔBP_{ND}) increases in striatal dopamine during fear conditioning, with the greatest release in the rodent tail of the striatum and nucleus accumbens core (Hamati et al., 2024). However, human studies have faced methodological challenges (Frick et al., 2022; Lissemore et al., 2020). Within the current thesis, we report methods to capture biologically valid fear-elicited dopamine release. Demonstrating task-based dopamine release provides a dynamic, real-time understanding of dopamine activity, complementing static molecular associations (i.e., NM-MRI) with paranoia. While molecular imaging reveals long-term dopamine levels, task-based studies show how dopamine responds during specific activities like fear conditioning. This allows for the investigation of how functional impairments in dopamine release, rather than just chronic elevations, contribute to symptoms such as paranoia.

4.3 functional MRI as a corroborating measure for PET

In the current thesis, functional MRI (fMRI) is used to corroborate our dopamine-related measures as an index of neuronal activity (Logothetis et al., 2001). fMRI is primarily sensitive to the concentration of paramagnetic deoxyhemoglobin. As regions of the brain are recruited to perform a task, they demand an increase in oxygenated blood, termed functional hyperemia (Hillman, 2014). This effectively decreases the concentration of deoxygenated blood within the region, and is interpreted as an increase in blood-oxygen-level-dependent (BOLD) signal characterized by a rise and fall (**figure 4**). Importantly, this haemodynamic response function (HRF) lags about 2-3 seconds after neuronal activity (Hillman, 2014; Logothetis et al., 2001). Nevertheless, fMRI is not a specific measure of

dopaminergic activity. In the current thesis, fMRI is used to confirm the task elicits BOLD signal in the expected areas and to support the observed increases in dopamine signal as physiologically relevant.

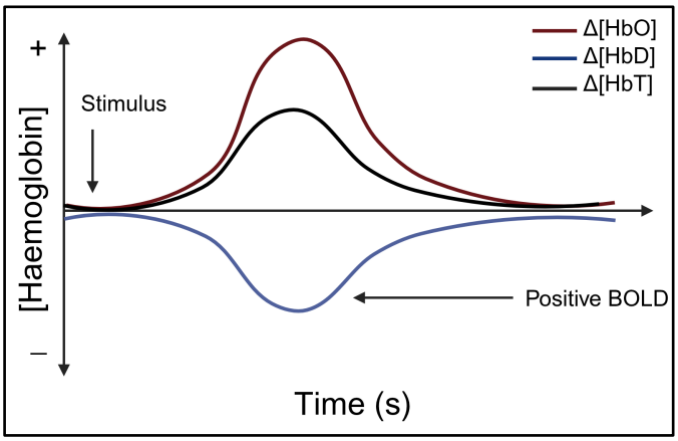

Figure 4. A few seconds after presentation of stimulus, BOLD signal is driven by an inflow of oxygenated haemoglobin concentration ([HbO]; red), increasing the total haemoglobin concentration ([HbT]; black) but also decreasing the relative concentration of deoxygenated haemoglobin ([HbD]; blue). Adapted from (Hillman, 2014) with modifications.

5. Rationale for studying dopamine dysregulation in family history of psychosis

In the current thesis, we examine NM-MRI, task-based dopamine neurotransmission using PET and fMRI in the first-degree relatives (FDRs) of those affected by psychotic disorders. This is because schizophrenia and related psychotic disorders are heritable; the disorder itself but also symptoms, cognitive function and the dopaminergic phenotype. By studying FDRs, we may investigate an attenuated phenotype without the confound of the disease itself and treatment duration. The evidence for heritability is reviewed in the following sections.

5.1 Heritability of schizophrenia and related disorders

Researchers have been examining the heritability of schizophrenia for more than a century. Older studies have reported lifetime risks of about 9% for siblings, 13% for offspring, 14% for dizygotic twins and 46% for monozygotic twins. Also, those adopted from mothers with schizophrenia tend to have a higher risk (9%) than kids adopted from mothers with no diagnosis of schizophrenia (2%) (Tsuang et al., 1999). Furthermore, national health databases have emerged as quality sources for examining risk in twins (Cannon et al., 1998; Cardno et al., 1999; Cheng et al., 2018; Hilker et al., 2018; Prescott et al., 2007; Rijsdijk et al., 2011; Sullivan et al., 2003). These reports point to a heritability of about 80% for schizophrenia and 70% for schizophrenia spectrum disorders, meaning that genetics contribute the majority of the risk. This does not preclude risk due to environmental factors. Importantly, a

study has shown that cannabis use and early childhood adversity can greatly exacerbate the risk of psychosis in FDRs (Radhakrishnan et al., 2019).

5.2 Heritability of specific symptoms

Further studies on large community samples of adolescent twins show that psychotic experiences are influenced by a combination of genetic and environmental factors. Although one study found that the majority of psychotic symptoms are heritable, some are more heritable than others. Notably, negative symptoms (59%) and paranoia (50%) were more heritable relative to hallucinations (15-30%) (Zavos et al., 2014). Another twin study examined how heritability changes with exposure to environmental risk factors. Anhedonia, cognitive disorganisation, paranoia and grandiosity were similarly heritable (41-49%) relative to hallucinations (30%). However, paranoia was more pronounced in those with exposure to more environmental risk factors (Taylor et al., 2022). Because paranoid thinking is also commonly expressed in the general population (20-40%) (Eaton et al., 1991; Ellett et al., 2003; Freeman et al., 2005, 2011), paranoia may be a suitable symptom to examine in both clinical and nonclinical populations.

5.3 Heritability of learning impairment

Learning impairments and their related cognitive functions also have a significant heritable component in FDRs. A broad meta-analysis including 170 published twin and family heritability studies comprised of >800 000 nonpsychiatric and schizophrenia participants found that general cognitive ability, verbal ability, visuospatial ability and executive function are all heritable (20-80%) (Blokland et al., 2017). Furthermore, another meta-analysis examining those with familial history of schizophrenia and bipolar disorder separately show deficits across most neuropsychological domains in both groups although it was more severe in those with familial schizophrenia history (Pedruzo et al., 2025).

5.4 Heritability of dopamine abnormalities

The heritability of dopamine abnormalities is nuanced. A few studies that examined FDRs and individuals with 22q11.2 deletion found evidence of increased dopamine synthesis capacity (Huttunen et al., 2008; Rogdaki et al., 2023), but a study on discordant twins did not replicate this finding in the unaffected and affected twin in remission (Shotbolt et al., 2011). This may be due to the idea that dopamine synthesis capacity increases are more pronounced during active psychosis than in remission (Avram et al., 2019). However, more recent and powerful genetic approaches, such as those using polygenic risk scores, have reinforced the link between genetic risk and elevated dopamine synthesis capacity (Eisenberg et al., 2024; Sportelli et al., 2024).

5.5 Outline of the current thesis

The overarching goal of the current work is to provide a way forward for studying dopamine dysregulation in psychosis. Studying dopamine dysregulation in psychosis is challenging because several ontological frameworks (biochemistry, neurobiology and psychology) should be thoroughly understood and linked together. Furthermore, technical limitations of PET and fMRI in humans precludes hypothesis testing. This is because measurement of endogenous dopamine release using [^{11}C]raclopride is highly specific to dopamine but lacks temporal resolution (i.e. one 60-minute measurement produces a single BP_{ND} value). Furthermore, measurement of brain activity using fMRI lacks molecular specificity. More recently, NM-MRI and simultaneous PET/fMRI have emerged as promising imaging methodologies to probe the dopamine system in humans. NM-MRI provides a long-term measure of dopamine accumulation. Whereas, simultaneous PET/fMRI can be used to link dopamine release to brain activity during specific time epochs (i.e. during presentation of a stimulus). In chapter 6, with my colleagues, I describe the use of NM-MRI to probe subclinical paranoia in a community sample including FDRs. We show a proxy of dopamine release over the lifespan (combined tonic and phasic dopamine) is associated with subclinical paranoid frequency irrespective of FDR group status. This finding supports the classical dopamine excess hypothesis of schizophrenia. In chapter 7, with my colleagues, I describe the use of simultaneous PET/fMRI to probe phasic dopamine release in the same community sample including FDRs. We show task-based dopamine release is measurable using a fear conditioning task. We then go on to show that this dopamine release is reduced in FDRs, providing support for the chaotic dopamine hypothesis of schizophrenia. Finally, we show lack of adaptive dopamine release is associated with more paranoia. In chapter 8, I discuss the implications of the main results and what they mean for the aberrant salience hypotheses, combining all current theories into a single cohesive framework.

5.6 Hypotheses

In general, we hypothesize that tonic dopamine would be increased in FDRs (chapter 6), whereas phasic dopamine would be decreased in FDRs (chapter 7). More detailed hypotheses are outlined in the respective chapters.

6. Article I: SN/VTA neuromelanin signal is associated with subclinical paranoia irrespective of familial risk for psychosis

Author list: Rami Hamati, Nour Kanaa, Bianca Chidiac, Synthia Guimond, Clifford Cassidy, Lauri Tuominen
Corresponding author: ltuominen@theroyal.ca
Manuscript accepted (*Schizophrenia*; submitted August 25, 2025).

Abstract

Subclinical paranoia is present in the relatives of patients with psychosis but it is also relatively common in the general population. Dopamine neurotransmission is increased in people with psychosis and is linked with positive symptoms, such as paranoia. Here, we examined if neuromelanin-sensitive MRI, a proxy of long-term dopamine turnover, is different between those with (n=25) and without (n=77) a first-degree relative with psychosis (N=102). We further tested whether neuromelanin-sensitive MRI was associated with the experience of subclinical paranoia as measured by the paranoia checklist. We found that there was no difference in neuromelanin-sensitive MRI signal between those with and without a first-degree relative. However, neuromelanin-sensitive MRI was significantly associated with the frequency subscore of the paranoia checklist, irrespective of familial risk (255 of 1879 voxels at $p < 0.05$, $p_{corrected} = 0.03$). This relationship was further supported by the association of neuromelanin-sensitive MRI and community assessment of psychic experience paranoia frequency subscore (316 of 1879 voxels at $p < 0.05$, $p_{corrected} = 0.01$). In summary, we show that subclinical paranoid thoughts are associated with a proxy of long-term dopamine turnover regardless of whether the person has a relative with psychosis or not. Thus, neuromelanin-MRI associates with positive subclinical symptomatology in those without psychotic illness, in addition to the link observed in patients.

Introduction

Schizophrenia is a neurodevelopmental disorder with a large genetic component [1,2]. Many symptoms of schizophrenia, including paranoia, are present at subclinical levels in the relatives of individuals with psychotic disorders [3,4]. In the general population, the prevalence of psychotic experiences is reported to be 5-8%, which is substantially higher than the prevalence of psychotic illness at 3%. That is, psychotic experiences exist along a continuum with a much larger cohort having subclinical psychotic experiences without a full-blown illness [5,6].

Paranoia is one such psychotic experience. It is common, heritable and exacerbated by exposure to environmental risk factors [7–12]. The two fundamental components of paranoia are i) a belief that harm will occur and ii) attribution of the

belief to the malicious intent of others. It is thought that paranoia may serve to be evolutionarily advantageous, particularly if the belief is true, unlike hallucinations which do not confer an evolutionary advantage at face value; however, paranoia becomes less advantageous as the conviction and distress due to these beliefs become disabling [13].

It is thought that paranoia may arise from maladaptive belief updating, caused by excess dopamine function [14]. More generally, elevated dopamine system function in the striatum is a hallmark of psychotic illness and represents a convergence of both genetic and environmental risk factors [15–17]. Individuals with schizophrenia show elevated dopamine synthesis capacity, increased release and synaptic dopamine levels compared to healthy controls [18–22]. Moreover, dopamine releasing drugs induce psychosis [23], dopamine blocking drugs attenuate psychosis [24] and dopamine synthesis capacity correlates with positive symptoms in psychotic illness [25,26]. Elevated dopamine system function has also been shown in those at clinical high-risk, i.e. those that present with attenuated symptomatology, using PET [27–30]. Similarly, people with a first-degree relative with schizophrenia (FDR) as well as those with higher polygenic risk scores have higher dopamine synthesis capacity in the striatum [31,32].

Striatal dopamine neurons largely originate from the midbrain substantia nigra and ventral tegmental area (SN/VTA complex) [33]. These dopamine producing neurons accumulate neuromelanin as a by-product of dopamine catabolism. Neuromelanin contains iron-rich deposits, which may be exploited and imaged using neuromelanin-sensitive MRI (NM-MRI) [34,35]. Accumulating evidence suggests NM-MRI can be a non-invasive means to capture this elevation in dopamine system function in psychotic illnesses [34,36–39] within the SN/VTA complex, that correlates to measures of dopamine synthesis and release [34,36,40]. Higher NM-MRI signal has been associated with positive symptom severity in individuals with schizophrenia and clinical high-risk [34,41], although results are mixed in clinical high-risk [35].

The extent to which familial risk factors and subclinical psychotic symptoms like paranoid thoughts are linked with SN/VTA NM-MRI CNR signal remains completely unexplored. Thus, the two objectives of the current study were to first test if substantia nigra NM signal is elevated in those with an FDR with psychosis compared to healthy controls without an FDR with psychosis (controls; CTRs). Secondly, to determine whether occurrence of self-reported paranoid thoughts *per se*, regardless of risk, is associated with substantia nigra NM signal. In the present study, we enrolled participants with and without an FDR with a diagnosis of schizophrenia, schizoaffective disorder or bipolar disorder with psychotic features to undergo a neuromelanin-MRI scan. We hypothesized that 1) the FDR group would have an elevated NM-MRI CNR signal (hereinafter referred to as **NM signal**) in the SN/VTA complex and 2) that NM signal correlates positively with the frequency of self-reported paranoid thoughts.

Methods

Participants

A total of 80 controls and 25 FDR individuals (N = 105) were pooled from two studies using identical NM-MRI sequences (n = 75 [study 1]; n = 30 [study 2]). The study protocols were approved by The Royal Ottawa Healthcare Group Research Ethics Board (REB #s: 2019003 [study 1] and 2018042 [study 2]) and Declaration of Helsinki. All participants gave a written informed consent before entering the study.

Participants with severe medical illness, head trauma resulting in unconsciousness, current substance use disorders, past psychosis, positive urine drug test on the day of scanning (amphetamines, barbiturates, benzodiazepines, codeine, fentanyl, MDMA, methadone, methamphetamine, opiates, oxycodone, phencyclidine and/or THC; using VeriCheck [Verify Diagnostics, Barrie, Ontario]), and/or contraindications for MRI scanning were excluded from the study.

Two FDR participants screened positively for a current mental health disorder (one with social anxiety disorder and the other with generalized anxiety disorder) as determined by a combination of medical history and the MINI international neuropsychiatric interview for DSM-5 [42]. Although they screened positively, these two FDRs were included in the study. They were not taking any medication to treat their disorders. Additionally, a total of 30 combined CTR and FDR individuals screened positively for a past mental health episode or disorder. This included 22 individuals with a past major depressive episode, 6 individuals with past major depressive disorder; 3 individuals with a past manic episode; 1 individual with a past hypomanic episode; 4 individuals with lifetime panic disorder; 2 individuals with past alcohol use disorder; 4 individuals with past substance use disorder; 1 individual with past generalized anxiety disorder; and 2 individuals with lifetime antisocial personality disorder.

FDRs were recruited by referral from psychiatrists at the Royal Ottawa Mental Health Centre or from the community. FDR status was confirmed using the family interview for genetic studies - psychosis checklist [43]. None of the control participants had first or second-degree relatives with psychotic illness. After discarding three scans due to misplacement of the field of view stack during scanning, a final sample of 77 controls and 25 FDRs (n = 102) were included in the analysis. **Table 1** presents the demographic variables and self-reported paranoia scores by FDR status [44–47].

Measures

Paranoia was primarily assessed using the paranoia checklist (PCL-18), an 18-item self-report questionnaire used to evaluate trait-like paranoid ideation on three dimensions: frequency, distress and conviction [44,45]. The frequency, distress and conviction of each item are rated on a five-point scale. Thus, the minimum score that can be acquired in each dimension is 18 and the minimum total score that can

be acquired is 54. Two controls scored more than three standard deviations above the mean on the PCL-18 conviction subscore (raw score > 70). All analyses were conducted with and without these two participants, which did not alter the main results (Table S4). Thus, the results for the full sample (n = 102) are reported in the main article.

We further support the primary analysis in two ways. We first support our primary analysis using a revised 13-item state paranoia checklist (PCL-13), in which five items were dropped due to poor sensitivity in experimental manipulations of paranoia [45]. In the PCL-13 (to evaluate state-like paranoid ideation), individuals are asked how the statement applies *at the moment* on a 10-point scale rather than asking about frequency, distress and conviction separately. For the purpose of this study, we used the PCL-13 but retained the 3-dimensional split (frequency, conviction, distress).

We also support the primary analysis using the Community Assessment of Psychic Experience (CAPE). The CAPE is a 42-item questionnaire, where the frequency and distress of each item is rated on a four-point Likert scale. The 42 items assess one of positive, negative or depressive symptom dimensions [46,48]. However, a factor analysis of the positive dimension revealed a 5-factor solution including paranoia as a subfactor [49,50]. Thus, the paranoia subscale of the CAPE was included as another analysis to support the brain-behaviour relationship as seen with the PCL.

MRI Acquisition

MRI data were acquired using a 3T mMR Biograph PET-MR system with a 12-channel head coil (Siemens, Erlangen, Germany). NM-MRI, first developed by Chen et al., (2014) [51], were collected as previously described [52]. Briefly, images were collected using a 2-dimensional gradient recalled echo sequence with magnetization transfer pulse; repetition time = 337 ms, echo time =3.97 ms, flip angle = 50, in-plane resolution = 0.43x0.43 mm, field of view = 165x220, 10 slices, slice thickness = 3 mm, magnetization transfer frequency offset = 1200 Hz, number of excitations = 6, acquisition time = 7.24 minutes. The 10 slices were positioned along the anterior commissure-posterior commissure line, starting 3 mm above the floor of the third ventricle. Additionally, T1-weighted MRI images were acquired using a multi-echo MPRAGE sequence [53]; spatial resolution = 1 mm isotropic; matrix = 256 x 256, number of slices = 192, repetition time (TR) = 2500 ms, echo time (TE) = 1.69, 3.55, 5.41, and 7.27 ms, flip angle = 7 degrees.

Processing of T1-weighted Images and NM-MRI

T1-weighted and NM-MRI scans were preprocessed using a previously validated pipeline in Matlab v9.1 (MathWorks, Natick, MA) [34,54]. First, T1-weighted images were inhomogeneity field corrected using the 'N4BiasFieldCorrection' function (advanced normalization tools [ANTs; v2.3.5]). Then, brains were extracted using the 'antsBrainExtraction' function (ANTs). Transformation matrices for 1) NM-MRI to

skull-stripped brain and 2) skull-stripped brain to MNI152 space were calculated using the 'antsRegistrationSyN' function (ANTs). Then, these transformations were applied to the NM-MRI image using the 'antsApplyTransforms' function in ANTs. The spatial normalized NM-MRI images were intensity normalized using the crus cerebri as a reference region. Finally, a 1 mm gaussian smoothing kernel was applied using the smooth3 function in SPM (v12.0) [55]. The final smoothed image was used for voxelwise analysis after visual inspection. Finally, the SN/VTA, psychosis and VTA NM-MRI averages were extracted for ROI-based robust regressions. The SN/VTA, psychosis, VTA and crus cerebri masks were generated from a previous study [34].

Visualization and Statistical Analysis

All visualizations were made with seaborn 0.13.2 [56] in python version 3.11. Independent-samples t-tests and chi-square tests on the demographic data were conducted using R (v4.5.1). To assess the voxelwise relationship between paranoia and NM-MRI, an SN/VTA voxelwise analysis controlling for age and sex was conducted in Matlab (MathWorks, Natick, MA) as previously described [34]. For each analysis, a robust regression was conducted for each voxel using the specified independent predictors and covariates (Table S2,4,5). The total number of significant positive voxels was computed and reported in Table S2,4,5. Then, permutation testing with 10 000 iterations was conducted, where subjects were randomly shuffled. Prior to permutation testing, voxels with CNR below -2.9% and above 21.5% were excluded to prevent undue influence of any single voxel. The lower and upper CNR thresholds were set to the lowest and highest 1% of values based on the distribution of all SN/VTA voxels in all subjects. Because some subjects have null (NaNs) on some values, we ensure that the permutation also excludes these values on a voxel-by-voxel basis. For each permutation, the total count of voxels that passed a one-tailed p-value threshold of 0.05 was computed. The observed count of significant voxels from the original analysis was compared against the null distribution generated from the 10 000 permutations. This max-T permutation test was conducted to preserve power while stringently correcting for false positives [57]. We supported the voxelwise analyses with independent-samples t-tests on whole SN/VTA, psychosis and VTA only masks using R (v4.5.1). Robust regressions on whole SN/VTA, psychosis, and VTA only masks were conducted using R (v4.5.1) as well.

Results

Sample Characteristics

Before comparing SN/VTA NM-MRI signals between groups, we looked for differences in age, sex, and paranoia frequency scores (**Table 1**). Individuals with an FDR and without a FDR had similar age and sex distributions (**Table 1**). There was no difference in PCL subscores or total score between groups (**Table 1**). Finally, the distribution of frequency, conviction and distress in the total group were not normal and differed from each other (**Table 1; Figure S1A**).

Table 1. Demographics and paranoia scores by FDR status.

	All (N=102)	Control (N= 77)	FDR (N= 25)	test	stats
Age					
Mean (SD)	32 (9.1)	32 (9.3)	31 (8.8)	t-test	t(100) = 0.28, p = 0.78
Sex					
Male	58 (56.9%)	46 (59.7%)	12 (48.0%)	chi-squared	X = 0.64, p = 0.43
Female	44 (42.6%)	31 (40.3%)	13 (52.0%)		
FDR Relationship					
None	77 (75.5%)	77 (100%)	0 (0%)		
Parent	14 (13.7%)	0 (0%)	14 (56.0%)		
Sibling	10 (9.8%)	0 (0%)	10 (40.0%)		
Both	1 (1.0%)	0 (0%)	1 (4.0%)		
PCL-18 - frequency				lilliefors	D = 0.28, p < 0.001
Mean (SD)	20 (3.1)	20 (2.9)	21 (3.6)		
Median [Min, Max]	18 [18, 33]	18 [18, 32]	20 [18, 33]	wilcoxon	W = 737, p = 0.06
PCL-18 - conviction				lilliefors	D = 0.31, p < 0.001
Mean (SD)	23 (9.0)	23 (10)	22 (4.2)		
Median [Min, Max]	21 [18, 87]	20 [18, 87]	21 [18, 34]	wilcoxon	W = 777, p = 0.14
PCL-18 - distress				lilliefors	D = 0.27, p < 0.001
Mean (SD)	20 (3.9)	20 (3.8)	21 (4.3)		
Median [Min, Max]	19 [18, 37]	18 [18, 37]	19 [18, 36]	wilcoxon	W = 835, p = 0.29
CAPE - paranoia (Frequency)				lilliefors	D = 0.21, p < 0.001
Mean (SD)	1.3 (0.26)	1.3 (0.25)	1.4 (0.30)		
Median [Min, Max]	1.2 [1.0, 2.0]	1.2 [1.0, 2.0]	1.4 [1.0, 1.8]	wilcoxon	W = 864, p = 0.43

SN/VTA NM Signal is Unaltered in FDRs

We first sought to examine differences in NM signal between CTRs and FDRs. Because the NM signal is a proxy of dopamine turnover over the lifespan, it is important to control for age [58,59]. A voxelwise analysis examining the effect of FDR status, controlling for age and sex, revealed scattered bidirectional changes with minimal clustering in the ventral SN that did not survive permutation testing (**Table S2**). Furthermore, ROI-based analysis using the whole SN/VTA, voxels previously associated with psychotic symptoms (referred to as the psychosis mask) or VTA [34] revealed no difference between CTR and FDR groups (t-test; p's > 0.05; **Figure S2A**; but also a robust regression controlling for age and sex; p's > 0.05; data not shown). We also examined the same ROIs with a binarized age variable (younger/older than 30 for both CTR and FDR) as in a previous analysis [39,60]. Here, we binarize groups by age because younger individuals are at a higher risk for psychosis. We found no differences in NM signal between younger CTRs and FDRs, or older CTRs and FDRs (t-test; p's > 0.05; **Figure S2B**). We examined the same ROIs across four groups: those with sibling, parent FDRs or both, separately as in a previous analysis [31]. Here, the rationale for splitting FDRs by genetic relationship is because children of affected individuals have a higher risk of developing psychosis relative to siblings [4]. We found no differences in NM signal between those without an FDR, siblings or children FDRs (one-way ANOVA; p's > 0.05; **Figure S2C**). Lastly, we examined these same ROIs across CTRs and FDRs with and without a past diagnosis to examine how past diagnosis could affect NM signal. In the whole group, past diagnosis was not associated with the ROI-based SN/VTA NM signal, controlling for age and sex ($F(1,98) = 0.26$, $p > 0.05$, robust regression, n = 102; data not shown). However, in an exploratory subgroup analysis, we found that FDRs with past diagnosis had elevated VTA NM signal compared to FDRs without a past diagnosis (t-test; $p < 0.05$, uncorrected; **Figure S2D**).

SN/VTA NM Signal is Associated with Self-reported Frequency of Paranoid Thoughts

Despite no group difference in SN/VTA NM signal, we asked whether individuals from the CTR and FDR groups combined, have elevated NM signal with respect to reported subclinical paranoia. A voxelwise analysis including FDR status, age and sex as covariates revealed a large number of voxels in the dorsomedial SN/VTA complex that were positively associated with self-reported frequency of paranoid thoughts (255 of 1879 voxels at $p < 0.05$, $p_{corrected} = 0.03$, n = 102, robust regression, **Figure 1A; Table S2**). This effect survived permutation correction for multiple comparisons (10,000 iterations). We also conducted an analysis more sensitive to state paranoia using the truncated 13-item state PCL frequency score [45] and further support our main finding (251 of 1879 voxels at $p < 0.05$, $p_{corrected} = 0.03$, n = 102, robust regression, **Table S2**)**.** The voxelwise effect was also supported by an ROI analysis using the whole SN/VTA ROI ($F(1,97) = 4.4$, $p = 0.04$, robust regression, n = 102; **Figure 1A; Table S3).** Lastly, we sought to supplement this brain-behaviour relationship using the CAPE paranoia frequency subscores [50,61]. A similar voxelwise analysis revealed a large number of voxels in the dorsomedial SN were also

associated with self-reported frequency using the CAPE (316 of 1879 voxels at $p < 0.05$, $p_{corrected} = 0.01$, n = 102, robust regression, **Figure 1B; Table S2)** but only trending when using the whole SN/VTA ROI ($F(1,97) = 3.8$, $p = 0.06$, robust regression, n = 102; **Figure 1B**). We also examined other aspects of paranoia severity. Although the frequency subscore was associated significantly with conviction and distress subscores (**Figure S1B**), the conviction, distress and total scores were not significantly associated with NM signal in the SN/VTA complex **(Table S2)**. Interestingly, past diagnosis was also associated with the PCL frequency score while controlling for age and sex ($F(1,98) = 13.5$, $p < 0.001$, robust regression, n = 102; data not shown).

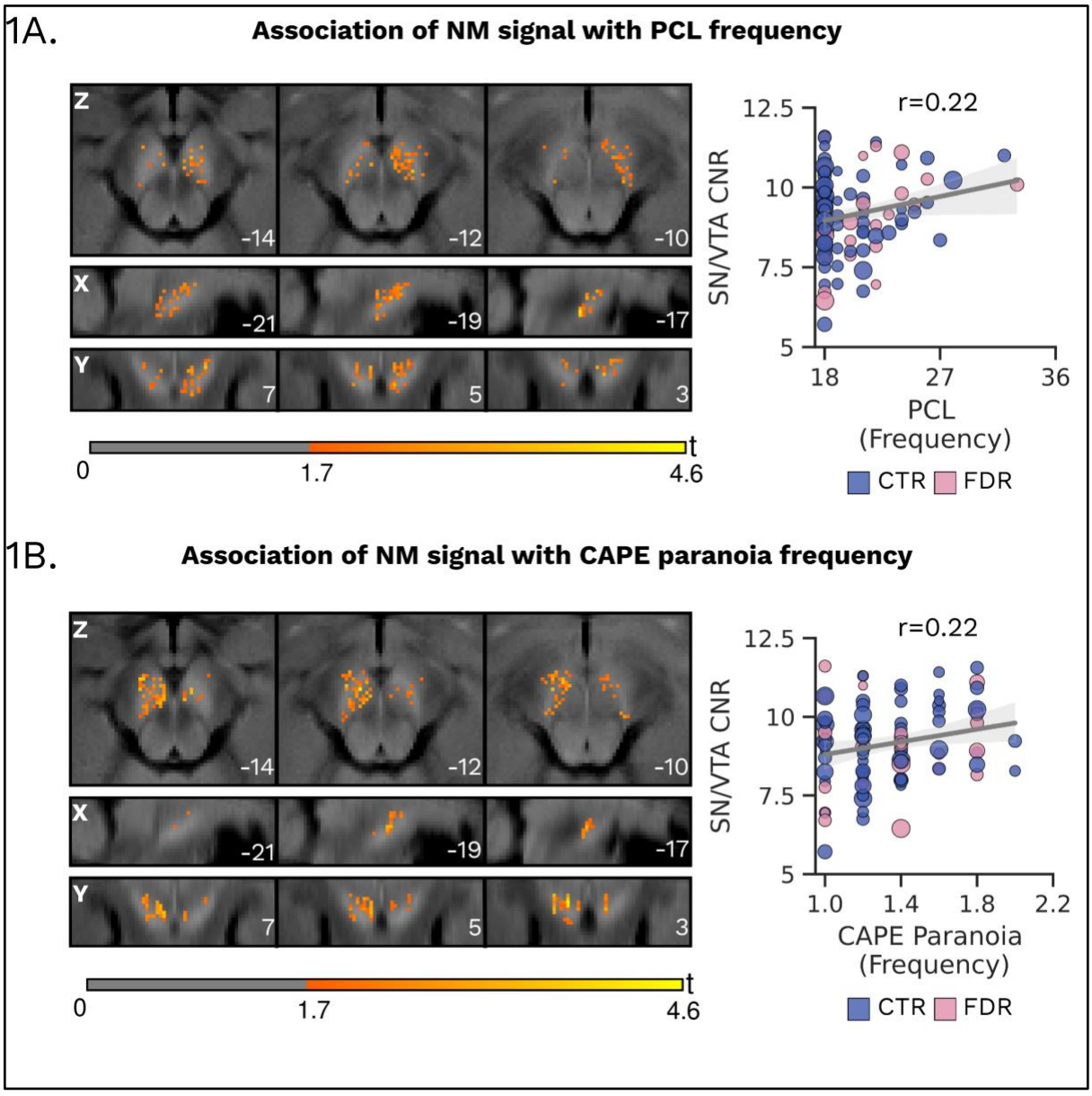

Figure 1. A) Voxelwise t-map of significant voxels only ($p < 0.05$, uncorrected) between PCL frequency score and SN/VTA CNR (axial view, z = -14, -12, -10). 255/1879 voxels along the dorsomedial SN were positively correlated with PCL

frequency score while controlling for group status, age and sex ($p_{corrected}$ = 0.03, robust regression, permutations = 10 000). Similar to voxelwise results, ROI analysis of the whole SN/VTA complex showed a significant association (bottom; robust regression, F(1,97) = 4.4, p = 0.04, r = 0.22 [effect size]). Note that the size of the data point indicates relative age. **B)** Voxelwise t-map of significant voxels only (p < 0.05, uncorrected) between CAPE paranoia frequency score and SN/VTA CNR (significant voxels only) (axial view, z = -14, -12, -10). 316/1879 voxels also along the dorsomedial SN were positively correlated with CAPE paranoia frequency score with controlling for group status, age and sex ($p_{corrected}$ = 0.01, robust regression, permutations = 10 000). When looking at the whole SN/VTA complex, the CAPE paranoia frequency score showed a borderline significant positive association (bottom; robust regression, F(1,97) = 3.8, p = 0.06, r = 0.22 [effect size]). Note that the size of the data point indicates relative age.

Discussion

The first objective of the current study was to examine if FDRs have elevated NM signal relative to CTRs. We report no difference in NM signal between those without and with a FDR when examining the signal in the whole SN/VTA complex, a psychosis mask and the VTA only [34] (**Figure S2A**). Additionally, there were no differences between CTRs and FDRs when examining younger versus older individuals, and FDR relationship status (**Figure S2B,C**). Our failure to find a difference in NM levels thus does not support the idea that dopamine neurons of the SN/VTA complex are overactive in this unaffected FDR sample. It is important to note, however, that our sample sizes were powered to detect moderate-to-large effect sizes; thus, we cannot rule out the existence of smaller group differences.

While increased NM signal in the SN/VTA complex is a well replicated result reported in several populations affected by psychosis [36,37,39,62], several factors may explain our null finding. First, we investigated FDRs unaffected by psychosis. This is in line with recent results reporting increased NM signal in more severe but not less severe psychosis [39] nor clinical high-risk individuals [41]. However, an exploratory analysis revealed those FDRs with a past mental health diagnosis may have higher NM signal (**Figure S2D**), suggesting dopamine neurons may be overactive in more mentally vulnerable FDRs.

A second key finding of our study is that NM signal correlates with subclinical measures of paranoid thought frequency (**Figure 1**). There are very few studies examining dopaminergic measures and their relation to psychotic experiences in healthy individuals [63,64]. Examining associations between dopaminergic measures and more common and more heritable symptoms, such as paranoia [8], may increase sensitivity. This interpretation may explain a lack of association of dopaminergic measures with auditory hallucination but not schizotypal personality traits [63,64]. Building on this, we show for the first time that a proxy of dopamine function

localized roughly to the dorsomedial SN correlates with the PCL frequency subscale, and that this association holds true regardless of FDR status. We further support this association using the CAPE paranoia frequency subscale as a comparable measure. This aligns with previous NM-MRI and PET studies where dopamine activity in the SN/VTA complex correlates with positive symptoms in schizophrenia and clinical high-risk in some, but not all, reports [25,30,34,41,65,66]. Our study adds to the literature by showing that this association exists for subclinical paranoia in a non-clinical population, irrespective of familial risk.

Interestingly, this correlation was present for the frequency of paranoid thoughts, but not their conviction or distress. This dissociation may be explained in several ways. One possibility is selection bias; by excluding participants with clinical psychosis, we may have also excluded those with high preoccupation and distress scores, which are factors that tend to differentiate clinical from non-clinical populations [67]. Alternatively, the frequency of paranoid thoughts may be directly reflected by elevated SN/VTA NM signal, while the associated distress and/or conviction are mediated by other mechanisms. This interpretation is supported by pharmacological studies, which show that the early phases of antipsychotic treatment reduce preoccupation and distress but not the conviction of delusional symptoms [68,69]. This implies that dopamine may be differently involved with distinct aspects of delusion severity.

The fact that NM signal accumulates slowly over the lifespan is more congruent with it being a trait marker of paranoia. Furthermore, state paranoia was not more strongly associated with NM-MRI than the total PCL score (**Table S2**). Paranoia is indeed present in the general population, suggesting paranoia exists on a continuum with clinical paranoid delusion [9,11,70]. Thus, paranoia may represent a sort of psychosis proneness [71,72]. Here, our data suggests overactive SN/VTA dopamine neurons, reflected by an increase in SN/VTA CNR, may be associated with the occurrence of paranoid thoughts, but relatively greater SN/VTA dopaminergic activity of the magnitude observed here is not sufficient to make these paranoid thoughts distressful.

There are several limitations to the current study. First, we used only familial status as a pseudo-quantitative marker of genetic risk. Studies examining the total burden of several genetic factors, such as polygenic risk score, may be more sensitive when examining differences in NM signal related to genetic risk. Furthermore, our subgroup analyses (binarized age, FDR relationship type, past diagnosis) may have been underpowered to detect small between-group differences in NM signal; as with our primary analysis, effects below a moderate-to-large size level cannot be ruled out.

In conclusion, this is the first study to examine self-reported paranoia in relation to NM signal in the SN/VTA complex in healthy individuals with and without an FDR. Our results suggest that elevated dopamine signaling, as indexed by NM-

MRI, confers susceptibility to the experience (i.e., frequency) of subclinical paranoia, regardless of familial risk. These data support the idea that while elevated SN/VTA NM signal is associated with the experience of subclinical paranoia, other factors, be it biological or environmental, may be necessary for these experiences to transition into distressing, convicted paranoia, as in clinical psychosis.

Data Availability Statement

The data are available upon reasonable request.

Acknowledgements

We would like to acknowledge our research participants, especially family members of patients with psychosis, for their participation.

Author Contributions (CRediT)

Rami Hamati: Investigation, Data Curation, Writing - Original Draft, Writing - Review & Editing, Formal Analysis, Visualization. Bianca Chidiac: Investigation, Data Curation. Nour Kanaa: Writing - Review & Editing Synthia Guimond: Resources, Writing - Review & Editing Clifford. Cassidy: Methodology, Software, Supervision, Writing - Review & Editing. Lauri Tuominen: Conceptualization, Methodology, Supervision, Writing - Review & Editing, Funding acquisition.

Funding

This research was supported by the Emerging Research Innovators in Mental Health Award (The Royal) to LT, the Brain and Behaviour foundation NARSAD Young Investigator Award to LT and the Canadian Institute of Health Research Project Grant to LT and SG.

Competing Interests

RH previously owned shares in Karuna Therapeutics Inc. and received two knowledge dissemination grants from Otsuka Canada Pharmaceutical Inc. to organize local trainee conferences. SG received honoraria/has been a consultant for Boehringer-Ingelheim (Canada) Ltd. CMC is inventor on a patent using the methodology employed in this study that is licensed to Terran Biosciences Inc. but has not received royalties. LT and SG received a knowledge dissemination grant from Otsuka Canada Pharmaceutical Inc. and Abbvie Inc. to organize a pan-Canadian schizophrenia conference. The remaining authors have nothing to disclose.

S1A.

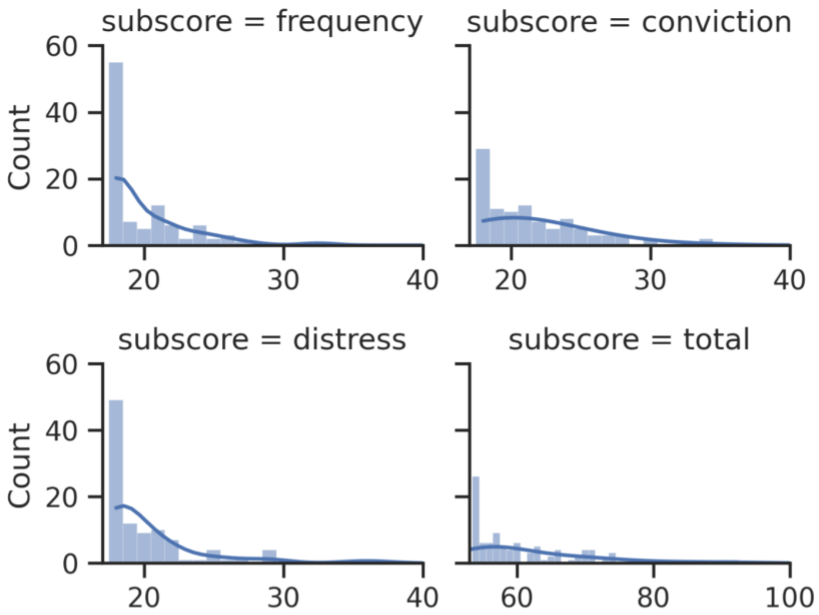

S1B.

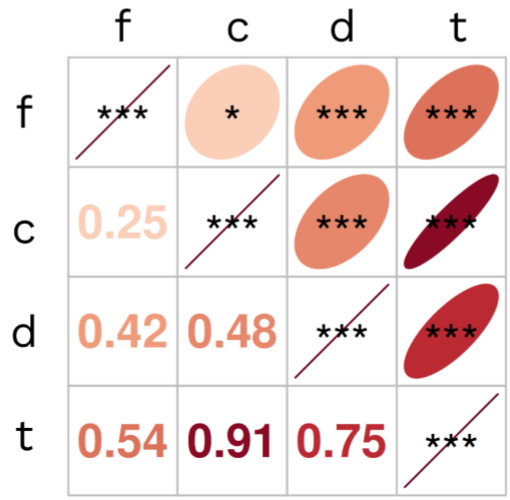

Figure S1A. Distribution of PCL subscores in the whole group (N =102). PCL-frequency and -conviction (Paired Pitman-Morgan test; $t(100) = -13.2$, $p < 0.05$), PCL-frequency and -distress (Paired Pitman-Morgan test; $t(100) = -2.6$, $p < 0.05$) and PCL-conviction and -distress (Paired Pitman-Morgan test; $t(100) = 10.6$, $p < 0.05$) distributions all differed from each other. Note that two control individuals who scored >70 on PCL conviction are not depicted here. **S1B.** Heatmap of PCL subscore correlations (f = frequency, c = conviction, d = distress, t = total). The rightward direction of the ellipse indicates a positive correlation. The numbers represent the Pearson r correlation coefficient. *p = 0.05; **p = 0.01; ***p = 0.001.

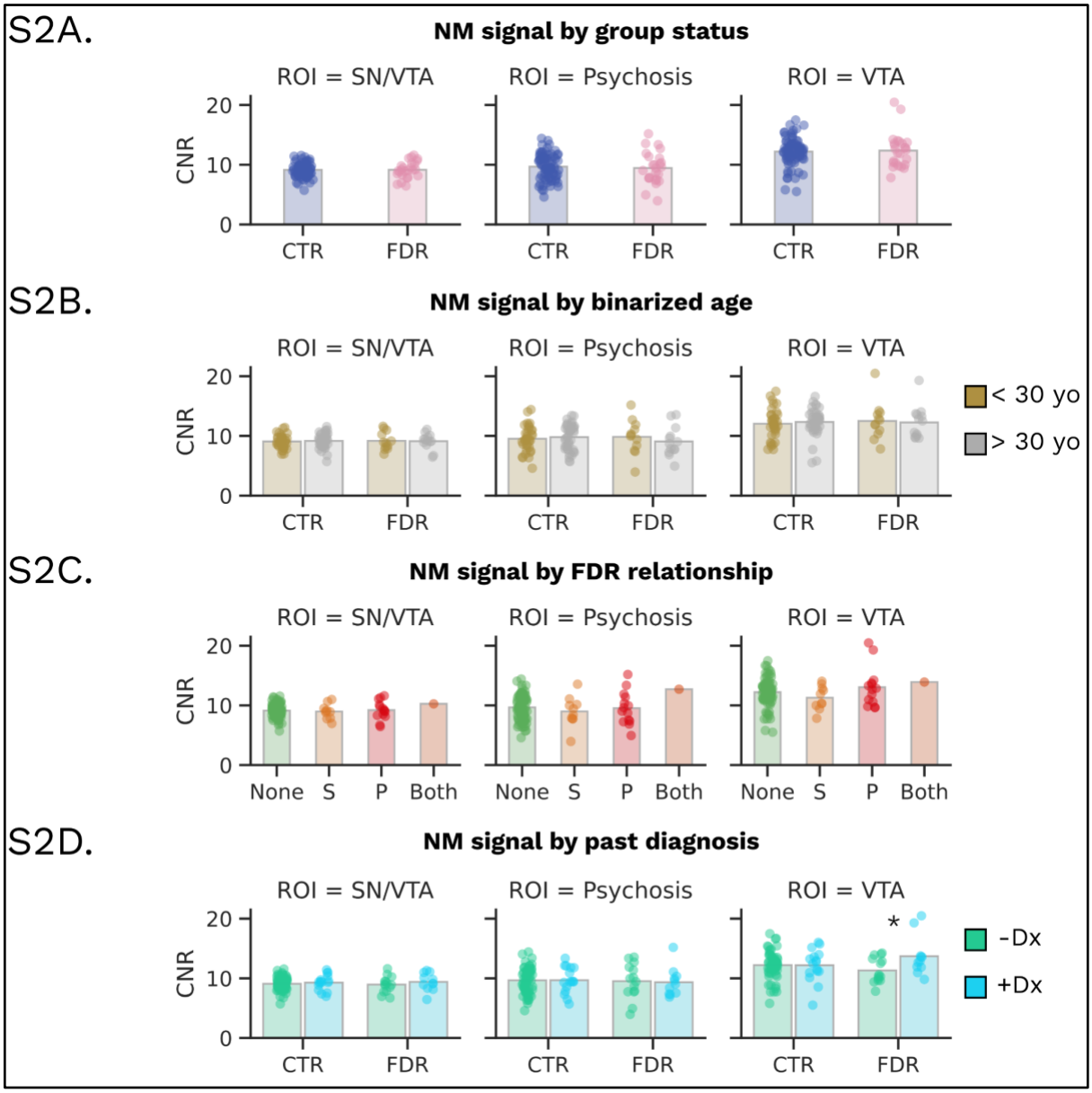

Figure S2. Uncorrected region of interest analyses. **A.** SN/VTA complex contrast-to-noise ratio (CNR) is not altered in FDR. Average of CNR in SN/VTA mask, psychosis mask and VTA mask is not different between groups using a t-test (SN/VTA: t(100) = -0.07, p = 0.94; Psychosis: t(100) = 0.44, p = 0.66; VTA: t(100) = -0.29, p = 0.78). **B.** SN/VTA complex CNR is not altered according to age status between groups using a t-test (under 30 yo; SN/VTA: t(100) = -0.25, p = 0.81. Psychosis: t(100) = -0.39, p = 0.70. VTA: t(100) = -0.51, p = 0.62. Over 30 yo; SN/VTA: t(100) = 0.14, p = 0.89. Psychosis: t(100) = 1.03, p = 0.31. VTA: t(100) = 0.12, p = 0.91. **C.** SN/VTA complex CNR is not altered according to FDR relationship type including 77 individuals without any FDR, 10 with an affected sibling and 14 with an affected parent and 1 individual with both an affected sibling and parent using a 1-way ANOVA (SN/VTA: F(3, 98) = 0.36, p = 0.78; Psychosis: F(3, 98) = 0.90, p = 0.44; VTA: F(3,98) = 1.2, p = 0.33). **D.** SN/VTA complex CNR is not altered according to past diagnosis status (+ or - Dx), but VTA CNR is altered in FDRs using a t-test

(CTRs; SN/VTA: t(100) = -0.61, p = 0.54. Psychosis: t(100) = -0.03, p = 0.98. VTA: t(100) = 0.05, p =0.43. FDRs; SN/VTA: t(100) = -0.80, p = 0.43. Psychosis: t(100) = 0.18, p = 0.86. VTA: t(100) = -2.2, p =0.04).

Table S1. Mean and standard deviations of CTR and FDR groups by ROI.

ROI	CTR (mean ± SD)	FDR (mean ± SD)
SN/VTA complex	9.13 ± 1.14	9.15 ± 1.40
Psychosis mask	9.68 ± 2.13	9.44 ± 2.66
VTA	12.21 ± 2.35	12.37 ± 2.88

Table S2. Robust regression model descriptions and results for the SN/VTA voxelwise analysis in 102 participants (n = 77 CTR; n = 25 FDR). In all the analyses, the dependent variable (DV) is the NM signal in the SN/VTA. The number of significant voxels (uncorrected p-value threshold = 0.05, one-tailed) and t-statistics are reported for the independent variable (IV). The covariates (COV) used are also described, where an asterisk (*) denotes it was examined in an interaction with the IV. The bolded analyses survived a correction for multiple comparisons using max-T permutations (iterations = 10 000). F= Frequency; C = Conviction, D = Distress; T = Total.

DV	IV	COV	N	# sig. + voxels	# sig. - voxels	Max T	Min T
NM	Group		102	64	59	3.0	-3.3
NM	Age		102	82	130	2.9	-3.7
NM	Group	Age	102	61	57	2.8	-3.3
NM	Group	Age, Sex	102	60	58	2.9	-3.43
NM	**PCL-F (18 item)**	**Group, Age, Sex**	**102**	**255**	**22**	**4.3**	**-3.2**
NM	PCL-F (18 item)	Group*, Age, Sex	102	157	43	3.6	-3.6
NM	PCL-C (18 item)	Group, Age, Sex	102	128	91	7.4	-3.3
NM	PCL-C (18 item)	Group*, Age, Sex	102	112	106	7.9	-3.5
NM	PCL-D (18 item)	Group, Age, Sex	102	94	83	3.8	-4.1
NM	PCL-D (18 item)	Group*, Age, Sex	102	96	120	3.8	-3.9
NM	PCL-T (18 item)	Group, Age, Sex	102	105	60	4.0	-3.2
NM	PCL-T (18 item)	Group*, Age, Sex	102	91	83	4.2	-3.4
NM	**PCL-F (13 item)**	**Group, Age, Sex**	**102**	**251**	**21**	**4.3**	**-3.2**
NM	**CAPE Paranoia-F**	**Group, Age, Sex**	**102**	**316**	**46**	**4.6**	**-3.3**

Table S3. A robust regression using the 'rlm' function from the 'MASS' package in R, with the following syntax: rlm(CNR (SN/VTA) ~ PCL-frequency + group + sex + age, data=filtered_data, method = "M"). P-values of the model were derived using the 'Anova' function from the 'car' package in R.

Independent Variable	DFs	F-value	p-value
PCL-frequency	1,97	4.4	0.04
Group	1,97	0.2	0.67
Sex	1,97	< 0.1	0.99
Age	1,97	< 0.1	0.85

Table S4. Robust regression model descriptions and results for the SN/VTA voxelwise analysis in 100 participants (n = 75 CTR; n = 25 FDR), excluding 2 CTRs for having high PCL conviction scores (> 3 SD above mean). In all the analyses, the dependent variable (DV) is the NM signal in the SN/VTA. The number of significant voxels (uncorrected p-value threshold = 0.05, one-tailed) and t-statistics are reported for the independent variable (IV). The covariates (COV) used are also described, where an asterisk (*) denotes it was examined in an interaction with the IV. The bolded analyses survived a correction for multiple comparisons using max-T permutations (iterations = 10 000). F= Frequency; C = Conviction, D = Distress; T = Total.

DV	IV	COV	N	# sig. + voxels	# sig. - voxels	Max T	Min T
NM	**PCL-F (18 item)**	**Group, Age, Sex**	**100**	**255**	**23**	**4.3**	**-3.4**
NM	PCL-C (18 item)	Group, Age, Sex	100	138	58	3.8	-3.6
NM	PCL-D (18 item)	Group, Age, Sex	100	83	127	3.4	-4.6
NM	PCL-T (18 item)	Group, Age, Sex	100	123	47	4.0	-3.6

Table S5. Robust regression model descriptions and results for the SN/VTA voxelwise analysis in 100 participants (n = 77 CTR; n = 23 FDR), excluding 2 FDRs for having current anxiety disorders according to the MINI. In all the analyses, the dependent variable (DV) is the NM signal in the SN/VTA. The number of significant voxels (uncorrected p-value threshold = 0.05, one-tailed) and t-statistics are reported for the independent variable (IV). The covariates (COV) used are also described, where an asterisk (*) denotes it was examined in an interaction with the IV. The bolded analyses survived a correction for multiple comparisons using max-T permutations (iterations = 10 000). F= Frequency; C = Conviction, D = Distress; T = Total.

DV	IV	COV	N	# sig. + voxels	# sig. - voxels	Max T	Min T
NM	**PCL-F (18 item)**	**Group, Age, Sex**	**100**	**222**	**28**	**4.3**	**-3.5**
NM	PCL-C (18 item)	Group, Age, Sex	100	115	106	6.9	-3.3
NM	PCL-D (18 item)	Group, Age, Sex	100	73	102	3.7	-4.1
NM	PCL-T (18 item)	Group, Age, Sex	100	93	69	3.6	-3.5

References

1. Sullivan, P. F., Yao, S. & Hjerling-Leffler, J. Schizophrenia genomics: genetic complexity and functional insights. *Nat. Rev. Neurosci.* **25**, 611–624 (2024).
2. Trubetskoy, V. *et al.* Mapping genomic loci implicates genes and synaptic biology in schizophrenia. *Nature* **604**, 502–508 (2022).
3. Torti, M. C. *et al.* Schizotypy and personality profiles of Cluster A in a group of schizophrenic patients and their siblings. *BMC Psychiatry* **13**, 245 (2013).
4. Tsuang, M. T., Stone, W. S. & Faraone, S. V. Schizophrenia: A review of genetic studies. *Harv. Rev. Psychiatry* **7**, 185–207 (1999).
5. McGrath, J. J. *et al.* Psychotic experiences in the general population: A cross-national analysis based on 31,261 respondents from 18 countries. *JAMA Psychiatry* **72**, 697–705 (2015).
6. van Os, J., Linscott, R. J., Myin-Germeys, I., Delespaul, P. & Krabbendam, L. A systematic review and meta-analysis of the psychosis continuum: evidence for a psychosis proneness-persistence-impairment model of psychotic disorder. *Psychol. Med.* **39**, 179–195 (2009).
7. van Os, J. Is there a continuum of psychotic experiences in the general population? *Epidemiol. Psichiatr. Soc.* **12**, 242–252 (2003).
8. Taylor, M. J., Freeman, D., Lundström, S., Larsson, H. & Ronald, A. Heritability of psychotic experiences in adolescents and interaction with environmental risk. *JAMA Psychiatry* **79**, 889–897 (2022).
9. Eaton, W., Romanoski, A., Anthony, J. & Nestadt, G. Screening for psychosis in the general population with a self-report interview. *J. Nerv. Ment. Dis.* **179**, 689–693 (1991).
10. Bebbington, P. E. *et al.* The structure of paranoia in the general population. *Br. J. Psychiatry* **202**, 419–427 (2013).
11. Elahi, A., Perez Algorta, G., Varese, F., McIntyre, J. C. & Bentall, R. P. Do paranoid delusions exist on a continuum with subclinical paranoia? A multi-method taxometric study. *Schizophr. Res.* **190**, 77–81 (2017).
12. Freeman, D. *et al.* Concomitants of paranoia in the general population. *Psychol. Med.* **41**, 923–936 (2011).
13. Raihani, N. J. & Bell, V. An evolutionary perspective on paranoia. *Nat. Hum. Behav.* **3**, 114–121 (2019).
14. Nour, M. M. *et al.* Dopaminergic basis for signaling belief updates, but not surprise, and the link to paranoia. *Proc. Natl. Acad. Sci. U. S. A.* **115**, E10167–E10176 (2018).
15. Dahoun, T. *et al.* The relationship between childhood trauma, dopamine release and dexamphetamine-induced positive psychotic symptoms: a [11C]-(+)-PHNO PET study. *Transl. Psychiatry* **9**, 287 (2019).
16. Egerton, A. *et al.* Adversity in childhood linked to elevated striatal dopamine function in adulthood. *Schizophr. Res.* **176**, 171–176 (2016).
17. Schalbroeck, R., van Hooijdonk, C. F. M., Bos, D. P. A., Booij, J. & Selten, J.-P. Chronic social stressors and striatal dopamine functioning in humans: A systematic review of SPECT and PET studies. *Mol. Psychiatry* **29**, 3841–3856 (2024).
18. Reith, J. *et al.* Elevated dopa decarboxylase activity in living brain of patients with psychosis. *Proc. Natl. Acad. Sci. U. S. A.* **91**, 11651–11654 (1994).
19. Hietala, J. *et al.* Depressive symptoms and presynaptic dopamine function in neuroleptic-naive schizophrenia. *Schizophr. Res.* **35**, 41–50 (1999).

20. Brugger, S. P. *et al.* Heterogeneity of striatal dopamine function in schizophrenia: Meta-analysis of variance. *Biol. Psychiatry* **87**, 215–224 (2020).
21. Lindström, L. H. *et al.* Increased dopamine synthesis rate in medial prefrontal cortex and striatum in schizophrenia indicated by L-(beta-11C) DOPA and PET. *Biol. Psychiatry* **46**, 681–688 (1999).
22. McCutcheon, R. A., Abi-Dargham, A. & Howes, O. D. Schizophrenia, dopamine and the striatum: From biology to symptoms. *Trends Neurosci.* **42**, 205–220 (2019).
23. Bell, D. S. The experimental reproduction of amphetamine psychosis. *Arch. Gen. Psychiatry* **29**, 35–40 (1973).
24. Seeman, P., Chau-Wong, M., Tedesco, J. & Wong, K. Brain receptors for antipsychotic drugs and dopamine: direct binding assays. *Proc. Natl. Acad. Sci. U. S. A.* **72**, 4376–4380 (1975).
25. Jauhar, S. *et al.* A test of the transdiagnostic dopamine hypothesis of psychosis using positron emission tomographic imaging in bipolar affective disorder and schizophrenia. *JAMA Psychiatry* **74**, 1206–1213 (2017).
26. Jauhar, S. *et al.* The relationship between cortical glutamate and striatal dopamine in first-episode psychosis: a cross-sectional multimodal PET and magnetic resonance spectroscopy imaging study. *Lancet Psychiatry* **5**, 816–823 (2018).
27. Howes, O. D. *et al.* Dopamine synthesis capacity before onset of psychosis: a prospective [18F]-DOPA PET imaging study. *Am. J. Psychiatry* **168**, 1311–1317 (2011).
28. Howes, O. *et al.* Progressive increase in striatal dopamine synthesis capacity as patients develop psychosis: a PET study. *Mol. Psychiatry* **16**, 885–886 (2011).
29. Mizrahi, R. *et al.* Increased stress-induced dopamine release in psychosis. *Biol. Psychiatry* **71**, 561–567 (2012).
30. Girgis, R. R. *et al.* Imaging synaptic dopamine availability in individuals at clinical high-risk for psychosis: a [11C]-(+)-PHNO PET with methylphenidate challenge study. *Mol. Psychiatry* **26**, 2504–2513 (2021).
31. Huttunen, J. *et al.* Striatal dopamine synthesis in first-degree relatives of patients with schizophrenia. *Biol. Psychiatry* **63**, 114–117 (2008).
32. Eisenberg, D. P. *et al.* Genetic risk for treatment resistant schizophrenia and corresponding variation in dopamine synthesis capacity and D2/3 receptor availability in healthy individuals. *Mol. Psychiatry* 1–8 (2024).
33. Weinstein, J. J. *et al.* Pathway-specific dopamine abnormalities in schizophrenia. *Biol. Psychiatry* **81**, 31–42 (2017).
34. Cassidy, C. M. *et al.* Neuromelanin-sensitive MRI as a noninvasive proxy measure of dopamine function in the human brain. *Proc. Natl. Acad. Sci. U. S. A.* **116**, 5108–5117 (2019).
35. Wengler, K., Trujillo, P., Cassidy, C. M. & Horga, G. Neuromelanin-sensitive MRI for mechanistic research and biomarker development in psychiatry. *Neuropsychopharmacology* **50**, 137–152 (2024).
36. Vano, L. J. *et al.* Mesostriatal dopaminergic circuit dysfunction in schizophrenia: A multimodal neuromelanin-sensitive magnetic resonance imaging and [18F]-DOPA positron emission tomography study. *Biol. Psychiatry* **96**, 674–683 (2024).
37. Wieland, L., Fromm, S., Hetzer, S., Schlagenhauf, F. & Kaminski, J. Neuromelanin-sensitive magnetic resonance imaging in schizophrenia: A meta-

analysis of case-control studies. *Front. Psychiatry* **12**, 770282 (2021).
38. van Hooijdonk, C. F. M. *et al.* Striatal dopamine synthesis capacity and neuromelanin in the substantia nigra: A multimodal imaging study in schizophrenia and healthy controls. *Neuroscience Applied* **2**, 101134 (2023).
39. Ueno, F. *et al.* Neuromelanin accumulation in patients with schizophrenia: A systematic review and meta-analysis. *Neurosci. Biobehav. Rev.* **132**, 1205–1213 (2022).
40. Zucca, F. A. *et al.* Neuromelanin of the human substantia nigra: an update. *Neurotox. Res.* **25**, 13–23 (2014).
41. Wengler, K. *et al.* Generalizability and Out-of-Sample Predictive Ability of Associations Between Neuromelanin-Sensitive Magnetic Resonance Imagingand Psychosis in Antipsychotic-Free Individuals. *JAMA Psychiatry* **81**, 198–208 (2024).
42. Sheehan, D. V. *et al.* The Mini-International Neuropsychiatric Interview (M.I.N.I.): The Development and Validation of a Structured Diagnostic Psychiatric Interview for DSM-IV and ICD-10. *J. Clin. Psychiatry* **59**, 22–33 (1998).
43. Maxwell, M. E. Manual for the FIGS. *Bethesda: National Institute of Mental Health* (1992).
44. Freeman, D. *et al.* Psychological investigation of the structure of paranoia in a non-clinical population. *Br. J. Psychiatry* **186**, 427–435 (2005).
45. Schlier, B., Moritz, S. & Lincoln, T. M. Measuring fluctuations in paranoia: Validity and psychometric properties of brief state versions of the Paranoia Checklist. *Psychiatry Res.* **241**, 323–332 (2016).
46. Brenner, K. *et al.* Validation of the English and French versions of the Community Assessment of Psychic Experiences (CAPE) with a Montreal community sample. *Schizophr. Res.* **95**, 86–95 (2007).
47. Mossaheb, N. *et al.* The Community Assessment of Psychic Experience (CAPE) questionnaire as a screening-instrument in the detection of individuals at ultra-high risk for psychosis. *Schizophr. Res.* **141**, 210–214 (2012).
48. Stefanis, N. C. *et al.* Evidence that three dimensions of psychosis have a distribution in the general population. *Psychol. Med.* **32**, 347–358 (2002).
49. Wigman, J. T. W. *et al.* The Structure of The Extended Psychosis Phenotype in Early Adolescence—A Cross-sample Replication. *Schizophrenia Bulletin* **37**, (2011).
50. Wigman, J. T. W. *et al.* Replication of the five-dimensional structure of positive psychotic experiences in young adulthood. *Psychiatry Res.* **197**, 353–355 (2012).
51. Chen, X. *et al.* Simultaneous imaging of locus coeruleus and substantia nigra with a quantitative neuromelanin MRI approach. *Magn. Reson. Imaging* **32**, 1301–1306 (2014).
52. McCall, A. *et al.* Evidence for locus coeruleus-norepinephrine system abnormality in military posttraumatic stress disorder revealed by neuromelanin-sensitive magnetic resonance imaging. *Biol. Psychiatry* **96**, 268–277 (2024).
53. van der Kouwe, A. J. W., Benner, T., Salat, D. H. & Fischl, B. Brain morphometry with multiecho MPRAGE. *Neuroimage* **40**, 559–569 (2008).
54. Wengler, K., He, X., Abi-Dargham, A. & Horga, G. Reproducibility assessment of neuromelanin-sensitive magnetic resonance imaging protocols for region-of-interest and voxelwise analyses. *Neuroimage* **208**, 116457 (2020).
55. The FIL Methods Group. SPM12 Manual. Preprint at

https://www.fil.ion.ucl.ac.uk/spm/doc/spm12_manual.pdf (2021).
56. Waskom, M. seaborn: statistical data visualization. *J. Open Source Softw.* **6**, 3021 (2021).
57. Nichols, T. E. & Holmes, A. P. Nonparametric permutation tests for functional neuroimaging: a primer with examples. *Hum. Brain Mapp.* **15**, 1–25 (2002).
58. Shibata, E. *et al.* Age-related changes in locus ceruleus on neuromelanin magnetic resonance imaging at 3 Tesla. *Magn. Reson. Med. Sci.* **5**, 197–200 (2006).
59. Xing, Y., Sapuan, A., Dineen, R. A. & Auer, D. P. Life span pigmentation changes of the substantia nigra detected by neuromelanin-sensitive MRI. *Mov. Disord.* **33**, 1792–1799 (2018).
60. Watanabe, Y. *et al.* Neuromelanin magnetic resonance imaging reveals increased dopaminergic neuron activity in the substantia nigra of patients with schizophrenia. *PLoS One* **9**, e104619 (2014).
61. Wigman, J. T. W. *et al.* The Structure of The Extended Psychosis Phenotype in Early Adolescence—A Cross-sample Replication. *Schizophrenia Bulletin* **37**, (2011).
62. Ahrens, J. *et al.* Convergence of cannabis and psychosis on the dopamine system. *JAMA Psychiatry* (2025) doi:10.1001/jamapsychiatry.2025.0432.
63. Woodward, N. D. *et al.* Correlation of individual differences in schizotypal personality traits with amphetamine-induced dopamine release in striatal and extrastriatal brain regions. *Am. J. Psychiatry* **168**, 418–426 (2011).
64. Howes, O. D. *et al.* Dopaminergic function in the psychosis spectrum: an [18F]-DOPA imaging study in healthy individuals with auditory hallucinations. *Schizophr. Bull.* **39**, 807–814 (2013).
65. Howes, O. D. *et al.* Midbrain dopamine function in schizophrenia and depression: a post-mortem and positron emission tomographic imaging study. *Brain* **136**, 3242–3251 (2013).
66. Tseng, H.-H. *et al.* Nigral stress-induced dopamine release in clinical high risk and antipsychotic-naïve schizophrenia. *Schizophr. Bull.* **44**, 542–551 (2018).
67. Sisti, D. *et al.* Preoccupation and distress are relevant dimensions in delusional beliefs. *Compr. Psychiatry* **53**, 1039–1043 (2012).
68. Mizrahi, R. *et al.* The selective effect of antipsychotics on the different dimensions of the experience of psychosis in schizophrenia spectrum disorders. *Schizophr. Res.* **88**, 111–118 (2006).
69. So, S. H.-W., Peters, E. R., Swendsen, J., Garety, P. A. & Kapur, S. Changes in delusions in the early phase of antipsychotic treatment - an experience sampling study. *Psychiatry Res.* **215**, 568–573 (2014).
70. Ellett, L., Lopes, B. & Chadwick, P. Paranoia in a nonclinical population of college students. *J. Nerv. Ment. Dis.* **191**, 425–430 (2003).
71. Thewissen, V., Bentall, R. P., Lecomte, T., van Os, J. & Myin-Germeys, I. Fluctuations in self-esteem and paranoia in the context of daily life. *J. Abnorm. Psychol.* **117**, 143–153 (2008).
72. Ellett, L. *et al.* Experimental studies of paranoid thinking in clinical and nonclinical populations: a systematic review and meta-analysis. *Psychol. Med.* **53**, 5933–5944 (2023).

7. Article II: Blunted fear-evoked striatal dopamine release in individuals with a family history of psychosis

Author list: Rami Hamati, Cecelia Shvetz, Bianca Chidiac, Hussein Bdair, Katie Dinelle, Daphne J. Holt, Clifford M. Cassidy, Lauri Tuominen
Corresponding author: ltuominen@theroyal.ca
Manuscript under consideration (*Molecular Psychiatry*; submitted January 12th, 2026).

Introduction

Schizophrenia is a disorder of excess tonic dopamine signaling [1–3]. Positron emission tomography (PET) studies have demonstrated elevated dopamine synthesis capacity, higher dopamine release in response to amphetamines, and increased synaptic dopamine levels in the striatum in individuals with schizophrenia [4]. Importantly, excess dopamine signaling extends to individuals with other psychotic disorders, clinical risk for psychosis, first degree relatives, and those with higher polygenic risk score for psychosis [5–8].

Yet, excess tonic dopamine signaling has been difficult to reconcile with findings of impaired dopamine-dependent learning in psychotic disorders. For example, individuals with psychotic disorders show reduced behavioural responses to reward predicting cues [9, 10]. In functional magnetic resonance imaging (fMRI) studies using reward tasks, individuals with psychotic disorders have blunted striatal BOLD responses during anticipation of reward, and to reward prediction errors [11–14]. In addition to reward learning, individuals with schizophrenia exhibit impaired discriminative fear conditioning, another dopamine dependent process [15–17]. If schizophrenia was simply a disorder of appropriately synchronized but excessive dopamine signaling, then presumably performance in dopamine dependent tasks would be better, not worse.

The chaotic dopamine hypothesis has emerged as a prominent theory trying to resolve this discrepancy [18, 19]. It postulates an increase in spontaneous dopamine release that contributes to higher tonic levels of dopamine and a reduction of adaptive, stimulus-driven phasic dopamine release in schizophrenia. Furthermore, the hypothesis predicts that increased spontaneous dopamine release is associated with positive symptoms, while decreased adaptive dopamine release is associated with negative symptoms. While compelling, so far there has been limited evidence supporting the chaotic dopamine hypothesis.

In this study, we use Pavlovian fear conditioning to directly test the chaotic dopamine hypothesis. Pavlovian fear conditioning requires adaptive, stimulus-driven dopamine release to form associations between aversive and neutral stimuli in rodents. However, definitive evidence that fear conditioning releases dopamine in humans is lacking [16]. Therefore, we first seek to demonstrate that fear conditioning leads to detectable dopamine release in the striatum in individuals without family

history of psychosis and explore the link between dopamine release and other fear responses. We measure dopamine release, neural, physiological, and behavioural responses simultaneously with [^{11}C]raclopride PET/fMRI, skin conductance, and behavioural ratings. Then, we set out to test the chaotic dopamine hypothesis in a group of first-degree relatives (FDRs) of individuals with psychotic disorders. We choose to study individuals with family history of psychosis because they display a hyperdopaminergic phenotype [5, 6] without the confounding treatment of antipsychotic medication, which directly competes with [^{11}C]raclopride. Specifically, our hypothesis is that first-degree relatives of individuals with psychotic disorders will show a reduction in adaptive, stimulus-driven dopamine release during fear conditioning. Finally, we test if lower dopamine release is associated with measures of subclinical negative or positive symptoms [20]. In a larger sample that only completed the Pavlovian fear conditioning fMRI task, we also test whether behavioural ratings of the cues are associated with subclinical negative and positive symptomatology.

Materials & Methods

General outline of the study

We employed a visual fear conditioning paradigm during which computer-generated faces were presented to participants [21, 22]. After completing the clinical interview, each participant underwent the fear conditioning task using simultaneous fMRI/SCR (*N* = 74). A subset of individuals underwent multimodal neuroimaging including a baseline T1-weighted MRI, baseline PET scan and the following day, another T1-weighted MRI, and simultaneous task-based PET/fMRI/SCR (*N* = 29). Four runs of fear conditioning were completed in the larger and smaller groups (see ***visual fear conditioning paradigm*** for more information on the task itself). Baseline and task PET days were counterbalanced and the inter-scan interval was approximately 24 hours for all participants, with the two scans never done on the same day. An explicit recall task was administered no more than 2 hours after acquisition. A second recall task was administered either in-person or virtually approximately 24 hours after acquisition (**Figure S1**).

The present methodology used to measure dopamine release during fear conditioning differs from prior studies in humans [23, 24]. First, administration of [^{11}C]raclopride with 2 separate bolus scans is the most established design used to quantify dopamine release in the living human brain [25]. Second, the analysis was restricted to the striatum since [^{11}C]raclopride binding is not displaceable elsewhere in the brain [26]. Lastly, we scanned individuals twice and used a task design that maximized the displacement of the tracer during the task PET session which avoids challenges in modeling bolus + constant infusion [27]. The logic is as follows; the first fear acquisition run is completed prior to injection of [^{11}C]raclopride. Under the assumption that fear acquisition releases dopamine, then this will prevent [^{11}C]raclopride from binding at injection time. Then, three more runs of fear

conditioning are conducted to continually displace [^{11}C]raclopride, as the learning of new CS-US pairings will also elicit dopamine release. In total, participants form four CS-US pairings. Thus, detection of dopamine release during fear acquisition is maximized with these considerations [28].

Participants

The study protocol was approved by The Royal Ottawa Healthcare Group Research Ethics Board (REB #: 2019003) and Declaration of Helsinki. All participants gave a written informed consent before entering the study. Control participant status was confirmed using the MINI International Neuropsychiatric Interview for the DSM-5 [29]. Control participants with severe medical illness, head trauma resulting in unconsciousness, current psychiatric illness including substance use disorders, past psychosis, positive urine drug test, and/or contraindications for MRI scanning were excluded from the study. FDRs were recruited in collaboration with psychiatrists at the ROMHC and through print advertisements in the community. FDR status was confirmed using the Family Interview for Genetic Studies - Psychosis Checklist [30] and confirmation of the proband's diagnosis through electronic medical records when possible. Two FDR participants screened positively for a current mental health disorder (one with social anxiety disorder and the other with generalized anxiety disorder). Although they screened positively, these two FDRs were included in the study. They were not taking any medication to treat their disorders.

Visual fear conditioning paradigm

The current paradigm consisted of a fear acquisition session, followed by two fear recall sessions [31]. The acquisition phase consisted of four runs (1932 s total; 483 s/ea) during which the CS+ and CS– stimuli were presented 20 and 14 times each, respectively, (34 total presentations; 4 s/ea) in pseudorandom order with a jittered inter-trial interval (range = 6–15 seconds). The CS+ was followed by the unconditioned stimulus (US; an electric shock to the ankle) in 30% of the trials (6/20 presentations), whereas the CS– was never followed by a shock. Thus, participants observed an equal number of nonreinforced CS+ and CS- stimuli in each run. Participants were told that each face stimulus may or may not be followed by an electrical shock, and were asked to recall which faces were followed by a shock after the experiment. The US (0.5 seconds in duration) was generated and delivered using a Coulbourne electric stimulator (Coulbourne Instruments, Allentown, PA) via a cable attached to the left ankle, 0.1 s prior to removal of the CS+. About 30 minutes prior to the scan, the intensity of the US was set by each participant at a level that was "highly annoying but not painful". Afterwards, participants were asked to recall the faces associated with the shock (CS+) approximately 2 and 24 hours after the fear conditioning session (*see* ***explicit recall task***).

Skin conductance recordings (SCR)

SCR were acquired during the fear conditioning task using two MRI-compatible electrodes placed on the participant's left palm. SCR were measured using a BIOPAC MP160 acquisition system (BIOPAC Systems Inc, Goleta, CA) equipped

with an EDA100C MRI amplifier. The SCR were collected at a gain of 5 µS/V, using a 1 Hz low pass filter during acquisition, then digitised at 200 Hz. The data were further filtered with a 3 Hz finite impulse response low pass filter, using the AcqKnowledge software package (BIOPAC Systems Inc, Goleta, CA). Stimulus presentations of CS+US, CS+ and CS- were time-stamped onto the SCR recordings using the LabJack u3-LV (LabJack Corporation, Lakewood, CO) digital-to-analogue converter.

Explicit recall task examining contingency memory

At the end of the fear conditioning task, participants were transferred into a separate procedure room where they completed an explicit recall task immediately after the experiment, no more than two hours after the last fear conditioning run. Participants were shown the four CS+, four CS-, and two novel faces and were asked to rate faces two times per face, in random order (a total of 20 ratings). For each face, participants were asked the following question: “How likely was this face paired with a shock?”. Participants rated the faces using a 4-point Likert scale; 1 = “very unlikely”, 2 = “somewhat unlikely”, 3 = “somewhat likely”, 4 = “very likely”. Participants repeated the same explicit recall task approximately 24 hours after fear acquisition.

PET/MR Image acquisition

Images were acquired using a 3T mMR Biograph PET-MR system with a 12-channel head coil (Siemens, Erlangen, Germany). T1-weighted images were acquired using an multiecho MPRAGE sequence[32]; spatial resolution = 1 mm isotropic; matrix = 256 x 256, number of slices = 192, repetition time (TR) = 2500 ms, echo time (TE) = 1.69, 3.55, 5.41, and 7.27 ms, flip angle = 7 degrees. T2*-weighted (functional MRI) images were acquired during the fear conditioning task; spatial resolution = [3 x 3 x 3.21 mm], matrix = 64 x 64, number of slices = 210, TR = 2300 ms, TE = 28 ms, flip angle = 80 degrees.

[^{11}C]raclopride PET acquisition

PET images were acquired once during baseline and once during the fear conditioning task; spatial resolution = [4.17 x 4.17 x 2.03 mm]; target injected dose = 300 MBq of [^{11}C]raclopride (bolus), number of sinograms = 2540, scan time = 60 minutes. All 58 [^{11}C]raclopride injections (N = 29) were administered between 11:00 and 15:00 (one scan per participant per day); 23 of 29 completed experiments are no more than one day apart, four experiments were completed two days apart and two experiments completed were eight to nine days apart.

MR preprocessing

Results included in this manuscript come from preprocessing performed using fMRIPrep 24.0.0 (Esteban et al. (2019); Esteban et al. (2018); RRID:SCR_016216), which is based on Nipype 1.8.6 (K. Gorgolewski et al. (2011); K. J. Gorgolewski et al. (2018); RRID:SCR_002502). To note, sessions one and two were analysed separately, and the boilerplate was modified to include the correct number of scans

(see ***supplementary methods***). All parameters are exactly the same between sessions.

Task-based fMRI analysis

Fully preprocessed BOLD images were post-processed using Nilearn 0.11.1 (RRID:SCR_001362 [33]) in python 3.11.9. Briefly, a first-level model was constructed with CS+, CS-, and CS+ shock events and a 'simple' confound strategy to fit a glover haemodynamic response function [34]. Afterwards, effect size contrast maps were computed per run, per participant: fear contrast (CS+ versus CS-). A total of four contrast images were computed, then averaged together to generate a single contrast map per participant. Then, the Glasser [35] and Tian atlases [36] were used to extract contrast beta values per parcel (196 parcels; 180 cortical and 16 subcortical parcels bilaterally).

PET preprocessing

For each of two 60-minute dynamic PET runs found per participant (across scanning sessions), the following preprocessing was performed. Attenuation correction was calculated using the pseudoCT method, which is an MR-based (T1w) technique to generate μ-maps [37]. Subsequently, PET images were reconstructed with the μ-map applying 3 mm Gaussian smoothing, grouped into 1-minute bins (60 frames per image) to allow for minute-by-minute motion correction. For the remainder of the PET preprocessing analysis, the PETsurfer pipeline was used [38, 39]. First, head motion correction [FreeSurfer mc-afni2] was applied to the reconstructed PET image, and the resulting motion-corrected image was used to generate a summed template volume for co-registration to the T1w [FreeSurfer mri_concat; [40]]. The PET template image was then co-registered to the T1w reference [FreeSurfer mri_coreg] and the resulting transformation matrix was applied to the PET image [FreeSurfer mri_vol2vol]. Finally, the T1w reference was co-registered to MNI152nlin6asym space [FreeSurfer mni152reg] and the transformation matrix was applied to the PET image in T1w space [FreeSurfer mri_vol2vol]. The resulting image is a PET scan in MNI152nlin6asym space with 60 motion-corrected frames.

PET analysis

A total of 58 [^{11}C]raclopride scans were collected (N = 29). There was no difference in the injected dose (paired-samples t-test: $t_{(28)}$ = 2.034, p = .0515) or injected molar activity (paired-samples t-test: $t_{(28)}$ = 0.8575, p = .3985) between the baseline session (dose: μ = 302.76 MBq, SD = 33.63; molar activity: μ = 1447.5 mCi/umol, SD = 839.64) and task session (dose: μ = 286.99 MBq, SD = 27.31; molar activity: μ = 1299.9 mCi/umol, SD = 526.89). D_2R BP_{ND} was quantified with multi-linear reference tissue model 2 (MRTM2) [41] using a custom FreeSurfer/kinfitr pipeline [ROI-wise] [38, 39, 42]. D_2R BP_{ND} is defined as the concentration of target protein ($D_{2/3}$ receptors) in the specifically bound compartment, relative to the non-displaceable compartment. ROIs were delineated using an unbiased striatal atlas [36] using the S2 level of granularity (each ROI >298 voxels). Then, average time-activity curves were generated for each striatal ROI (FreeSurfer mri_binarize & mri_segstats). The

time-activity curves were inputted to the software package kinfitr for the kinetic modeling of D_2R BP_{ND} [42]. Because we do a minute-by-minute motion correction, we only excluded participants that produced less than excellent goodness-of-fit in the kinetic modelling (less than $R^2 < 0.80$). This resulted in one exclusion, and a total of 28 individuals for the final analysis (16 CTR/12 FDR). Importantly, participant motion did not differ between baseline and fear conditioning sessions (N = 28, paired-samples t-test: $t_{(27)} = -0.691$, $p = 0.495$). MRTM2 goodness-of-fits using the Tian S2 atlas remained above 0.8 (range of $R^2 = 0.84 – 0.99$) only when the nucleus accumbens shell and core were combined into a single ROI; otherwise, R^2 values failed to reach this standard. Thus, to balance accurate BP_{ND} estimates and retain granularity, all of our primary analyses use a total of five striatal ROIs: nucleus accumbens, anterior caudate, anterior putamen, posterior caudate and posterior putamen. Finally, $\%\Delta D_2R$ BP_{ND}, our index of dopamine release, was calculated using the following equation:

$$\%\Delta BP_{ND} = [\frac{(BP_{ND}task - BP_{ND}baseline)}{BP_{ND}baseline}] \times 100$$

Statistical analysis

All statistical analyses were conducted in R v4.5.1. Linear mixed effects models and subsequent marginal means were conducted and then extracted using the ‘nlme’ package. Then marginal means were inputted for post-hoc comparisons using the ‘emmeans’ package. Correlations were done using the native R ‘cor’ function. Ordinary least squares (OLS) regressions were done using the native R ‘lm’ function. All post-hoc comparisons were corrected using False Discovery Rate (FDR). All plots were made using seaborn v0.13.2 [43]. All cortical and subcortical visualizations were made using surfplot v0.2.0 [44] and subcortex_visualization v0.1.12 [45].

Results

Dopamine is released in the striatum during fear conditioning in humans

Prior to characterizing fear-elicited dopamine release in those with a family history of psychosis, we sought to quantify dopamine release in individuals without a family history. Sixteen individuals without a family history of psychotic disorders (N = 16) completed the Pavlovian fear acquisition task over four runs. Age, sex, injected tracer dose, injected molar activity, motion during the PET scan, US shock intensity, self-reported subclinical symptoms and behavioural fear responses of this control group are presented in **Table 1** and **Table S1**.

Table 1. This study includes two groups of participants: a simultaneous PET/fMRI group (*N* = 28) and a second fMRI only group that completed the same task without PET (*N* = 46) that was combined for fMRI analysis (*N* = 74).

	Simultaneous PET/fMRI (N = 28)			**fMRI (N = 74)**		
	CTR n = 16	**FDR n = 12**	**test**	**CTR n = 50**	**FDR n = 24**	**test**
Age (SD)	33 (9.8)	33 (11)	$t_{(26)} = 0.03$, p = .97	30 (8.5)	32 (9.0)	$t_{(72)} = -0.71$, p = .48
Sex (male)	9/16 (56.3%)	7/12 (58.3%)	$X^2 < 0.01$, p = 1.0	26/50 (52%)	12/24 (50%)	$X^2 < 0.01$, p = 1.0
US (SD) [mA]	2.7 (0.95)	2.9 (1.04)	$t_{(26)} = 0.48$, p = .63	2.2 (0.98)	2.7 (1.0)	$t_{(72)} = 2.0$, p = .04
Baseline dose (SD) [MBq]	300 (42)	310 (19)	$t_{(26)} = 1.04$, p = .31			
Task dose (SD) [MBq]	280 (31)	290 (22)	$t_{(26)} = 1.08$, p = .29			
Baseline MA (SD) [mCi/umol]	1600 (1100)	1300 (410)	$t_{(26)} = -0.67$, p = .51			
Task MA (SD) [mCi/umol]	1300 (420)	1300 (680)	$t_{(26)} = 0.28$, p = .78			
Baseline FD (SD) [mm]	1.6 (0.64)	1.5 (0.50)	$t_{(26)} = -0.74$, p = .46			
Task FD (SD) [mm]	1.6 (0.81)	1.6 (0.66)	$t_{(26)} < 0.01$, p = .99			

Note: Demographics (age and sex), the average of four runs of unconditioned stimulus (US) ankle shock intensity in milliamperes (mA) during the fear conditioning session are reported separately for the simultaneous PET/fMRI and combined fMRI only group. Furthermore, the injected dose of the radioligand in megabecquerels (MBq), the injected molar activity (MA) of the radioligand in millicuries per micromole (mCi/umol) and the average framewise displacement (FD; a metric of motion) in millimetres (mm) during the baseline and fear conditioning sessions, are reported for the combined PET/fMRI group. In the combined PET/MR group (*N* =28, 16 CTRs, 12 FDRs), there were no significant differences between control (CTR) and first-degree relative (FDR) participants in age, sex, US shock intensity, injected baseline and task doses/molar activity, or motion on baseline and task day as indexed by FD. In the

larger fMRI-only group (*N* =74, 50 CTRs, 24 FDRs), CTR and FDR participants did not differ significantly in age or sex, but the US shock intensity significantly differed.

Dopamine release is quantified as a percent change in dopamine $D_{2/3}$ receptor binding potential (%ΔD_2R BP_{ND}) between the baseline scan and the scan during the Pavlovian fear conditioning paradigm (see *methods* and **Figure S1A**). First, we examine D_2R BP_{ND} in a session by region analysis because striatal-projecting dopamine neurons respond differently to fear versus reward [46–49]. We find that the fear conditioning task leads to the release of dopamine in the posterior caudate (n = 16, μ = 0.116, SE = 0.044, $t_{(75)}$ = 2.626, p = .011 p_{FDR} = .032) and posterior putamen (n = 16, μ = 0.112, SE = 0.044, $t_{(75)}$ = 2.549, p = .013 p_{FDR} = .032) of the striatum in CTRs (**Figure 1a,b; Table S2**).

We then examine the link between dopamine release and neural activity. During the fear conditioning two stimuli are presented: the conditioned stimulus (CS+) which is partially reinforced with an unconditioned shock stimulus (US), signalling fear, and a second stimulus that is never reinforced (CS-), signalling safety (see *methods*). We observe an association between %ΔD_2R BP_{ND} and fMRI activation (BOLD response to the contrast of CS+ vs CS-) in the posterior caudate (n = 16, r = -0.607, p = .013, p_{FDR} = .025; **Figure 1c**) but not the posterior putamen (n = 16, r = -0.369, p = .159; data not shown). In summary, the largest magnitude of phasic dopamine release occurs in the posterior caudate during fear acquisition and is associated with BOLD activity in the same region.

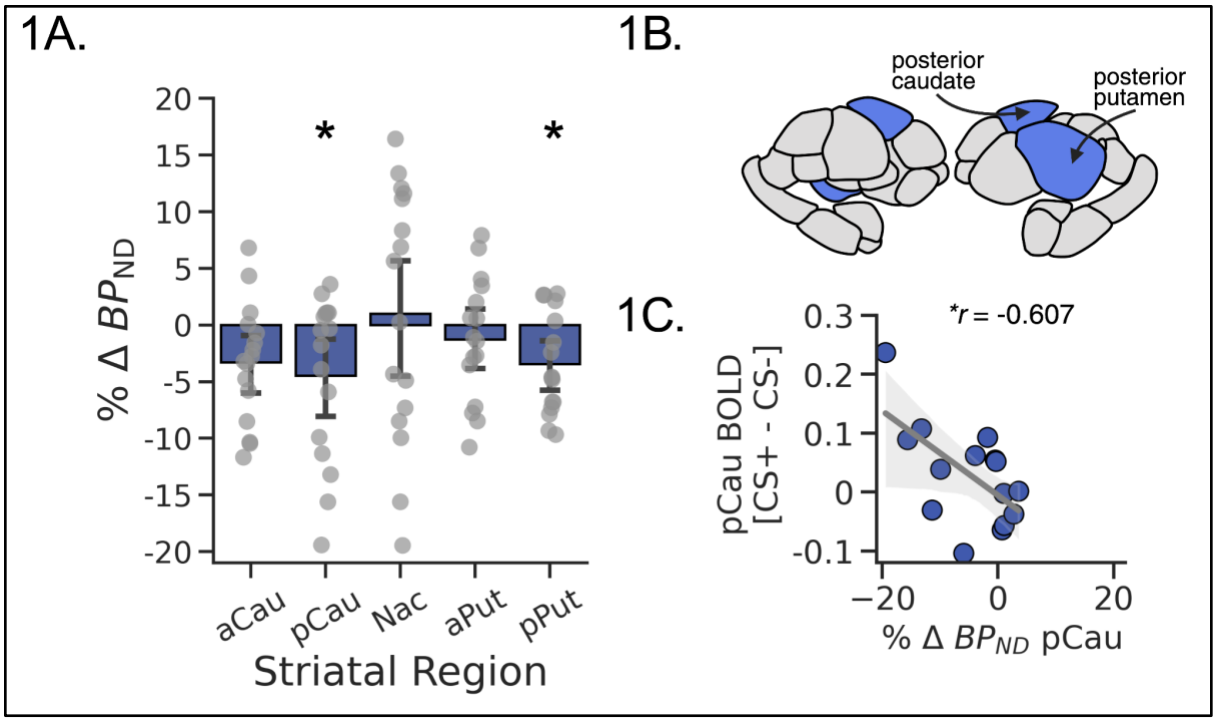

Figure 1. Dopamine is released in the posterior caudate and posterior putamen during fear conditioning in humans. **a.** A linear mixed effects model is used to determine dopamine release. The model included region and session as fixed

effects, as well as region and participant as crossed random effects. Post-hoc comparison of regions between sessions reveal D_2R BP_{ND} in the posterior caudate and putamen are significantly decreased during fear conditioning (n = 16, μ = 0.112-0.116, SE = 0.042, $t_{(75)}$ = 2.55-2.62, p_{FDR} = .032 [baseline - fear conditioning D_2R BP_{ND}]; bar plots with error bars indicate mean %Δ $D_2R BP_{ND}$ ± 95% CI, dot plots represent individual values). **b.** Dopamine is released in the posterior striatal regions (Tian S2 atlas). **c.** Dopamine release in the posterior caudate is associated with greater BOLD signal to the CS+ relative to the CS- (n = 16, Pearson's correlation: r = -0.607, p = .013, p_{FDR} = .025; regression line indicates slope ± 95% CI, scatter plot represents individual values). aCau = anterior caudate; pCau = posterior caudate; Nac = Nucleus accumbens; aPut = anterior putamen, pPut = posterior putamen; %Δ BP_{ND} = percent change in binding potential. * = significant p-value.

Adaptive dopamine release is blunted during fear acquisition in first-degree relatives

To determine if those with an FDR with a psychotic disorder differentially release dopamine during fear acquisition, we compared data from 16 control participants and 12 FDR participants after excluding one FDR for excess motion that compromised the PET kinetic fits (see *methods*) (see **Table 2** for proband information). A linear mixed effects analysis was conducted to examine the interaction between group and striatal region on %ΔD_2R BP_{ND}. We find that during fear conditioning, FDR participants release significantly less dopamine in the posterior caudate (n = 28, μ = 7.047%, SE = 2.762%, $t_{(26)}$ = 2.551, p = .017, p_{FDR} = .034), but not the posterior putamen (n = 28, μ = 5.099%, SE = 2.762%, $t_{(26)}$ = -1.846, p = .076) (**Figure 2a,b; Table S3**). To determine if dopamine release is associated with striatal BOLD responses, we also conducted a regression using %ΔD_2R BP_{ND} and group as predictors. We further show that even when controlling for family history of a psychotic disorder, %ΔD_2R BP_{ND} is associated with greater BOLD response to the contrast of CS+ vs CS- (n = 28, group: β = -0.067, SE = 0.035, $t_{(25)}$ = -1.918, p = .067; %ΔD_2R BP_{ND}: β = -0.005, SE = 0.002, $t_{(25)}$ = -2.652, p = .014) (**Figure 2c**). Importantly, change of participant motion between sessions did not correlate with %ΔD_2R BP_{ND} in the posterior caudate or putamen (N = 28, Pearson's correlation: all r < 0.15, all p > 0.44; data not shown). Furthermore, this reduction in dopamine release is not due to between-group differences in US shock intensity, injected dose, baseline D_2 BP_{ND}, or motion. Likewise, behavioural learning as indexed by skin conductance recordings during fear acquisition and explicit recall, is not different between FDR and CTR groups of the combined PET/fMRI experiment (**Table 1; Table S1; Table S4**). However, we did find modest differences in fMRI responses in the amygdala and visual association areas in the larger CTR and FDR groups (**Table S8**).

Table 2. Proband relationship status and diagnosis.

	Simultaneous PET/fMRI (N = 12)	**fMRI (N = 24)**
Relationship (Sibling/Parent/Both)	6/6/0	10/13/1
Diagnosis (SCZ/SA/BP/PNOS)	7/1/0/3	15/5/2/3

Note: The FDR with both a parent and sibling affected by psychosis contributes 2 individuals to the diagnosis count. SCZ = schizophrenia; SA; schizoaffective disorder; BP; bipolar with psychosis; PNOS; psychosis not otherwise specified.

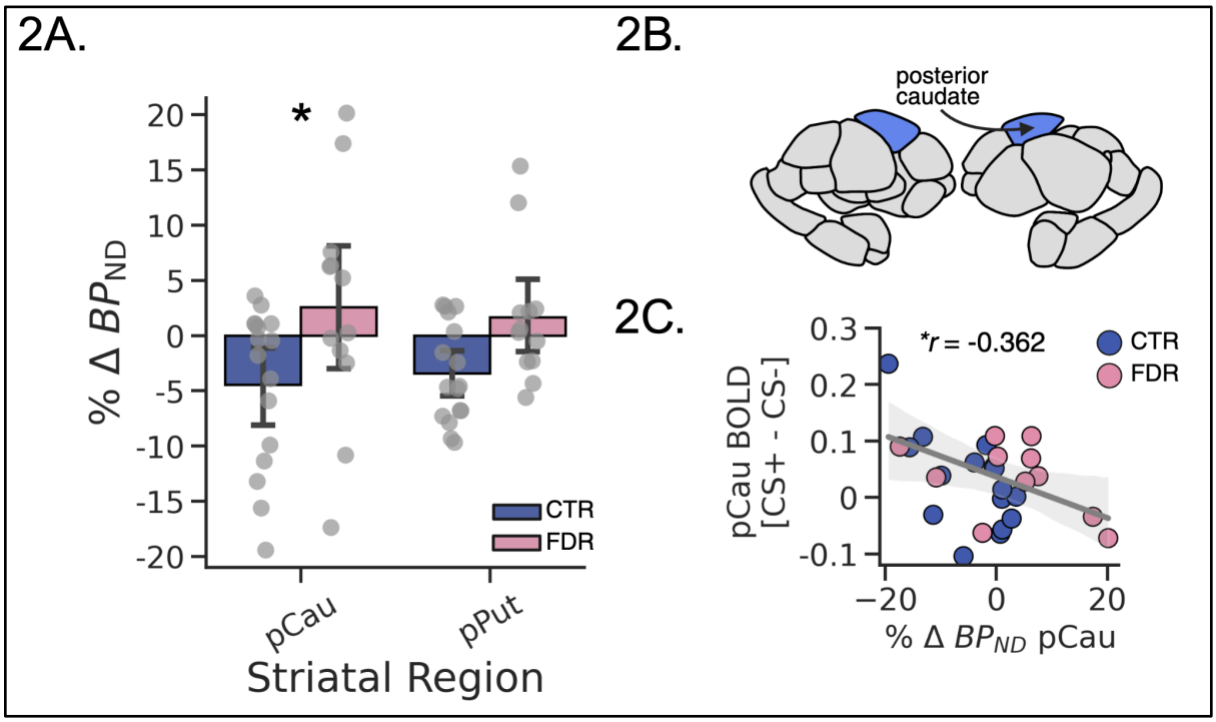

Figure 2. Dopamine release in the posterior caudate is reduced in FDR participants compared to CTRs. **a.** A linear mixed effects model is used to determine differences in dopamine release between FDR and control participants. The model included region and session as fixed effects, and region nested within-participants as a random effect. Post-hoc comparisons indicate that %ΔD_2R BP_{ND} in the posterior caudate is significantly reduced during fear acquisition (n = 28, μ = 7.047%, SE = 2.762%, $t_{(26)}$ = 2.551, p = .017, p_{FDR} = .034 [FDR - CTR ΔD_2R BP_{ND}]; bar plots with error bars indicate mean %ΔD_2R BP_{ND} ± 95% CI, dot plots represent individual values), **b.** Illustration of the localization of the group difference in the posterior caudate (Tian S2 atlas). **c.** Dopamine release in the posterior caudate is associated with greater BOLD signal to the CS+ relative to the CS- in the whole group when correcting for family history of a psychotic disorder (n = 28, regression model, group: β = -0.067, SE = 0.035, $t_{(25)}$ = -1.918, p = .067; %ΔD_2R BP_{ND}: β = -0.005, SE = 0.002, $t_{(25)}$ = -2.652, p = .014; regression line indicates slope ± 95% CI, scatter plot

represents individual values). pCau = posterior caudate; pPut = posterior putamen; %ΔBP_{ND} = percent change in non-displaceable binding potential. * = significant *p*-value.

Lack of adaptive dopamine release is associated with more paranoid thinking but not with anhedonia

We next examine whether adaptive dopamine release is associated with measures of subclinical positive and negative symptoms, as predicted by the chaotic dopamine hypothesis [19]. Subclinical anhedonia, a negative symptom of schizophrenia, is measured here with the Temporal Experience of Pleasure Scale (TEPS) [50]. We measure subclinical paranoia, a positive symptom, with the Paranoia Checklist (PCL) [51]. We see that a lack of adaptive dopamine release in the posterior caudate is associated with higher PCL total scores even when taking family history of psychosis into account (n = 28, %ΔD_2R BP_{ND} β = 0.004, SE = 0.002, $t_{(25)}$ = 2.074, p = .049; group: β = -0.043, SE = 0.033, $t_{(25)}$ = 1.257, p = .22). The association between fear learning and paranoia is driven by higher frequency of self-reported paranoid thoughts, but not conviction or distress subscores (N = 28, %ΔD_2R BP_{ND} β = 0.003, SE = 0.001, $t_{(25)}$ = 2.199, p = .037; group: β = -0.008, SE = 0.024, $t_{(25)}$ = -0.334, p = .741) (**Figure 3a**) (**Table S9**). In an exploratory analysis, a lack of adaptive dopamine release in the posterior putamen is also associated with a higher PCL total score (N = 28, %ΔD_2R BP_{ND} β = 0.008, SE = 0.003, t(25) = 2.806, p = .009; group: β = -0.057, SE = 0.033, $t_{(25)}$ = 1.727, p = .097) and a higher frequency score (N = 28, regression model: %ΔD2R BP_{ND} β = 0.006, SE = 0.002, $t_{(25)}$ = 2.866, p = .008; group: β = 0.002, SE = 0.023, $t_{(25)}$ = 0.076, p = .940) (**Figure 3b**). This link between fear learning and paranoia is further supported in a larger sample that completed the same task without PET, where lower explicit ratings of the threatening CS+ faces, but not the safe CS- faces, also predicted higher PCL frequency subscores (n = 74, CS+: β = -0.024, SE = 0.011, $t_{(71)}$ = -2.041, p = 0.045; CS-: β = -0.003, SE = 0.012, $t_{(71)}$ = -0.259, p = .789) (**Figure 3c**). In contrast, associations with the TEPS were not supported. That is, we did not find an association between dopamine release in the posterior caudate and self-reported anhedonia, as %ΔD_2R BP_{ND} was unrelated to total, anticipatory, or consummatory subscores on the TEPS (**Table S9**). Altogether, our behavioral results suggest that a lack of adaptive dopamine release during fear learning is associated specifically with the frequency of paranoid thoughts.

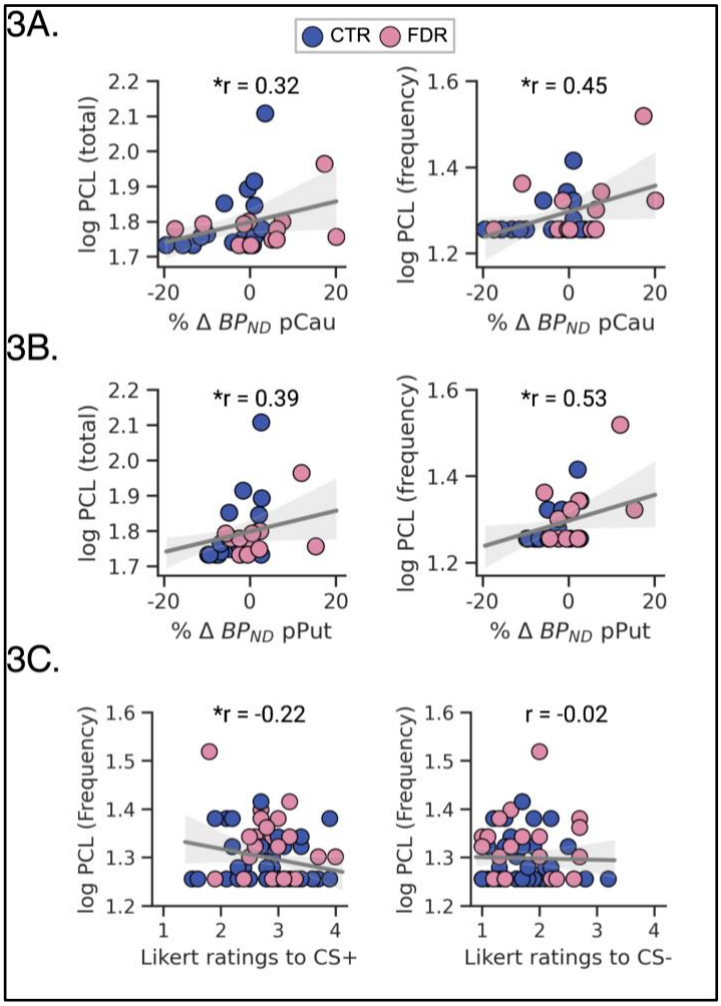

Figure 3. Lack of dopamine release and poor learning about the CS+ predict PCL frequency scores. **a.** Lack of dopamine release in the posterior caudate is associated with the PCL total score (N = 28, regression model: %ΔD_2R BP_{ND} β = 0.004, SE = 0.002, $t_{(25)}$ = 2.074, p = 0.049; group: β = -0.043, SE = 0.033, t(25) = 1.257, p = 0.22) and frequency of paranoid thinking (N = 28, regression model: %ΔD_2R BP_{ND} β = 0.003, SE = 0.001, $t_{(25)}$ = 2.199, p = .037; group: β = -0.008, SE = 0.024, $t_{(25)}$ = -0.334, p = .741). **b.** Lack of dopamine release in the posterior putamen is associated with the PCL total score (N = 28, regression model: %ΔD_2R BP_{ND} β = 0.008, SE = 0.003, $t_{(25)}$ = 2.806, p = .009; group: β = -0.057, SE = 0.033, $t_{(25)}$ = 1.727, p = .097) and frequency of paranoid thinking (N = 28, regression model: %ΔD_2R BP_{ND} β = 0.006, SE = 0.002, $t_{(25)}$ = 2.866, p = .008; group: β = 0.002, SE = 0.023, $t_{(25)}$ = 0.076, p = .940). **c.** Paranoid thinking is predicted by Likert ratings of the CS+ (n = 74, regression model for CS+ on day 1: β = -0.024, SE = 0.011, $t_{(71)}$ = -2.041, p = .045) but not Likert ratings of the CS- (n = 74, regression model for CS- on day 1: β = -0.003, SE = 0.012, $t_{(71)}$ = -0.259, p = .789). pCAU = posterior caudate; pPUT = posterior putamen; * = significant p-value.

Baseline D_2Rs but not dopamine release is associated with fear recall

We also examined whether adaptive dopamine release is associated with behavioural indices of fear conditioning. We did not see an association between dopamine release and autonomic responding (skin conductance) or explicit recall (**Table S9**). We also conducted an exploratory analysis between baseline D_2Rs and these same indices of fear conditioning. Unlike dopamine release, baseline D_2Rs in the posterior caudate are associated with better recall of the CS+ relative to the CS- (N = 28, regression model: D_2R BP_{ND} β = 0.606, SE = 0.218, $t_{(52)}$ = 2.777, p = 0.008; group: β = 0.083, SE = 0.183, $t_{(52)}$ = 0.454, p = 0.65; day: β = -0.103, SE = 0.177, $t_{(52)}$ = -0.579, p = 0.56). However, baseline D_2Rs in the posterior caudate are not associated with greater skin conductance towards CS+ relative to CS- (N = 28, regression model: D_2R BP_{ND} β = 0.046, SE = 0.071, $t_{(25)}$ = 0.648, p = 0.523; group: β = 0.067, SE = 0.822, $t_{(25)}$ = 0.082, p = 0.94). In summary, we show that baseline measurements of D_2Rs in the whole group are associated with better fear discrimination during recall.

Discussion

Here, we first show that in humans, fear conditioning releases dopamine in the striatum using [^{11}C]raclopride PET. This dopamine release is greatest in the posterior caudate and is proportional to neural activation in the same region measured as BOLD contrast between responses to CS+ and CS- stimuli. Using this paradigm, we then test the chaotic dopamine hypothesis of schizophrenia. We find that dopamine release is blunted during fear conditioning in people with a family history of a psychotic disorder. The blunted dopamine release is not associated with any differences in fear learning, nor did we find any learning differences between those who had a family history and those who did not. In the whole group, blunted dopamine release is associated with greater paranoia , but not with anhedonia. Altogether, we provide the first evidence for the impairment in adaptive striatal dopamine release in first-degree relatives of individuals with a psychotic disorder and those who experience subclinical paranoid thoughts.

We report dopamine release in the posterior caudate and putamen during fear acquisition. This finding aligns with rodent studies showing dopamine release in the rodent analogue (striatal tail), a region known to generate a dopamine prediction error that drives fear acquisition, but not recall [48, 49, 52–55]. Our finding contrasts with the few available human studies, potentially due to methodological differences like measurement timing (fear acquisition vs. recall), tracer choice, and experimental design [23, 24]. While one study observed indiscriminate striatal dopamine release, our findings highlight subregion-specific release within the posterior caudate, supported by correlations between %ΔD_2R BP_{ND} and fMRI activations. This is further supported by a rodent study that reported concurrent dopamine release and striatal neural activity during fear acquisition [55]. In summary, our study is the first to demonstrate dopamine release in two dorsoposterior striatal areas during fear acquisition in humans.

We find reduced task-based dopamine release in the posterior caudate in a group with a family history of psychotic disorders. There are three previous PET only studies on task-induced dopamine release in psychotic disorders that found a lack of cortical dopamine release during a working memory task and increased nigrostriatal dopamine release during acute nonspecific stress [56–58]. However, none of those studies assessed adaptive dopamine release in the striatum. Here, using a simultaneous PET/fMRI design, we present the first *in vivo* evidence of reduced adaptive dopamine release in those with an FDR with a psychotic disorder. We see that the difference in dopamine release between groups is not due to differences in fear learning or engagement on the task, as behavioural indices of learning were not different between those with and without a first degree relative with a psychotic disorder. Given that tonic dopamine release constitutes a small fraction (approximately 0.01%) of the total dopamine released in the synaptic cleft [59, 60], the absence of a detectable change in D_2 BP_{ND} likely indicates a deficiency in adaptive, stimulus-driven dopamine release in response to the CS+, rather than an increase in baseline tonic dopamine release. Furthermore, we found no evidence for baseline D_2 BP_{ND} differences between the two groups. Altogether, these findings support the chaotic dopamine hypothesis by demonstrating a reduction in adaptive dopamine release [19].

On the other hand, we found that a decrease in adaptive dopamine release and poor recall of the CS+ are linked to subclinical, self-reported paranoid thinking, but not to anhedonia. Paranoid thoughts are common in the general population, and paranoia is one of the most heritable symptoms in schizophrenia, often emerging early in the development of psychosis [51, 61−64]. Because delusions, like paranoia, are thought to arise from chaotic and out-of-context dopamine release, our finding of reduced adaptive dopamine release correlating with paranoia contrasts with a subcomponent of the chaotic dopamine hypothesis of schizophrenia [19]. Indeed, lack of adaptive dopamine release may lead to the emergence of paranoid delusion, which may help explain why antipsychotics are generally not effective in preventing psychosis in those at clinical high risk [65].

Previous research has shown that tonic increases in dopamine signaling are linked to positive symptoms [66–70]. In contrast, reduced adaptive dopamine release, especially towards rewards, is postulated to be related to negative symptoms [19]. A potential pitfall of current dopaminergic theories of schizophrenia (and psychotic disorders) is that they are primarily based on reward learning tasks that typically target the ventral striatum. Yet, it is currently thought that dopaminergic dysregulation in these disorders is more prominent in the dorsal, associative, and sensorimotor striatal areas [11, 71, 72]. Therefore, it is worth noting that the dopamine dysregulation observed in our study is located in the posterior area of the dorsal striatum, an area involved in integrating both sensory and reward prediction errors (Fritsche et al. 2026). Fear conditioning might thus be a valuable paradigm for studying dopaminergic dysregulation in psychotic disorders, potentially contributing

to the refinement of existing theories and our understanding of symptom emergence. We propose that inefficiencies in fear learning, possibly mediated by subcortical reductions in phasic dopamine release, might contribute to the development of positive symptoms, like paranoia. One possibility is that a distorted dopamine-reinforced probabilistic map of future risks and rewards might allow less probable explanations to take hold, leading to paranoia [73, 74].

Interestingly, although dopamine release is not associated with behavioural indices of fear learning in the current study, we demonstrate an association with increased baseline D_2Rs and better fear discrimination at recall, irrespective of FDR status. Indeed, silencing Adora+ (putative D_2R expressing) tail of striatum neurons increased fear behaviour in the absence of a learned CS [54]. Furthermore, raclopride administration (at pharmacological, not tracer, doses) immediately after fear acquisition reduced fear discrimination at recall [75]. Together, these preclinical studies suggest D_2Rs in the posterior striatum are essential for computing the appropriate behavioural response towards a CS. Our finding further strengthens this view by demonstrating an association between D_2R availability in the living human brain and fear discrimination recall, both a few hours after fear acquisition and one day later.

This study is not without limitations. First, despite including 56 [^{11}C]raclorpide PET/fMRI scans, our sample size remains modest. Associations between brain activations and behaviour are notoriously difficult to detect and this might explain why we did not detect a link between dopamine release and other fear-related measures [76]. Second, we studied first-degree relatives of individuals with schizophrenia and psychotic disorders and not those individuals themselves. While evidence suggests that the dopamine system is similarly affected in first-degree relatives, future studies should still attempt to test the chaotic dopamine hypothesis in unmedicated individuals with psychotic disorders.

In summary, we show dopamine release in the tail of the striatum of humans during discriminative fear acquisition, and a reduction of this release in the first-degree relatives of those with psychotic disorders. This deficient release is not explained by group differences in fear learning; instead, dopamine release is correlated inversely with self-reported paranoia but not anhedonia. Poor performance on the explicit recall task, reflected by lower Likert ratings towards the shock-paired stimulus (CS+), also correlates inversely with self-reported paranoid thinking. We believe these findings support the hypothesis that lack of stimulus-driven dopamine release, here observed subcortically, may be a component of schizophrenia and psychotic disorders. In conclusion, fear conditioning emerges as a valuable paradigm for investigating dopamine dysregulation in psychosis, offering avenues for refining existing theories and providing a deeper understanding of how psychotic symptoms arise.

Supplementary Methods

Anatomical data preprocessing

A total of two T1-weighted (T1w) (one T1w ses-001; one T1w ses-002) images are found within the input BIDS dataset. The T1w image is corrected for intensity non-uniformity (INU) with N4BiasFieldCorrection (Tustison et al. 2010), distributed with ANTs 2.5.1 (Avants et al. 2008, RRID:SCR_004757), and used as T1w-reference throughout the workflow. The T1w-reference is then skull-stripped with a Nipype implementation of the antsBrainExtraction.sh workflow (from ANTs), using OASIS30ANTs as target template. Brain tissue segmentation of cerebrospinal fluid (CSF), white-matter (WM) and gray-matter (GM) is performed on the brain-extracted T1w using fast (FSL (version unknown), RRID:SCR_002823, [77]). Brain surfaces are reconstructed using recon-all (FreeSurfer 7.3.2, RRID:SCR_001847, [78]), and the brain mask previously estimated is refined with a custom variation of the method to reconcile ANTs-derived and FreeSurfer-derived segmentations of the cortical gray-matter of Mindboggle (RRID:SCR_002438, [79]). Volume-based spatial normalization to two standard spaces (MNI152NLin6Asym, MNI152NLin2009cAsym) is performed through nonlinear registration with antsRegistration (ANTs 2.5.1), using brain-extracted versions of both T1w reference and the T1w template. The following templates are were selected for spatial normalization and accessed with TemplateFlow (24.2.0, [80]): FSL's MNI ICBM 152 non-linear 6th Generation Asymmetric Average Brain Stereotaxic Registration Model [[81], RRID:SCR_002823; TemplateFlow ID: MNI152NLin6Asym], ICBM 152 Nonlinear Asymmetrical template version 2009c [[82], RRID:SCR_008796; TemplateFlow ID: MNI152NLin2009cAsym].

Functional data preprocessing

For each of the eight BOLD runs (three resting-state fMRI ses-001; four task-based fMRI ses-002; one resting state fMRI ses-002) found per participant (across all tasks and sessions), the following preprocessing is performed. First, a reference volume is generated, using a custom methodology of fMRIPrep, for use in head motion correction. Head-motion parameters with respect to the BOLD reference (transformation matrices, and six corresponding rotation and translation parameters) are estimated before any spatiotemporal filtering using mcflirt (FSL, [83]). The BOLD reference is then co-registered to the T1w reference using bbregister (FreeSurfer) which implements boundary-based registration [84]. Co-registration is configured with six degrees of freedom. Several confounding time-series are calculated based on the preprocessed BOLD: framewise displacement (FD), DVARS and three region-wise global signals. FD is computed using two formulations following Power (absolute sum of relative motions [85]) and Jenkinson (relative root mean square displacement between affines [83]). FD and DVARS are calculated for each functional run, both using their implementations in Nipype (following the definitions by [86]. The three global signals are extracted within the CSF, the WM, and the whole-brain masks. Additionally, a set of physiological regressors are extracted to

allow for component-based noise correction (CompCor, [87]). Principal components are estimated after high-pass filtering the preprocessed BOLD time-series (using a discrete cosine filter with 128s cut-off) for the two CompCor variants: temporal (tCompCor) and anatomical (aCompCor). tCompCor components are then calculated from the top 2% variable voxels within the brain mask. For aCompCor, three probabilistic masks (CSF, WM and combined CSF+WM) are generated in anatomical space. The implementation differs from that of Behzadi et al. in that instead of eroding the masks by 2 pixels on BOLD space, a mask of pixels that likely contain a volume fraction of GM is subtracted from the aCompCor masks. This mask is obtained by dilating a GM mask extracted from the FreeSurfer's aseg segmentation, and it ensures components are not extracted from voxels containing a minimal fraction of GM. Finally, these masks are resampled into BOLD space and binarized by thresholding at 0.99 (as in the original implementation). Components are also calculated separately within the WM and CSF masks. For each CompCor decomposition, the k components with the largest singular values are retained, such that the retained components' time series are sufficient to explain 50% of variance across the nuisance mask (CSF, WM, combined, or temporal). The remaining components are dropped from consideration. The head-motion estimates calculated in the correction step are also placed within the corresponding confounds file. The confounding time series derived from head motion estimates and global signals are expanded with the inclusion of temporal derivatives and quadratic terms for each [88]. Frames that exceeded a threshold of 0.5 mm FD or 1.5 standardized DVARS are annotated as motion outliers. Additional nuisance time series are calculated by means of principal components analysis of the signal found within a thin band (crown) of voxels around the edge of the brain [89]. The BOLD time-series are resampled onto the following surfaces (FreeSurfer reconstruction nomenclature): fsaverage5. All resamplings can be performed with a single interpolation step by composing all the pertinent transformations (i.e. head-motion transform matrices, susceptibility distortion correction when available, and co-registrations to anatomical and output spaces). Gridded (volumetric) resamplings are performed using nitransforms, configured with cubic B-spline interpolation. Non-gridded (surface) resamplings are performed using mri_vol2surf (FreeSurfer).

Many internal operations of fMRIPrep use Nilearn 0.10.4 (RRID:SCR_001362 [33]), mostly within the functional processing workflow. For more details of the pipeline, see the section corresponding to workflows in fMRIPrep's documentation.

Supplementary Results

The visual fear discrimination paradigm elicits fear responses but these do not differ between groups

Before examining differences in fear learning between controls and FDRs, the expected learning in the combined PET/fMRI group (N = 28) and the larger fMRI group (N = 74) are first confirmed. Here, we examine if the fear conditioning task

elicited greater skin conductance responses to the CS+, correct recall of the CS+ and typical fMRI responses during fear conditioning across all four runs of fear acquisition using linear mixed effect models. Indeed, expected skin conductance responses, Likert ratings during explicit recall and fMRI responses towards the CS+ are confirmed (**Figure S2; Tables S5, S6**). Reaction times during explicit ratings did not differ between CS+ and CS- (**Figure S2; Table S7**). Next, we find no between-group differences in skin conductance recordings and the explicit recall task (**Tables S5, S6, S7**). Thus, differences in behavioural indices of fear expression between groups do not explain differences in dopamine release between the groups. Finally, we examine between-group differences in the CS+ versus CS- fMRI BOLD responses using the Glasser atlas for the extraction of cortical ROIs and the Tian S2 atlas for the extraction of subcortical ROIs. An exploratory linear mixed effects model reveals several higher order visual and associative areas are differentially activated in controls versus FDRs, as well as the medial amygdala (**Table S8**). Activity in significantly different regions between-groups are not predicted by dopamine release in the posterior caudate (**Table S8**). Thus, BOLD differences between groups do not explain the difference in dopamine release between groups.

Supplementary Figures

Visual depiction of the experimental design

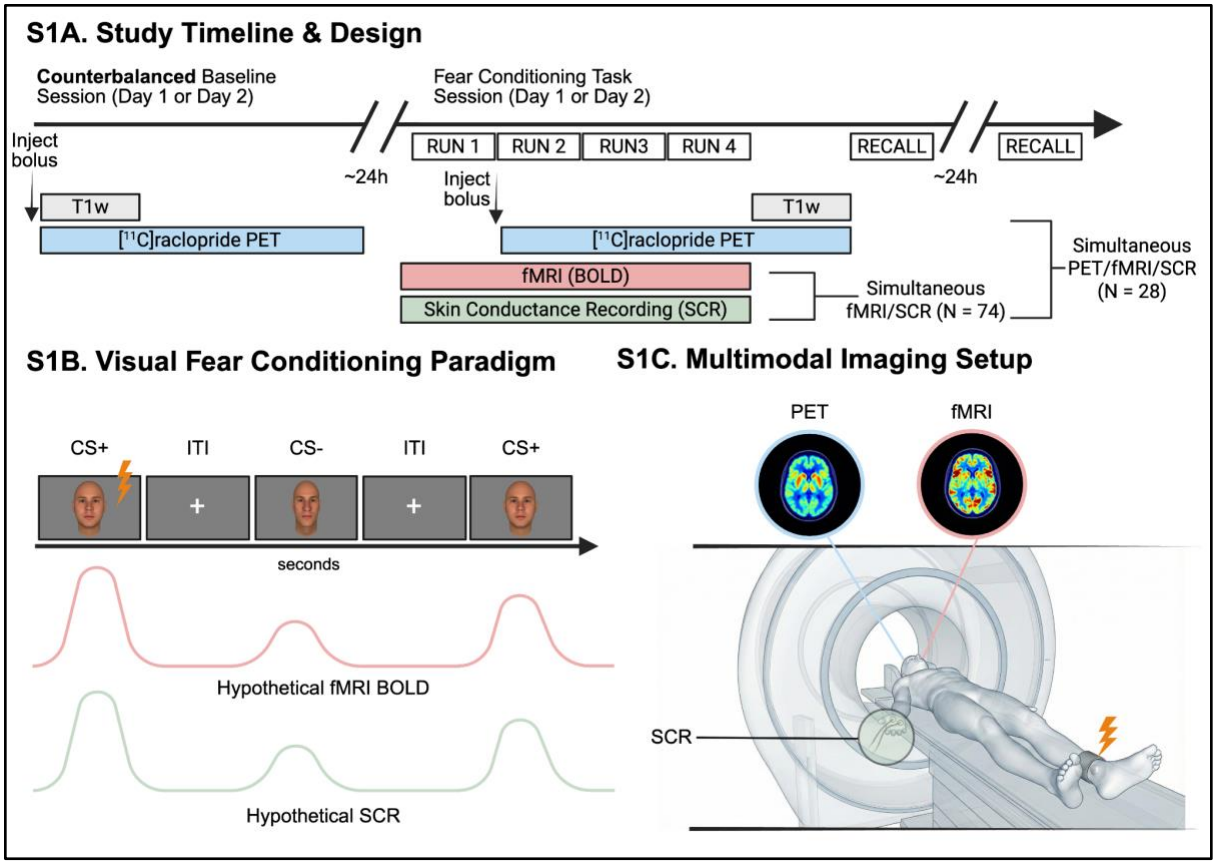

Figure S1. Visual depiction of the experimental design and fear conditioning task. **A.** A subset of 28 individuals completed the combined PET/fMRI arm. Here, participants completed one 60-minute [^{11}C]raclopride PET scan during baseline. Approximately one day later, participants are brought back for a fear acquisition scan. Participants complete four runs of a visual fear conditioning paradigm in the MRI scanner, with simultaneous acquisitions of fMRI and SCR. [^{11}C]raclopride is injected immediately after termination of the first fear conditioning run, and then participants complete three more runs. Afterwards, participants complete an explicit recall of the visual pairings no more than two hours after the last fear conditioning run. Finally, participants complete a second explicit recall approximately one day after the last fear conditioning run. These 28 individuals that completed the combined PET/fMRI arm are part of a larger group (*N* = 74) that completed simultaneous fMRI and SCR, then recall. **B.** The top panel depicts an example of a single fear conditioning run. Participants are presented with a new pair of pseudorandomized faces at each run to ensure continuous learning throughout the scan. One run of fear acquisition consisted of 20 CS+ presentations (6 paired with a shock, ~33% reinforcement rate, 4 seconds each), 14 CS- presentations (4 seconds each) and a jittered inter-trial interval (6-15 seconds each) for a total of 483 seconds (see *methods* for more details). The bottom panel represents theoretical blood-oxygen-dependent-level

(BOLD) and SCR signals. **C.** An example illustration of an individual undergoing simultaneous PET/fMRI/SCR.

The visual fear discrimination paradigm elicits fear responses but these do not differ between groups

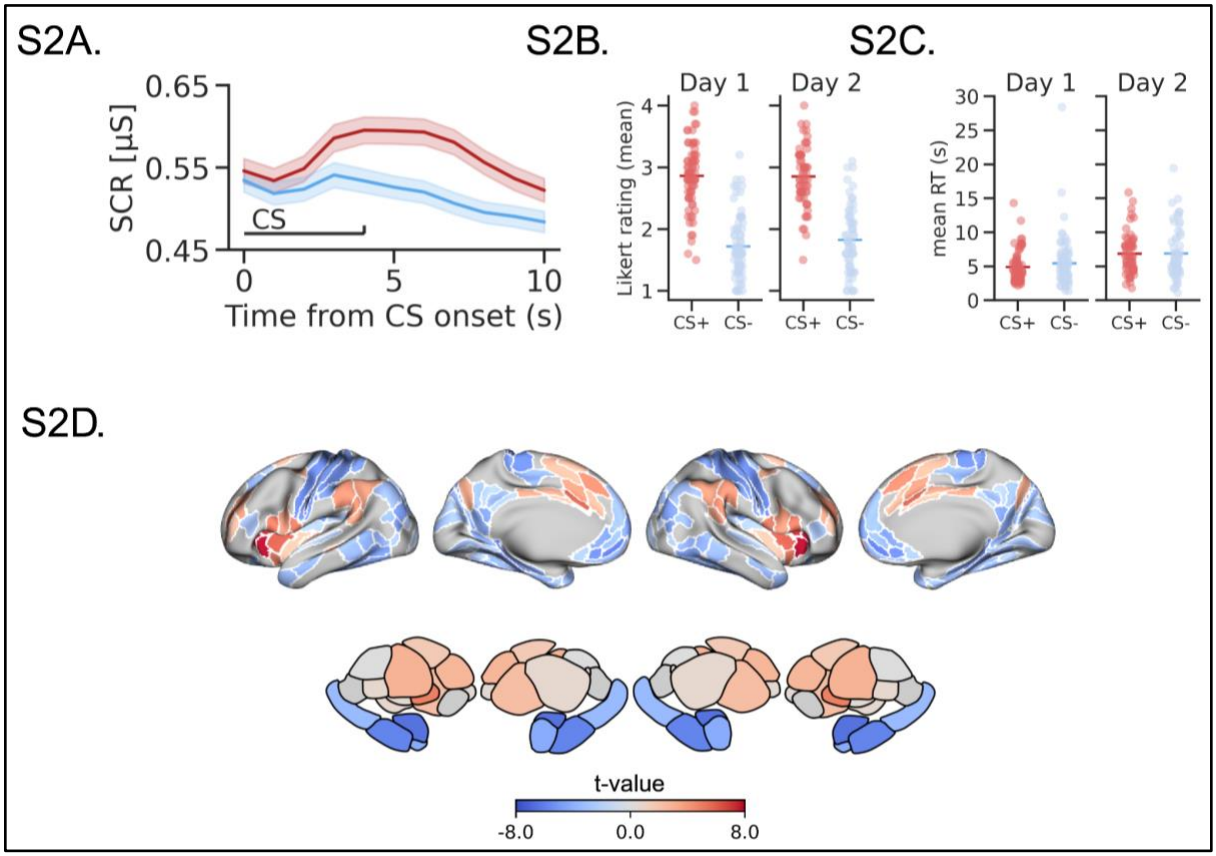

Figure S2. Area Under the Curve (AUC) of the deconvolved phasic skin conductance response from 0-10 s (measured in microsiemens [µS]), explicit recall scores representing contingency memory and BOLD responses confirm learning during the visual fear discrimination paradigm. **a.** A linear mixed effects model reveals the CS+ (red) elevated skin conductance responses relative to the CS- (blue). Examination of the main effects of the model using ANOVA reveals a significant effect of CS type, but not group, in the combined PET/fMRI (N = 28, $F_{(1,111)}$ = 6.404, p = .0128) and the larger fMRI group (N = 69, $F_{(1,275)}$ = 12.02, p = .0006). **b.** A linear mixed effects model reveals that participants rated the CS+ (red) as more likely to be paired with the shock relative to the CS- (blue), 2 hours after the last fear conditioning run and the next day. Examination of the main effects of the model using ANOVA reveals a significant effect of CS type, but not group or day, in the combined PET/fMRI (N = 28, $F_{(1,334)}$ = 246.1, p < .0001) and the larger fMRI group (N = 74, $F_{(1,782)}$ = 578.4, p < .0001) **c.** However, a linear mixed effects model did not reveal differences in reaction time (RT) when rating CS+ and CS- stimuli when examining main effects in the combined PET/fMRI (N = 28, $F_{(1,334)}$ = 0.207, p = .6491) and the larger fMRI group (N = 74, $F_{(1,782)}$ = 1.452, p = .2285). **d.** A one-sample *t*-test of BOLD activity during the fear conditioning task indicates that 38

parcels exhibit BOLD activity favoring the CS+ relative to CS- (red), while 75 parcels show BOLD activity favoring the CS- relative to CS+ (blue) (N = 74, all $t_{(73)} > |2.2|$, all $p < 0.05$; fdr-adjusted for 196 parcels). Importantly, we find similar changes in BOLD activity in these regions as previous meta-analyses of fear conditioning [90, 91].

Supplementary Tables

Table S1. Temporal Experience of Pleasure Scale (TEPS), State Paranoia Checklist (PCL), explicit recall, and skin conductance from the combined PET/fMRI group (*N* = 28).

	Controls (N = 16)	FDRs (N = 12)	Test	Statistic
TEPS				
Anticipatory Subscore | Mean (SD)	42 (8.0)	43 (5.5)	t-test	t(26) = -0.22, p = 0.83
Consummatory Subscore | Mean (SD)	39 (6.4)	38 (5.4)	t-test	t(26) = 0.42, p = 0.68
Total Score | Mean (SD)	81 (13)	81 (9.4)	t-test	t(26) = 0.08, p = 0.94
PCL				
Frequency Subscore | Median [Min, Max]	18 [18,26]	19 [18,33]	wilcoxon	W = 75.5, p = 0.29
Conviction Subscore | Median [Min, Max]	20 [18,73]	21 [18, 34]	wilcoxon	W = 89, p = 0.76
Distress Subscore | Median [Min, Max]	19 [18, 37]	18 [18, 25]	wilcoxon	W = 112.5, p = 0.42
Total Score | Median [Min, Max]	57 [54, 130]	60 [54,92]	wilcoxon	W = 86, p = 0.66
Explicit Recall				
Day 1				
CS+ | Mean (SD)	3.22 (0.96)	3.03 (0.98)	Linear mixed effect model	F(1,111) = 122, p < 0.0001 **[CS- vs. CS+]** F(1,26) = 0.03, p = 0.86 **[group]**
CS- | Mean (SD)	1.73 (1.00)	1.86 (1.02)		

Table S1 Continued…				
	Controls (N = 16)	**FDRs (N = 12)**	**Test**	**Statistic**
Day 2				
CS+ | Mean (SD)	3.17 (0.94)	3.07 (1.07)	Linear mixed effect model	F(1,111) = 91.1, p < 0.0001 **[CS- vs. CS+]** F(1,25) = 0.15, p = 0.69 **[group]**
CS- | Mean (SD)	1.90 (1.00)	1.86 (1.07)		
Skin conductance				
CS+ | Mean (SD)	6.81 (7.49)	9.74 (12.3)	Linear mixed effect model	F(1,111) = 6.40, p = 0.013 **[CS- vs. CS+]** F(1,26) = 0.75, p = 0.39 **[group]**
CS- | Mean (SD)	6.21 (6.77)	8.74 (10.1)		

Table S2. %ΔD_2R BP_{ND} data are fit using a linear fixed effects model in 16 control participants x 2 timepoints x 5 regions = 150 total observations. As per the equation below [lme(bpnd ~ session*region, random = list(*participant*_id = ~ 1, region = ~ 1), data=filtered_data, method="REML")], we specify fixed effects of *region* and *session*. We also specify two random effects of *participant_id* and *region.* This syntax specifies *1|participant_id* to model both overall individual differences as well as *1|region in participant_id* to model region-specific individual differences. Then, the *emmeans* package in R is used to extract marginal means from the model. The results of the pairwise comparisons [BL - FC] are presented below. SE = standard error; df = degrees of freedom.

region	estimate	SE	df	t.ratio	p.value	fdr.adj.p
Nucleus accumbens	-0.017	0.044	75	-0.378	0.7064	0.706
Anterior caudate	0.084	0.044	75	1.916	0.0592	0.099
Anterior putamen	0.038	0.044	75	0.871	0.3866	0.483
Posterior caudate	0.116	0.044	75	2.626	0.0105	0.032
Posterior putamen	0.115	0.044	75	2.549	0.0129	0.032

Table S3. %ΔD_2R BP_{ND} data are fit using a linear fixed effects model in 16 control participants + 12 FDR participants. One difference value was obtained from each participant x 2 regions = 54 total observations. As per the equation [*lme(bpnd ~ region*group, random = list(participant_id = ~ 1, region = ~ 1), data=filtered_data, method="REML")*], we specify fixed effects of *region* and *session*. We also specify two random effects of *participant_id* and *region.* This syntax specifies *1|participant_id* to model both overall individual differences as well as *1|region in participant_id* to model region-specific individual differences. Then, the *emmeans* package in R is used to extract marginal means from the model. The results of the pairwise comparisons [FDR - CTR] are presented below. SE = standard error; df = degrees of freedom.

region	estimate	SE	df	t.ratio	p.value	fdr.adj.p
Posterior caudate	7.047	2.762	26	2.551	0.017	0.034
Posterior putamen	5.100	2.762	26	1.846	0.076	0.076

Table S4. Baseline D_2R BP_{ND} data are fit using a linear fixed effects model in 16 control participants + 12 FDR participants. One BP_{ND} value is obtained from each participant x 2 regions = 54 total observations. As per the equation *[lme(bpnd ~ group*region, random = list(participant_id = ~ 1, region = ~ 1), data=filtered_data, method="REML")*], we specify fixed effects of *region* and *group*. We also specify two random effects of *participant_id* and *region.* This syntax specifies *1|participant_id* to model both overall individual differences as well as *1|region in participant_id* to model region-specific individual differences. Then, the emmeans package in R is used to extract marginal means from the model. The results of the pairwise comparisons [FDR - CTR] are presented below. SE = standard error; df = degrees of freedom.

region	estimate	SE	df	t.ratio	p.value	fdr.adj.p
Posterior caudate	-0.179	0.144	26	-1.238	0.227	0.453
Posterior putamen	-0.045	0.144	26	-0.314	0.756	0.756

Table S5. SCR data are fit using a linear mixed effects model in *N* = 28 and *N* = 69 individuals (after discarding 5 SCR recordings from the fMRI only arm). As per the equation [*lme(scr ~stimtype, random =~ 1|subid/run, data=filtered_data, method="REML")],* we specified the fixed effects of stimulus type (CS+ or CS-) and group. We also specify two random effects of *run (1, 2, 3, 4)* and participant*_id*. This syntax specifies *1|participant_id* to model both overall individual differences as well as *1|run in* participant*_id* to model run-specific individual differences. Because we are interested in main effects of stimulus type and group, we used the anova.lme function to extract main effects, presented below. numDF = numerator degrees of freedom, denDF = denominator degrees of freedom.

N	Effect	numDF	denDF	F-value	p-value
28	Intercept	1	111	13.80	0.0003
	Stimulus type	1	111	6.404	0.0128
	Group	1	26	0.752	0.3936
69	Intercept	1	275	21.62	< 0.0001
	Stimulus type	1	275	12.02	0.0006
	Group	1	67	0.8112	0.3710

Table S6. Explicit recall data are fit using a linear mixed effects model in *N* = 28 and *N* = 74 individuals. As per the equation [*lme(Response ~stimtype + group + day, random =~ 1|subid/run, data=filtered_data, method="REML")],* we specify the fixed effects of stimulus type (CS+ or CS-), group and day (1, 2). We also specify two random effects of *run (1, 2, 3, 4)* and *participantt_id*. This syntax specifies *1|participantt_id* to model both overall individual differences as well as *1|run in participantt_id* to model run-specific individual differences. Because we are interested in main effects of stimulus type and group, we used the anova.lme function to extract main effects, presented below. numDF = numerator degrees of freedom, denDF = denominator degrees of freedom.

N	Effect	numDF	denDF	F-value	p-value
28	Intercept	1	334	115.4	< 0.0001
	Stimulus type	1	334	246.1	< 0.0001
	Group	1	26	0.089	0.7671
	Day	1	334	0.263	0.6083
74	Intercept	1	782	240.1	< 0.0001
	Stimulus type	1	782	578.4	< 0.0001
	Group	1	72	0.104	0.7485
	Day	1	782	0.045	0.8321

Table S7. Reaction time data during recall are fit using a linear mixed effects model in *N* = 28 and *N* = 74 individuals. As per the equation [*lme(Response ~stimtype + group + day, random =~ 1|subid/run, data=filtered_data, method="REML")],* we specify the fixed effects of stimulus type (CS+ or CS-), group and day (1, 2). We also specify two random effects of *run (1, 2, 3, 4)* and *participant_id*. This syntax specifies *1|participant_id* to model both overall individual differences as well as *1|run in participant_id* to model run-specific individual differences. Because we are interested in main effects of stimulus type and group, we used the anova.lme function to extract main effects, presented below. numDF = numerator degrees of freedom, denDF = denominator degrees of freedom.

N	Effect	numDF	denDF	F-value	p-value
28	Intercept	1	334	29.24	< 0.0001
	Stimulus type	1	334	0.207	0.6491
	Group	1	26	0.008	0.9315
	Day	1	334	4.489	0.0348
74	Intercept	1	782	29.47	< 0.0001
	Stimulus type	1	782	1.452	0.2285
	Group	1	72	0.144	0.7056
	Day	1	782	20.72	< 0.0001

Table S8. fMRI contrast data during acquisition are fit using a linear mixed effects model *N* = 74 individuals. As per the equation *[lme(beta ~region*group+run, random =~ 1|participant_id, data=filtered_data, method="ML")],* we specify the fixed effects of region, group and run (1, 2,3,4). We also specify the random effect of *participant_id*. This syntax specifies *1|participant_id* to model overall individual differences. Then, the emmeans package in R is used to extract marginal means from the model. The results of the pairwise comparisons [FDR - CTR] are presented below only for significant parcels surviving FDR correction. Exploratory regressions are performed between the significant parcels and $\%\Delta BP_{ND}$ to rule out fMRI group differences on dopamine release. SE = standard error; df = degrees of freedom.

contrast	Region (acronym)	estimate	SE	df	t.ratio	fdr.adj.p	Correlation with $\%\Delta BP_{ND}$
fdr - hc	Area V6A (V6A)	0.074	0.015	72	5.071	0.0006	No
fdr - hc	Seventh Visual Area (V7)	0.075	0.018	72	4.244	0.0063	No
fdr - hc	Posterior InferoTempo ral complex (PIT)	0.063	0.018	72	3.560	0.0374	No
fdr - hc	Eighth Visual Area (V8)	0.062	0.018	72	3.516	0.0374	No
fdr - hc	Medial amygdala (mAMY)	0.061	0.018	72	3.439	0.0381	No
fdr - hc	Fourth visual area (V4)	0.059	0.018	72	3.348	0.0424	No
fdr - hc	Area Lateral IntraParietal dorsal (LIPd)	0.058	0.018	72	3.271	0.0432	No
fdr - hc	Area V3CD (V3CD)	0.057	0.018	72	3.235	0.0432	No
fdr - hc	Ventral IntraParietal Complex (VIP)	0.057	0.018	72	3.210	0.0432	No

Table S9. Predictions of the chaotic dopamine hypothesis using the posterior caudate striatal ROI.

Prediction	Variables	Equation	Statistic (%ΔBP$_{ND}$)
↓release → ↓BOLD for positive prediction error	%ΔBP$_{ND}$ ΔBOLD [CS+ - CS-]	ΔBOLD ~ %ΔBP$_{ND}$+Group	**t(25) = -2.65, p = 0.014**
↓release → ↓autonomic responding	%Δ*BP*$_{ND}$ Skin conductance Δ CS [CS+ - CS-]	Autonomic response ~ %Δ*BP*$_{ND}$+Group +Stimulus	t(25) = -0.21, p = 0.84
↓release → ↓valuation of stimuli	%Δ*BP*$_{ND}$ Explicit recall Δ CS [CS+ - CS-]	Likert response ~ %Δ*BP*$_{ND}$+Group +Day(1+2)	t(52) = 0.47, p = 0.64
↓release → ↑negative symptoms	%Δ*BP*$_{ND}$ TEPS total	TEPS ~ %Δ*BP*$_{ND}$+Group	t(25) = -0.076, p = 0.94
↓release → ↑negative symptoms	%Δ*BP*$_{ND}$ TEPS anticipatory	TEPS ~ %Δ*BP*$_{ND}$+Group	t(25) = -0.723, p = 0.476
↓release → ↑negative symptoms	%Δ*BP*$_{ND}$ TEP consummatory	TEPS ~ %Δ*BP*$_{ND}$+Group	t(25) = 0.709, p = 0.485
↓release → ↓positive symptoms	**%Δ*BP*$_{ND}$ PCL total**	**log(PCL) ~ %Δ*BP*$_{ND}$+Group**	**t(25) = 2.07, p = 0.049**
↓release → ↓positive symptoms	**%Δ*BP*$_{ND}$ PCL frequency**	**log(PCL) ~ %Δ*BP*$_{ND}$+Group**	**t(25) = 2.20 p = 0.037**
↓release → ↓positive symptoms	%Δ*BP*$_{ND}$ PCL conviction	log(PCL) ~ %Δ*BP*$_{ND}$+Group	t(25) = 1.498, p = 0.147
↓release → ↓positive symptoms	%Δ*BP*$_{ND}$ PCL distress	log(PCL) ~ %Δ*BP*$_{ND}$+Group	t(25) = 1.977, p = 0.059

Data Availability

Anonymized data is available upon request. Supplementary information is available at MP's website.

Code Availability

Code for the project including aggregate data, analysis and figures are available at https://github.com/rami-hamati/avlraclo.

Funding

This research was supported by the Emerging Research Innovators in Mental Health Award (The Royal) and a NARSAD grant (The Brain & Behavior Research Foundation).

Acknowledgements

We would like to acknowledge the participants of the study, especially the first-degree relatives of patients with psychotic illness. Also, thanks to Drs. Pierre Blier, Jeanne Talbot, Georg Northoff and Timothy Lau for providing medical supervision during the positron emission tomography sessions. Also, thanks to the Brain Imaging Centre at The Royal for facilitating this study. Finally, we would like to thank the anonymous donors who provided funding for the Emerging Researchers in Mental Health Award, and ultimately, this study. An oral presentation and conference proceeding related to this data was previously published in *Biological Psychiatry:* https://doi.org/10.1016/j.biopsych.2025.02.236.

Author Contributions

RH: Investigation, Data Curation, Writing - Original Draft, Writing - Review & Editing, Formal Analysis, Visualization. **CS:** Investigation, Data Curation; Writing - Review & Editing. **BC:** Investigation, Data Curation. **HB:** Investigation, Writing - Review & Editing. **KD:** Writing - Review & Editing. **DJH:** Writing - Review & Editing. **CMC:** Methodology, Supervision, Writing - Review & Editing, Funding acquisition. **LT:** Conceptualization, Methodology, Software, Supervision, Writing - Original Draft, Writing - Review & Editing, Funding acquisition.

Competing Interests

RH previously owned shares in Karuna Therapeutics Inc. and received two knowledge dissemination grants from Otsuka Canada Pharmaceutical Inc. to organize local trainee conferences. **CMC** is inventor on a patent using the methodology employed in this study that is licensed to Terran Biosciences Inc. but has not received royalties. **LT** received one knowledge dissemination grant from Otsuka Canada Pharmaceutical Inc. & AbbVie Inc. to organize a pan-Canadian schizophrenia conference. The remaining authors have nothing to disclose.

Materials & Correspondence

Correspondence and requests for materials should be addressed to Lauri Tuominen.

References

1. Meltzer HY, Stahl SM. The dopamine hypothesis of schizophrenia: a review. Schizophr Bull. 1976;2:19–76.
2. Snyder SH. The dopamine hypothesis of schizophrenia: focus on the dopamine receptor. Am J Psychiatry. 1976;133:197–202.
3. Carlsson A. The current status of the dopamine hypothesis of schizophrenia. Neuropsychopharmacology. 1988;1:179–186.
4. Brugger SP, Angelescu I, Abi-Dargham A, Mizrahi R, Shahrezaei V, Howes OD. Heterogeneity of striatal dopamine function in schizophrenia: Meta-analysis of variance. Biol Psychiatry. 2020;87:215–224.
5. Eisenberg DP, Blackman RK, Tietcheu MG, Kohn PD, Bettina JS, Kolachana B, et al. Genetic risk for treatment resistant schizophrenia and corresponding variation in dopamine synthesis capacity and D2/3 receptor availability in healthy individuals. Mol Psychiatry. 2024:1–8.
6. Huttunen J, Heinimaa M, Svirskis T, Nyman M, Kajander J, Forsback S, et al. Striatal dopamine synthesis in first-degree relatives of patients with schizophrenia. Biol Psychiatry. 2008;63:114–117.
7. Howes OD, Bonoldi I, McCutcheon RA, Azis M, Antoniades M, Bossong M, et al. Glutamatergic and dopaminergic function and the relationship to outcome in people at clinical high risk of psychosis: a multi-modal PET-magnetic resonance brain imaging study. Neuropsychopharmacology. 2020;45:641–648.
8. Jauhar S, Nour MM, Veronese M, Rogdaki M, Bonoldi I, Azis M, et al. A test of the transdiagnostic dopamine hypothesis of psychosis using positron emission tomographic imaging in bipolar affective disorder and schizophrenia. JAMA Psychiatry. 2017;74:1206–1213.
9. Strauss GP, Waltz JA, Gold JM. A review of reward processing and motivational impairment in schizophrenia. Schizophr Bull. 2014;40 Suppl 2:S107–S116.
10. Barch DM, Carter CS, Gold JM, Johnson SL, Kring AM, MacDonald AW, et al. Explicit and implicit reinforcement learning across the psychosis spectrum. J Abnorm Psychol. 2017;126:694–711.
11. Winton-Brown TT, Fusar-Poli P, Ungless MA, Howes OD. Dopaminergic basis of salience dysregulation in psychosis. Trends Neurosci. 2014;37:85–94.
12. Radua J, Schmidt A, Borgwardt S, Heinz A, Schlagenhauf F, McGuire P, et al. Ventral striatal activation during reward processing in psychosis: A neurofunctional meta-analysis: A neurofunctional meta-analysis. JAMA Psychiatry. 2015;72:1243–1251.
13. Zeng J, Yan J, Cao H, Su Y, Song Y, Luo Y, et al. Neural substrates of reward anticipation and outcome in schizophrenia: a meta-analysis of fMRI findings in the monetary incentive delay task. Transl Psychiatry. 2022;12:448.
14. Yang X, Song Y, Zou Y, Li Y, Zeng J. Neural correlates of prediction error in patients with schizophrenia: evidence from an fMRI meta-analysis. Cereb Cortex. 2024;34:bhad471.
15. Tuominen L, Romaniuk L, Milad MR, Goff DC, Hall J, Holt DJ. Impairment in acquisition of conditioned fear in schizophrenia. Neuropsychopharmacology. 2022;47:681–686.
16. Hamati R, Ahrens J, Shvetz C, Holahan MR, Tuominen L. 65 years of

research on dopamine's role in classical fear conditioning and extinction: A systematic review. Eur J Neurosci. 2024;59:1099–1140.
17. Quarmley M, Gur RC, Turetsky BI, Watters AJ, Bilker WB, Elliott MA, et al. Reduced safety processing during aversive social conditioning in psychosis and clinical risk. Neuropsychopharmacology. 2019;44:2247–2253.
18. Millard SJ, Bearden CE, Karlsgodt KH, Sharpe MJ. The prediction-error hypothesis of schizophrenia: new data point to circuit-specific changes in dopamine activity. Neuropsychopharmacology. 2022;47:628–640.
19. Maia TV, Frank MJ. An integrative perspective on the role of dopamine in schizophrenia. Biol Psychiatry. 2017;81:52–66.
20. Hamati R, Kanaa N, Chidiac B, Guimond S, Cassidy C, Tuominen L. SN/VTA neuromelanin signal is associated with subclinical paranoia irrespective of familial risk for psychosis. NPJ Schizophr. 2026. In press.
21. Tuominen L, Boeke E, DeCross S, Wolthusen RP, Nasr S, Milad M, et al. The relationship of perceptual discrimination to neural mechanisms of fear generalization. Neuroimage. 2019;188:445–455.
22. Tuominen L, DeCross SN, Boeke E, Cassidy CM, Freudenreich O, Shinn AK, et al. Neural abnormalities in fear generalization in schizophrenia and associations with negative symptoms. Biol Psychiatry Cogn Neurosci Neuroimaging. 2021;6:1165–1175.
23. Frick A, Björkstrand J, Lubberink M, Eriksson A, Fredrikson M, Åhs F. Dopamine and fear memory formation in the human amygdala. Mol Psychiatry. 2022;27:1704–1711.
24. Lissemore JI, Nagano-Saito A, Smart K, Gravel P, Leyton M, Benkelfat C. Dopaminergic plasticity in the bilateral hippocampus following threat reversal in humans. Sci Rep. 2020;10:7627.
25. Egerton A, Mehta MA, Montgomery AJ, Lappin JM, Howes OD, Reeves SJ, et al. The dopaminergic basis of human behaviors: A review of molecular imaging studies. Neurosci Biobehav Rev. 2009;33:1109–1132.
26. Alakurtti K, Johansson JJ, Joutsa J, Laine M, Bäckman L, Nyberg L, et al. Long-term test-retest reliability of striatal and extrastriatal dopamine D2/3 receptor binding: study with [(11)C]raclopride and high-resolution PET. J Cereb Blood Flow Metab. 2015;35:1199–1205.
27. Mandeville JB, Levine MA, Arsenault JT, Vanduffel W, Rosen BR, Sander CY. A reference tissue forward model for improved PET accuracy using within-scan displacement studies. J Cereb Blood Flow Metab. 2022;42:1007–1019.
28. Monchi O, Ko JH, Strafella AP. Striatal dopamine release during performance of executive functions: A [(11)C] raclopride PET study. Neuroimage. 2006;33:907–912.
29. Sheehan DV, Lecrubier Y, Harnett Sheehan K, Amorim P, Janavs J, Emmanuelle Weiller MS, et al. The Mini-International Neuropsychiatric Interview (M.I.N.I.): The Development and Validation of a Structured Diagnostic Psychiatric Interview for DSM-IV and ICD-10. J Clin Psychiatry. 1998;59:22–33.
30. Maxwell ME. Manual for the FIGS. Bethesda: National Institute of Mental Health. 1992. 1992.
31. Lonsdorf TB, Menz MM, Andreatta M, Fullana MA, Golkar A, Haaker J, et al. Don't fear 'fear conditioning': Methodological considerations for the design and analysis of studies on human fear acquisition, extinction, and return of fear. Neurosci Biobehav Rev. 2017;77:247–285.

32. van der Kouwe AJW, Benner T, Salat DH, Fischl B. Brain morphometry with multiecho MPRAGE. Neuroimage. 2008;40:559–569.
33. Abraham A, Pedregosa F, Eickenberg M, Gervais P, Mueller A, Kossaifi J, et al. Machine learning for neuroimaging with scikit-learn. Front Neuroinform. 2014;8:14.
34. Fox MD, Snyder AZ, Vincent JL, Corbetta M, Van Essen DC, Raichle ME. The human brain is intrinsically organized into dynamic, anticorrelated functional networks. Proc Natl Acad Sci U S A. 2005;102:9673–9678.
35. Glasser MF, Coalson TS, Robinson EC, Hacker CD, Harwell J, Yacoub E, et al. A multi-modal parcellation of human cerebral cortex. Nature. 2016;536:171–178.
36. Tian Y, Margulies DS, Breakspear M, Zalesky A. Topographic organization of the human subcortex unveiled with functional connectivity gradients. Nat Neurosci. 2020;23:1421–1432.
37. Izquierdo-Garcia D, Hansen AE, Förster S, Benoit D, Schachoff S, Fürst S, et al. An SPM8-based approach for attenuation correction combining segmentation and nonrigid template formation: application to simultaneous PET/MR brain imaging. J Nucl Med. 2014;55:1825–1830.
38. Greve DN, Svarer C, Fisher PM, Feng L, Hansen AE, Baare W, et al. Cortical surface-based analysis reduces bias and variance in kinetic modeling of brain PET data. Neuroimage. 2014;92:225–236.
39. Greve DN, Salat DH, Bowen SL, Izquierdo-Garcia D, Schultz AP, Catana C, et al. Different partial volume correction methods lead to different conclusions: An (18)F-FDG-PET study of aging. Neuroimage. 2016;132:334–343.
40. Nichols T, Brett M, Andersson J, Wager T, Poline J-B. Valid conjunction inference with the minimum statistic. Neuroimage. 2005;25:653–660.
41. Ichise M, Liow J-S, Lu J-Q, Takano A, Model K, Toyama H, et al. Linearized reference tissue parametric imaging methods: application to [11C]DASB positron emission tomography studies of the serotonin transporter in human brain. J Cereb Blood Flow Metab. 2003;23:1096–1112.
42. Tjerkaski J, Cervenka S, Farde L, Matheson GJ. Kinfitr - an open-source tool for reproducible PET modelling: validation and evaluation of test-retest reliability. EJNMMI Res. 2020;10:77.
43. Waskom M. seaborn: statistical data visualization. J Open Source Softw. 2021;6:3021.
44. Gale DJ, Vos de Wael. R, Benkarim O, Bernhardt B. Surfplot: Publication-ready brain surface figures. Zenodo; 2021.
45. Bryant AG. anniegbryant/subcortex_visualization: Initial Zenodo release. Zenodo; 2025.
46. Pauli WM, Larsen T, Collette S, Tyszka JM, Seymour B, O'Doherty JP. Distinct contributions of ventromedial and dorsolateral subregions of the human substantia nigra to appetitive and aversive learning. J Neurosci. 2015;35:14220–14233.
47. Matsumoto M, Hikosaka O. Two types of dopamine neuron distinctly convey positive and negative motivational signals. Nature. 2009;459:837–841.
48. Menegas W, Babayan BM, Uchida N, Watabe-Uchida M. Opposite initialization to novel cues in dopamine signaling in ventral and posterior striatum in mice. Elife. 2017;6.

49. Zafiri D, Salinas-Hernández XI, De Biasi ES, Rebelo L, Duvarci S. Dopamine prediction error signaling in a unique nigrostriatal circuit is critical for associative fear learning. Nat Commun. 2025;16:1–22.
50. Gard DE, Gard MG, Kring AM, John OP. Anticipatory and consummatory components of the experience of pleasure: A scale development study. J Res Pers. 2006;40:1086–1102.
51. Freeman D, Garety PA, Bebbington PE, Smith B, Rollinson R, Fowler D, et al. Psychological investigation of the structure of paranoia in a non-clinical population. Br J Psychiatry. 2005;186:427–435.
52. van Elzelingen W, Goedhoop J, Warnaar P, Denys D, Arbab T, Willuhn I. A unidirectional but not uniform striatal landscape of dopamine signaling for motivational stimuli. Proc Natl Acad Sci U S A. 2022;119:e2117270119.
53. Menegas W, Bergan JF, Ogawa SK, Isogai Y, Umadevi Venkataraju K, Osten P, et al. Dopamine neurons projecting to the posterior striatum form an anatomically distinct subclass. Elife. 2015;4:e10032.
54. Kintscher M, Kochubey O, Schneggenburger R. A striatal circuit balances learned fear in the presence and absence of sensory cues. Elife. 2023;12.
55. Chen APF, Chen L, Shi KW, Cheng E, Ge S, Xiong Q. Nigrostriatal dopamine modulates the striatal-amygdala pathway in auditory fear conditioning. Nat Commun. 2023;14:7231.
56. Rao N, Northoff G, Tagore A, Rusjan P, Kenk M, Wilson A, et al. Impaired prefrontal cortical dopamine release in schizophrenia during a cognitive task: A [11C]FLB 457 positron emission tomography study. Schizophr Bull. 2019;45:670–679.
57. Mizrahi R, Addington J, Rusjan PM, Suridjan I, Ng A, Boileau I, et al. Increased stress-induced dopamine release in psychosis. Biol Psychiatry. 2012;71:561–567.
58. Tseng H-H, Watts JJ, Kiang M, Suridjan I, Wilson AA, Houle S, et al. Nigral stress-induced dopamine release in clinical high risk and antipsychotic-naïve schizophrenia. Schizophr Bull. 2018;44:542–551.
59. Grace AA, Floresco SB, Goto Y, Lodge DJ. Regulation of firing of dopaminergic neurons and control of goal-directed behaviors. Trends Neurosci. 2007;30:220–227.
60. Liu C, Goel P, Kaeser PS. Spatial and temporal scales of dopamine transmission. Nat Rev Neurosci. 2021;22:345–358.
61. Mourgues-Codern C, Benrimoh D, Gandhi J, Farina EA, Vin R, Zamorano T, et al. Emergence and dynamics of delusions and hallucinations across stages in early psychosis. Biol Psychiatry. 2025;98:679–688.
62. Eaton W, Romanoski A, Anthony J, Nestadt G. Screening for psychosis in the general population with a self-report interview. J Nerv Ment Dis. 1991;179:689–693.
63. Taylor MJ, Freeman D, Lundström S, Larsson H, Ronald A. Heritability of psychotic experiences in adolescents and interaction with environmental risk. JAMA Psychiatry. 2022;79:889–897.
64. Freeman D, McManus S, Brugha T, Meltzer H, Jenkins R, Bebbington P. Concomitants of paranoia in the general population. Psychol Med. 2011;41:923–936.
65. Minichino A, Davies C, Karpenko O, Christodoulou N, Ramalho R, Nandha S, et al. Preventing psychosis in people at clinical high risk: an updated

meta-analysis by the World Psychiatric Association Preventive Psychiatry section. Mol Psychiatry. 2025;30:2773–2782.
66. Woodward ND, Cowan RL, Park S, Ansari MS, Baldwin RM, Li R, et al. Correlation of individual differences in schizotypal personality traits with amphetamine-induced dopamine release in striatal and extrastriatal brain regions. Am J Psychiatry. 2011;168:418–426.
67. Laruelle M, Abi-Dargham A, van Dyck CH, Gil R, D'Souza CD, Erdos J, et al. Single photon emission computerized tomography imaging of amphetamine-induced dopamine release in drug-free schizophrenic subjects. Proc Natl Acad Sci U S A. 1996;93:9235–9240.
68. Abi-Dargham A, Gil R, Krystal J, Baldwin RM, Seibyl JP, Bowers M, et al. Increased striatal dopamine transmission in schizophrenia: confirmation in a second cohort. Am J Psychiatry. 1998;155:761–767.
69. Dahoun T, Nour MM, McCutcheon RA, Adams RA, Bloomfield MAP, Howes OD. The relationship between childhood trauma, dopamine release and dexamphetamine-induced positive psychotic symptoms: a [11C]-(+)-PHNO PET study. Transl Psychiatry. 2019;9:287.
70. Cassidy CM, Zucca FA, Girgis RR, Baker SC, Weinstein JJ, Sharp ME, et al. Neuromelanin-sensitive MRI as a noninvasive proxy measure of dopamine function in the human brain. Proc Natl Acad Sci U S A. 2019;116:5108–5117.
71. McCutcheon RA, Abi-Dargham A, Howes OD. Schizophrenia, dopamine and the striatum: From biology to symptoms. Trends Neurosci. 2019;42:205–220.
72. Corlett PR, Fraser KM. 20 years of aberrant salience in psychosis: What have we learned? Am J Psychiatry. 2025:appiajp20240556.
73. Mohebi A, Wei W, Pelattini L, Kim K, Berke JD. Dopamine transients follow a striatal gradient of reward time horizons. Nat Neurosci. 2024;27:737–746.
74. Sousa M, Bujalski P, Cruz BF, Louie K, McNamee DC, Paton JJ. A multidimensional distributional map of future reward in dopamine neurons. Nature. 2025;642:691–699.
75. De Bundel D, Zussy C, Espallergues J, Gerfen CR, Girault J-A, Valjent E. Dopamine D2 receptors gate generalization of conditioned threat responses through mTORC1 signaling in the extended amygdala. Mol Psychiatry. 2016;21:1545–1553.
76. Marek S, Tervo-Clemmens B, Calabro FJ, Montez DF, Kay BP, Hatoum AS, et al. Reproducible brain-wide association studies require thousands of individuals. Nature. 2022;603:654–660.
77. Zhang Y, Brady J, Smith SM, Fmrib. An HMRF-EM algorithm for partial volume segmentation of brain MRI FMRIB technical report TR 01 YZ 1. 2001. 2001.
78. Dale AM, Fischl B, Sereno MI. Cortical surface-based analysis. I. Segmentation and surface reconstruction. Neuroimage. 1999;9:179–194.
79. Klein A, Ghosh SS, Bao FS, Giard J, Häme Y, Stavsky E, et al. Mindboggling morphometry of human brains. PLoS Comput Biol. 2017;13:e1005350.
80. Ciric R, Thompson WH, Lorenz R, Goncalves M, MacNicol EE, Markiewicz CJ, et al. TemplateFlow: FAIR-sharing of multi-scale, multi-species brain models. Nat Methods. 2022;19:1568–1571.
81. Evans AC, Janke AL, Collins DL, Baillet S. Brain templates and

atlases. Neuroimage. 2012;62:911–922.
82. Fonov VS, Evans AC, McKinstry RC, Almli CR, Collins DL. Unbiased nonlinear average age-appropriate brain templates from birth to adulthood. Neuroimage. 2009;47:S102.
83. Jenkinson M, Bannister P, Brady M, Smith S. Improved optimization for the robust and accurate linear registration and motion correction of brain images. Neuroimage. 2002;17:825–841.
84. Greve DN, Fischl B. Accurate and robust brain image alignment using boundary-based registration. Neuroimage. 2009;48:63–72.
85. Power JD, Barnes KA, Snyder AZ, Schlaggar BL, Petersen SE. Spurious but systematic correlations in functional connectivity MRI networks arise from subject motion. Neuroimage. 2012;59:2142–2154.
86. Power JD, Mitra A, Laumann TO, Snyder AZ, Schlaggar BL, Petersen SE. Methods to detect, characterize, and remove motion artifact in resting state fMRI. Neuroimage. 2014;84:320–341.
87. Behzadi Y, Restom K, Liau J, Liu TT. A component based noise correction method (CompCor) for BOLD and perfusion based fMRI. Neuroimage. 2007;37:90–101.
88. Satterthwaite TD, Elliott MA, Gerraty RT, Ruparel K, Loughead J, Calkins ME, et al. An improved framework for confound regression and filtering for control of motion artifact in the preprocessing of resting-state functional connectivity data. Neuroimage. 2013;64:240–256.
89. Patriat R, Reynolds RC, Birn RM. An improved model of motion-related signal changes in fMRI. NeuroImage. 2017;144:74–82.
90. Fullana MA, Harrison BJ, Soriano-Mas C, Vervliet B, Cardoner N, Àvila-Parcet A, et al. Neural signatures of human fear conditioning: an updated and extended meta-analysis of fMRI studies. Mol Psychiatry. 2016;21:500–508.
91. Radua J, Savage HS, Vilajosana E, Jamieson A, Abler B, Åhs F, et al. Neural correlates of human fear conditioning and sources of variability in 2199 individuals. Nat Commun. 2025;16:1–18.

8. General Discussion

8.1 Summary of main findings

In summary, the first manuscript shows that dorsomedial SN/VTA NM-MRI signal correlates with paranoid delusions. This suggests that a long-term measure of dopamine reflecting both tonic and phasic dopamine, as measured by NM-MRI, is positively linked to subclinical paranoia. The second manuscript indicates that dorsoposterior striatal dopamine release, likely reflecting phasic dopamine, is inversely associated with subclinical paranoia. Collectively, these studies suggest that while a static dopamine measure may be linked to paranoia, a lack of adaptive dopamine release might also contribute to positive symptoms. Together, these two studies highlight that two dopamine subsystems (dorsomedial SN/VTA → ventral striatum and ventrolateral SN/VTA → dorsal striatum) potentially contribute to paranoia. Furthermore, tonic and/or phasic dopamine release may be involved in the dysregulation of these two dopamine subsystems. Ultimately, these changes might reduce the dynamic range in which dopamine can signal value and impair the ability to discriminate stimuli, leading to paranoia.

8.1.1 Two components of the dopamine signal may contribute to positive symptoms

Interestingly, these studies collectively demonstrate that two separate parts of the midbrain dopamine system may contribute to positive symptoms. Dorsomedial SN/VTA projects to ventral striatum, whereas ventrolateral SN/VTA projects to dorsal striatum (Haber, 2003). Dopamine neurons across the mediolateral axis are thought to reflect different aspects of value encoding. Medial dopamine neurons are more likely to reflect a valence signal, differentiating between rewarding and aversive stimuli. Whereas, lateral dopamine neurons are more likely to reflect a general salience signal (Hamati et al., 2024). Together, these neurons may reflect the total value of a given stimulus association, providing information on whether an outcome is generally good or bad (valence) and how important it is (salience). This computation of the value signal for a stimulus may be important in understanding positive symptoms.

8.1.2 Two modes of dopamine release in each dopamine subsystem may reduce the dynamic range of the value signal

Our findings highlight that two modes of dopamine release, tonic and phasic dopamine, may contribute to positive symptoms like paranoia. Increased SN/VTA NM-MRI may reflect hyperdopaminergia in the tonic component. On the other hand, decreased fear-elicited dopamine release may reflect hypodopaminergia in the phasic component. Importantly, tonic and phasic dopamine set the range in which the brain can represent the value of a given stimulus. By increasing tonic and decreasing phasic release, the ability of the dopamine system to represent distinct stimuli in the brain is reduced. Consequently, this severely impacts the ability of an individual to discriminate stimuli. This idea is supported by a study which reported an

increased fear response to a safety stimulus, when dopamine release towards a fear stimulus was reduced, in a fear discrimination paradigm (Jo et al., 2018).

8.1.3 Phasic release as measured by [^{11}C]raclopride may reflect a predominantly D_2 receptor mediated signal

In the present study, fear conditioning evoked dopamine release was assessed by [^{11}C]raclopride, which has affinity for D_2 and D_3 receptors (Köhler et al. 1985). Thus, it could be argued that raclopride could be displaced by both types of dopamine receptors. However, D_2 and D_3 receptors are expressed in almost opposing gradients within the striatum (Gurevich and Joyce 1999). In the caudate and putamen where [^{11}C]raclopride was displaced in the current study, D_2 receptors are relatively more expressed than D_3 receptors, and so it is mainly these receptors that were activated during fear conditioning with only some contribution from D_3 receptors. In contemporary theories, striatal D_2 receptors are thought to mediate value learning and inhibit competing actions (**see section 2.5.2**). This suggests a reduction in striatal D_2 receptor-mediated signalling may lead to supra-additive features. This idea is supported by a study which reported an increased fear response in the absence of sensory cues, when D_2 receptor expressing striatal neurons are silenced (Kintscher et al., 2023). Overall, a reduction in D_2 receptor mediated signaling may be one way in which reduced dopamine release may contribute to positive symptoms.

8.2 A new integrated hypothesis of schizophrenia

The present thesis presents new empirical data that complicates the dopamine hypothesis of schizophrenia even further. On one hand, the dopamine imbalance hypothesis attributes increased striatal dopamine to positive symptoms and decreased cortical dopamine to negative symptoms. On the other hand, the chaotic dopamine hypothesis attributes increased tonic dopamine release to positive symptoms and decreased phasic dopamine release at relevant times to negative symptoms. However, our data suggests that there may be a case for reduced phasic striatal dopamine release in the emergence of positive symptoms, which does not fit either hypothesis neatly. Thus, I propose an updated integrated hypothesis that combines insights from a systems neuroscience view of dopamine, bayesian uncertainty, prediction errors, and tonic versus phasic dopamine signalling (Corlett & Fraser, 2025; Hamati et al., 2024; Maia & Frank, 2017; Millard et al., 2022).

In this new integrated model we will start by describing 1) an individual who observes the association between a face stimulus and a shock. 2) Dopaminergic neurons then produce a prediction error signal. This signal represents the mismatch between current sensory input and prior experience. If the current input is greatly different from prior experience, then a large dopamine signal will drive learning to update the probability of occurrence. In this model, we reconcile motivational salience and general salience by recognizing that dopaminergic neurons can signal

either type of salience. 3) These two types of saliences are represented by dopaminergic neurons projecting along a dorsoventral axis. Dorsomedial dopaminergic neurons signal motivational salience (A.K.A valence - is it good or bad?) and project to ventral striatum. Ventrolateral dopaminergic neurons signal general salience (Is it important?) and project to dorsal striatum (Menegas et al., 2017). The dorsoventral striatal axis may also have distinct time horizons for discounting events (Mohebi et al., 2024). General salience, maintained by sensory information, may be discounted at a faster rate in the sensorimotor striatum. Whereas, motivational salience, maintained by internal representations may be discounted at a slower rate in the ventral striatum. 4) Thus, striatal dopamine represents a probabilistic map of future risk and reward for a given stimulus (in this case, the face-shock pair), which is stored in a 'library' of stimulus-shock pairings in the cortex (or allocortex such as the hippocampus). In the case of the face-shock pair, this is a net positive salience signal and a net negative valence signal. 5) Finally, the relative risk or reward assessment of a given environment is produced by the evaluation of all stimuli within the environment and their corresponding value as given by the striatal dopamine representation (**figure 4**).

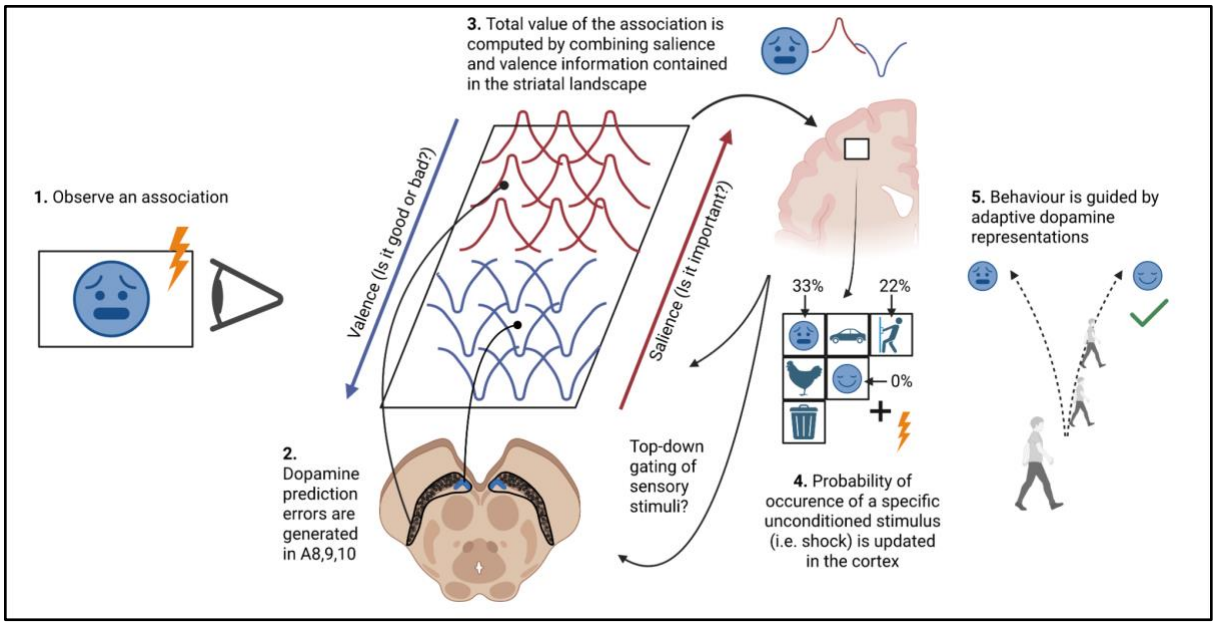

Figure 4. A model of how individuals learn about the world.

In the case of psychosis, there may be reduced adaptive dopamine release (i.e. there may be excess dopamine but it is not released at appropriate times and magnitudes; as we present evidence for in the current thesis) and increased tonic dopamine release. One or both of these changes in dopamine release may reduce the dynamic range in which dopamine may signal salience and valence. Overall, this results in a reduced ability to discriminate between various stimuli in the environment and inhibit competing responses. In the case of pain or fear related associations, this lack of ability to discriminate between stimuli leads to paranoia (**figure 5**).

To illustrate this new integrated hypothesis of schizophrenia, a hypothetical scenario will be described. In this scenario, there is a fatal virus circulating town. This virus, although fatal, is asymptomatic at the beginning stages. If a person is to step out of their home, then all individuals within that person's field of view would be considered highly dangerous. This is because there is no way to discriminate between who has the virus versus who does not. In the same way, a person with paranoia has no way of discriminating who is safe versus who is not. Thus I propose that excess perceived danger, combined with a reduced ability to discriminate fear from safety, are two essential components to the formation of paranoid delusion.

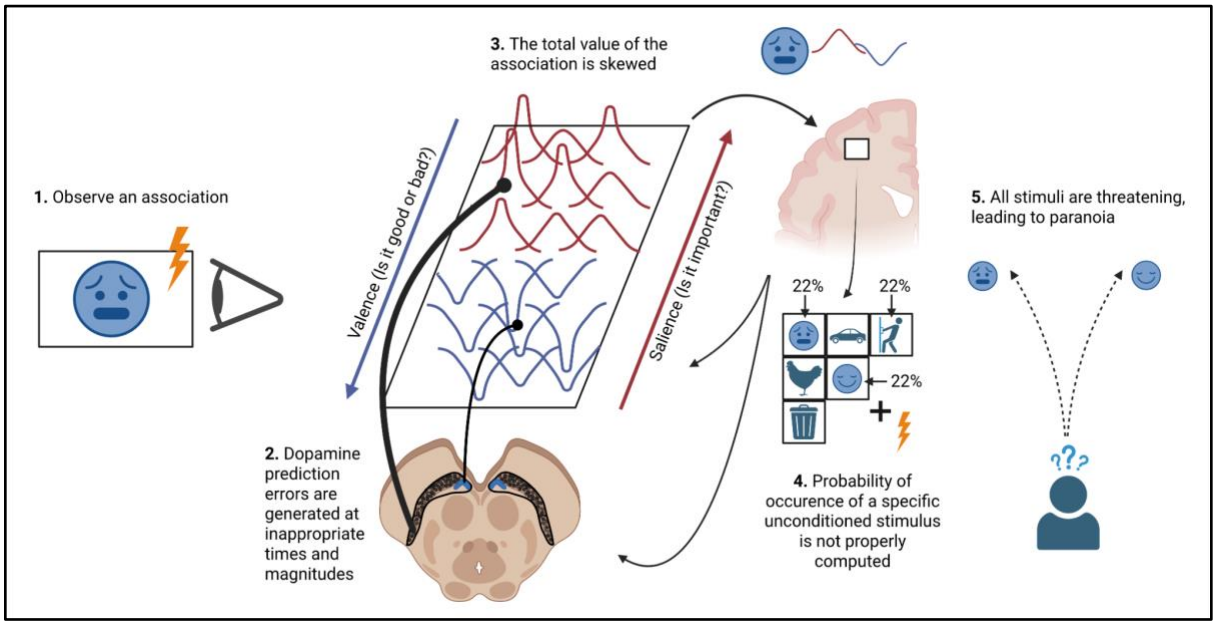

Figure 5. A new integrated model of schizophrenia.

8.3 Future avenues: What does this mean for the study of schizophrenia?

8.3.1 Solidifying a reduction of phasic dopamine in more severe presentations and by sex

Although the link between excess tonic dopamine release and positive symptoms has been extensively supported by the existing literature, this thesis is the first to demonstrate the idea that reduced phasic dopamine may also contribute to positive symptoms. However, this data is preliminary and additional studies using populations with more severe symptom presentation and different learning tasks are warranted. First, the current population of study are FDR individuals, the majority of which did not have any current mental health disorders, and some past the age of conversion to psychosis. Thus, we likely studied learning in individuals that were resilient and did not reflect paranoia severity in populations such as CHR-P or first-episode psychosis. Second, we used a fear conditioning task to study dopamine

release. It would be beneficial to see if this reduction in dopamine release is replicated using similar fear conditioning tasks, but further if this reduction occurs in reward conditioning tasks, and cognitive tasks such as working memory. One future direction would be to examine if deficits in dopamine release are related to specific symptoms. In the current thesis, lack of dopamine release during fear conditioning was related to paranoia, a fear-based delusion. Logically, then, lack of dopamine release during reward conditioning may be related to anhedonia; and lack of dopamine release during a working memory task may be related to cognitive deficits. Finally, we did not find any statistically significant differences in dopamine release between male and females, which we were underpowered to detect in the current studies. However, future studies should examine sex differences in task-evoked dopamine release, as the oestrous cycle may modulate this release.

8.3.2 Implications for treatment of schizophrenia and related disorders

Up until recently, schizophrenia and related disorders were thought of as disorders of dopamine excess subcortically and dopamine scarcity cortically. By teasing out tonic and phasic components of dopamine signaling, we may take dopamine dysregulation one step further. That is, baseline or tonic levels of dopamine are likely higher, and phasic or learning levels of dopamine are likely lower, irrespective of the brain region examined. Through this understanding, we may be able to tailor treatments to balance tonic and phasic dopamine signalling in the brain. One way would be to reduce the number of spontaneously active dopamine neurons responsible for tonic dopamine release while leaving phasic release and postsynaptic dopamine receptor binding intact. Another way would be to boost phasic dopamine activity. These manipulations would require an in-depth understanding of the molecular and systems-level substrates underlying the transitory switches from silent, spontaneously active, to phasic states. One potential therapeutic could be an NMDA receptor agonist or positive allosteric modulator, as NMDA receptors expressed dopamine neurons are responsible for their bursting activity and the maintenance of phasic dopamine levels (Zweifel et al. 2009; Paladini and Roeper 2014).

8.3.3 Concluding remark

In conclusion, the current thesis brings forward a new perspective on dopamine dysregulation in schizophrenia and related disorders: Paranoid delusion may not emerge because of "too much dopamine." It is likely a dysregulation of the signal-to-noise produced by the individual tonic and phasic signaling components. And so I close the thesis with this final statement in the hopes that it leads to new ways of treating schizophrenia and related disorders.

9. References

Abi-Dargham, A., Gil, R., Krystal, J., Baldwin, R. M., Seibyl, J. P., Bowers, M., van Dyck, C. H., Charney, D. S., Innis, R. B., & Laruelle, M. (1998). Increased striatal dopamine transmission in schizophrenia: confirmation in a second cohort. *The American Journal of Psychiatry*, *155*(6), 761–767.

Abi-Dargham, A., Rodenhiser, J., Printz, D., Zea-Ponce, Y., Gil, R., Kegeles, L. S., Weiss, R., Cooper, T. B., Mann, J. J., Van Heertum, R. L., Gorman, J. M., & Laruelle, M. (2000). Increased baseline occupancy of D2 receptors by dopamine in schizophrenia. *Proceedings of the National Academy of Sciences of the United States of America*, *97*(14), 8104–8109.

Aghajanian, G. K., & Bunney, B. S. (1973). CENTRAL DOPAMINERGIC NEURONS: NEUROPHYSIOLOGICAL IDENTIFICATION AND RESPONSES TO DRUGS**this research was supported by NIMH grant MH-17871, USPHS research scientist development award MH-14459 (to G. k. a.), and the state of Connecticut. In *Frontiers in Catecholamine Research* (pp. 643–648). Elsevier.

Alakurtti, K., Johansson, J. J., Joutsa, J., Laine, M., Bäckman, L., Nyberg, L., & Rinne, J. O. (2015). Long-term test-retest reliability of striatal and extrastriatal dopamine D2/3 receptor binding: study with [(11)C]raclopride and high-resolution PET. *Journal of Cerebral Blood Flow and Metabolism: Official Journal of the International Society of Cerebral Blood Flow and Metabolism*, *35*(7), 1199–1205.

Albanese, A., Altavista, M. C., & Rossi, P. (1986). Organization of central nervous system dopaminergic pathways. *Journal of Neural Transmission. Supplementum*, *22*, 3–17.

Alsharaeh, T., Salahat, A.-J., Alhajahjeh, A., Khudirat, M., Alashoor, A., Shuriquie, L., Alquabeh, B., & AlRyalat, S. A. (2024). The incidence of psychosis among Parkinson's disease patients and associated factors: A meta-analysis. *Jordan Medical Journal*, *58*(4). https://doi.org/10.35516/jmj.v58i4.893

Angrist, B., Sathananthan, G., & Gershon, S. (1973). Behavioral effects of L-dopa in schizophrenic patients. *Psychopharmacologia*, *31*(1), 1–12.

Angrist, B., Sathananthan, G., Gershon, S., & Wilk, S. (1973). BEHAVIOURAL AND BIOCHEMICAL EFFECTS OF L-DOPA IN PSYCHIATRIC PATIENTS. In *Frontiers in Catecholamine Research* (pp. 991–994). Elsevier.

Arakawa, R., Ichimiya, T., Ito, H., Takano, A., Okumura, M., Takahashi, H., Takano, H., Yasuno, F., Kato, M., Okubo, Y., & Suhara, T. (2009). Increase in thalamic binding of [(11)C]PE2I in patients with schizophrenia: a positron emission tomography study of dopamine transporter. *Journal of Psychiatric Research*, *43*(15), 1219–1223.

Avram, M., Brandl, F., Cabello, J., Leucht, C., Scherr, M., Mustafa, M., Leucht, S., Ziegler, S., & Sorg, C. (2019). Reduced striatal dopamine synthesis capacity in patients with schizophrenia during remission of positive symptoms. *Brain: A Journal of Neurology*, *142*(6), 1813–1826.

Beckstead, M. J., Grandy, D. K., Wickman, K., & Williams, J. T. (2004). Vesicular dopamine release elicits an inhibitory postsynaptic current in midbrain dopamine neurons. *Neuron*, *42*(6), 939–946.

Bell, D. S. (1973). The experimental reproduction of amphetamine psychosis. *Archives of General Psychiatry*, *29*(1), 35–40.

Bertolino, A., Breier, A., Callicott, J. H., Adler, C., Mattay, V. S., Shapiro, M., Frank,

J. A., Pickar, D., & Weinberger, D. R. (2000). The relationship between dorsolateral prefrontal neuronal N-acetylaspartate and evoked release of striatal dopamine in schizophrenia. *Neuropsychopharmacology: Official Publication of the American College of Neuropsychopharmacology*, *22*(2), 125–132.

Björklund, A., Divac, I., & Lindvall, O. (1978). Regional distribution of catecholamines in monkey cerebral cortex, evidence for a dopaminergic innervation of the primate prefrontal cortex. *Neuroscience Letters*, *7*(2-3), 115–119.

Björklund, A., & Dunnett, S. B. (2007). Dopamine neuron systems in the brain: an update. *Trends in Neurosciences*, *30*(5), 194–202.

Blokland, G. A. M., Mesholam-Gately, R. I., Toulopoulou, T., Del Re, E. C., Lam, M., DeLisi, L. E., Donohoe, G., Walters, J. T. R., GENUS Consortium, Seidman, L. J., & Petryshen, T. L. (2017). Heritability of neuropsychological measures in schizophrenia and nonpsychiatric populations: A systematic review and meta-analysis. *Schizophrenia Bulletin*, *43*(4), 788–800.

Breier, A., Su, T. P., Saunders, R., Carson, R. E., Kolachana, B. S., de Bartolomeis, A., Weinberger, D. R., Weisenfeld, N., Malhotra, A. K., Eckelman, W. C., & Pickar, D. (1997). Schizophrenia is associated with elevated amphetamine-induced synaptic dopamine concentrations: evidence from a novel positron emission tomography method. *Proceedings of the National Academy of Sciences of the United States of America*, *94*(6), 2569–2574.

Brugger, S. P., Angelescu, I., Abi-Dargham, A., Mizrahi, R., Shahrezaei, V., & Howes, O. D. (2020). Heterogeneity of striatal dopamine function in schizophrenia: Meta-analysis of variance. *Biological Psychiatry*, *87*(3), 215–224.

Cannon, T. D., Kaprio, J., Lönnqvist, J., Huttunen, M., & Koskenvuo, M. (1998). The genetic epidemiology of schizophrenia in a Finnish twin cohort. A population-based modeling study. *Archives of General Psychiatry*, *55*(1), 67–74.

Caravaggio, F., Borlido, C., Wilson, A., & Graff-Guerrero, A. (2015). Examining endogenous dopamine in treated schizophrenia using [^{11}C]-(+)-PHNO positron emission tomography: A pilot study. *Clinica Chimica Acta; International Journal of Clinical Chemistry*, *449*, 60–62.

Cardno, A. G., Marshall, E. J., Coid, B., Macdonald, A. M., Ribchester, T. R., Davies, N. J., Venturi, P., Jones, L. A., Lewis, S. W., Sham, P. C., Gottesman, I. I., Farmer, A. E., McGuffin, P., Reveley, A. M., & Murray, R. M. (1999). Heritability estimates for psychotic disorders: the Maudsley twin psychosis series. *Archives of General Psychiatry*, *56*(2), 162–168.

Carlsson, A. (1988). The current status of the dopamine hypothesis of schizophrenia. *Neuropsychopharmacology: Official Publication of the American College of Neuropsychopharmacology*, *1*(3), 179–186.

Carlsson, A., & Carlsson, M. L. (2006). A dopaminergic deficit hypothesis of schizophrenia: the path to discovery. *Dialogues in Clinical Neuroscience*, *8*(1), 137–142.

Carlsson, A., & Lindqvist, M. (1963). Effect of chlorpromazine or haloperidol on formation of 3methoxytyramine and normetanephrine in mouse brain. *Acta Pharmacologica et Toxicologica*, *20*(2), 140–144.

Carlsson, A., Roos, B. E., Wålinder, J., & Skott, A. (1973). Further studies on the mechanism of antipsychotic action: potentiation by alpha-methyltyrosine of thioridazine effects in chronic schizophrenics. *Journal of Neural Transmission*, *34*(2), 125–132.

Carter, M. J. (2014). Diagnostic and statistical manual of mental disorders. *Therapeutic Recreation Journal*, *48*(3), 275.

Cassidy, C. M., Zucca, F. A., Girgis, R. R., Baker, S. C., Weinstein, J. J., Sharp, M. E., Bellei, C., Valmadre, A., Vanegas, N., Kegeles, L. S., Brucato, G., Kang, U. J., Sulzer, D., Zecca, L., Abi-Dargham, A., & Horga, G. (2019). Neuromelanin-sensitive MRI as a noninvasive proxy measure of dopamine function in the human brain. *Proceedings of the National Academy of Sciences of the United States of America*, *116*(11), 5108–5117.

Cesarec, Z., & Nyman, A. K. (1985). Differential response to amphetamine in schizophrenia. *Acta Psychiatrica Scandinavica*, *71*(5), 523–538.

Charalampous, K. D., & Brown, S. (1967). A clinical trial of a-methyl-para-tyrosine in mentally ill patients. *Psychopharmacologia*, *11*(5), 422–429.

Cheng, C.-M., Chang, W.-H., Chen, M.-H., Tsai, C.-F., Su, T.-P., Li, C.-T., Tsai, S.-J., Hsu, J.-W., Huang, K.-L., Lin, W.-C., Chen, T.-J., & Bai, Y.-M. (2018). Co-aggregation of major psychiatric disorders in individuals with first-degree relatives with schizophrenia: a nationwide population-based study. *Molecular Psychiatry*, *23*(8), 1756–1763.

Citrome, L. (2015). The ABC's of dopamine receptor partial agonists - aripiprazole, brexpiprazole and cariprazine: the 15-min challenge to sort these agents out. *International Journal of Clinical Practice*, *69*(11), 1211–1220.

Corlett, P. R., & Fraser, K. M. (2025). 20 years of aberrant salience in psychosis: What have we learned? *The American Journal of Psychiatry*, appiajp20240556.

Corlett, P. R., Frith, C. D., & Fletcher, P. C. (2009). From drugs to deprivation: a Bayesian framework for understanding models of psychosis. *Psychopharmacology*, *206*(4), 515–530.

Cui, G., Jun, S. B., Jin, X., Pham, M. D., Vogel, S. S., Lovinger, D. M., & Costa, R. M. (2013). Concurrent activation of striatal direct and indirect pathways during action initiation. *Nature*, *494*(7436), 238–242.

Dahlstroem, A., & Fuxe, K. (1964). Evidence for the existence of monoamine-containing neurons in the central nervous system. I. Demonstration of monoamines in the cell bodies of brain stem neurons. *Acta Physiologica Scandinavica. Supplementum*, SUPPL 232:1–55.

Davis, J. M., & Janowsky, D. S. (1973). AMPHETAMINE AND METHYLPHENIDATE PSYCHOSIS. In *Frontiers in Catecholamine Research* (pp. 977–981). Elsevier.

Eaton, W., Romanoski, A., Anthony, J., & Nestadt, G. (1991). Screening for psychosis in the general population with a self-report interview. *The Journal of Nervous and Mental Disease*, *179*(11), 689–693.

Efthimiou, O., Taipale, H., Radua, J., Schneider-Thoma, J., Pinzón-Espinosa, J., Ortuño, M., Vinkers, C. H., Mittendorfer-Rutz, E., Cardoner, N., Tanskanen, A., Fusar-Poli, P., Cipriani, A., Vieta, E., Leucht, S., Tiihonen, J., & Luykx, J. J. (2024). Efficacy and effectiveness of antipsychotics in schizophrenia: network meta-analyses combining evidence from randomised controlled trials and real-world data. *The Lancet. Psychiatry*, *11*(2), 102–111.

Eisenberg, D. P., Blackman, R. K., Tietcheu, M. G., Kohn, P. D., Bettina, J. S., Kolachana, B., Gregory, M. D., & Berman, K. F. (2024). Genetic risk for treatment resistant schizophrenia and corresponding variation in dopamine synthesis capacity and D2/3 receptor availability in healthy individuals. *Molecular Psychiatry*, 1–8.

Ellett, L., Lopes, B., & Chadwick, P. (2003). Paranoia in a nonclinical population of college students. *The Journal of Nervous and Mental Disease*, *191*(7), 425–430.

Ellwood, I. T., Patel, T., Wadia, V., Lee, A. T., Liptak, A. T., Bender, K. J., & Sohal, V. S. (2017). Tonic or phasic stimulation of dopaminergic projections to

prefrontal cortex causes mice to maintain or deviate from previously learned behavioral strategies. *The Journal of Neuroscience: The Official Journal of the Society for Neuroscience*, *37*(35), 8315–8329.
Fabiano, N., Wong, S., Zhou, C., Correll, C. U., Højlund, M., & Solmi, M. (2025). Efficacy, tolerability, and safety of xanomeline-trospium chloride for schizophrenia: A systematic review and meta-analysis. *European Neuropsychopharmacology: The Journal of the European College of Neuropsychopharmacology*, *92*, 62–73.
Farde, L., Hall, H., Ehrin, E., & Sedvall, G. (1986). Quantitative analysis of D2 dopamine receptor binding in the living human brain by PET. *Science (New York, N.Y.)*, *231*(4735), 258–261.
Farde, L., Wiesel, F. A., Stone-Elander, S., Halldin, C., Nordström, A. L., Hall, H., & Sedvall, G. (1990). D2 dopamine receptors in neuroleptic-naive schizophrenic patients. A positron emission tomography study with [11C]raclopride. *Archives of General Psychiatry*, *47*(3), 213–219.
Feber, L., Peter, N. L., Chiocchia, V., Schneider-Thoma, J., Siafis, S., Bighelli, I., Hansen, W.-P., Lin, X., Prates-Baldez, D., Salanti, G., Keefe, R. S. E., Engel, R. R., & Leucht, S. (2025). Antipsychotic drugs and cognitive function: A systematic review and Network Meta-analysis. *JAMA Psychiatry (Chicago, Ill.)*, *82*(1), 47–56.
Filimontseva, A., Fu, Y., Vila, M., & Halliday, G. M. (2025). Neuromelanin and selective neuronal vulnerability to Parkinson's disease. *Trends in Neurosciences*, *48*(6), 445–459.
François, C., Yelnik, J., Tandé, D., Agid, Y., & Hirsch, E. C. (1999). Dopaminergic cell group A8 in the monkey: anatomical organization and projections to the striatum. *The Journal of Comparative Neurology*, *414*(3), 334–347.
Frankle, W. G., Himes, M., Mason, N. S., Mathis, C. A., & Narendran, R. (2022). Prefrontal and striatal dopamine release are inversely correlated in schizophrenia. *Biological Psychiatry*, *92*(10), 791–799.
Frankle, W. G., Paris, J., Himes, M., Mason, N. S., Mathis, C. A., & Narendran, R. (2018). Amphetamine-induced striatal dopamine release measured with an agonist radiotracer in schizophrenia. *Biological Psychiatry*, *83*(8), 707–714.
Frederick, J. M., Rayborn, M. E., Laties, A. M., Lam, D. M., & Hollyfield, J. G. (1982). Dopaminergic neurons in the human retina. *The Journal of Comparative Neurology*, *210*(1), 65–79.
Freeman, D., Garety, P. A., Bebbington, P. E., Smith, B., Rollinson, R., Fowler, D., Kuipers, E., Ray, K., & Dunn, G. (2005). Psychological investigation of the structure of paranoia in a non-clinical population. *The British Journal of Psychiatry: The Journal of Mental Science*, *186*, 427–435.
Freeman, D., McManus, S., Brugha, T., Meltzer, H., Jenkins, R., & Bebbington, P. (2011). Concomitants of paranoia in the general population. *Psychological Medicine*, *41*(5), 923–936.
Frick, A., Björkstrand, J., Lubberink, M., Eriksson, A., Fredrikson, M., & Åhs, F. (2022). Dopamine and fear memory formation in the human amygdala. *Molecular Psychiatry*, *27*(3), 1704–1711.
Fusar-Poli, P. (2017). The Clinical High-risk state for psychosis (CHR-P), Version II. *Schizophrenia Bulletin*, *43*(1), 44–47.
Fusar-Poli, P., Borgwardt, S., Bechdolf, A., Addington, J., Riecher-Rössler, A., Schultze-Lutter, F., Keshavan, M., Wood, S., Ruhrmann, S., Seidman, L. J., Valmaggia, L., Cannon, T., Velthorst, E., De Haan, L., Cornblatt, B., Bonoldi, I.,

Birchwood, M., McGlashan, T., Carpenter, W., … Yung, A. (2013). The psychosis high-risk state: a comprehensive state-of-the-art review: A comprehensive state-of-the-art review. *JAMA Psychiatry (Chicago, Ill.)*, *70*(1), 107–120.
Fusar-Poli, P., & Politi, P. (2008). Paul Eugen Bleuler and the birth of schizophrenia (1908). *The American Journal of Psychiatry*, *165*(11), 1407.
GBD 2017 Disease and Injury Incidence and Prevalence Collaborators. (2018). Global, regional, and national incidence, prevalence, and years lived with disability for 354 diseases and injuries for 195 countries and territories, 1990-2017: a systematic analysis for the Global Burden of Disease Study 2017. *Lancet*, *392*(10159), 1789–1858.
Gerlach, J., & Lühdorf, K. (1975). The effect of L-dopa on young patients with simple schizophrenia, treated with neuroleptic drugs: a double-blind cross-over trial with Madopar and placebo. *Psychopharmacologia*, *44*(1), 105–110.
German, D. C., & Manaye, K. F. (1993). Midbrain dopaminergic neurons (nuclei A8, A9, and A10): three-dimensional reconstruction in the rat. *The Journal of Comparative Neurology*, *331*(3), 297–309.
Gershon, S., Hekimian, L. J., Floyd, A., Jr, & Hollister, L. E. (1967). Alpha-methyl-p-tyrosine (AMT) in schizophrenia. *Psychopharmacologia*, *11*(2), 189–194.
Goldsmith, P. C., Thind, K. K., Song, T., Kim, E. J., & Boggant, J. E. (1990). Location of the neuroendocrine dopamine neurons in the monkey hypothalamus by retrograde tracing and immunostaining. *Journal of Neuroendocrinology*, *2*(2), 169–179.
Government of Canada. (2019, September 30). *Canada's Population, July 1 2019*. https://www150.statcan.gc.ca/n1/pub/11-627-m/11-627-m2019061-eng.htm
Grace, A. A. (1991). Phasic versus tonic dopamine release and the modulation of dopamine system responsivity: a hypothesis for the etiology of schizophrenia. *Neuroscience*, *41*(1), 1–24.
Grace, A. A. (2008). Physiology of the normal and dopamine-depleted basal ganglia: insights into levodopa pharmacotherapy: Insights into Levodopa Pharmacotherapy. *Movement Disorders: Official Journal of the Movement Disorder Society*, *23 Suppl 3*(S3), S560–S569.
Grace, A. A. (2016). Dysregulation of the dopamine system in the pathophysiology of schizophrenia and depression. *Nature Reviews. Neuroscience*, *17*(8), 524–532.
Grace, A. A., & Bunney, B. S. (1983). Intracellular and extracellular electrophysiology of nigral dopaminergic neurons--1. Identification and characterization. *Neuroscience*, *10*(2), 301–315.
Grace, A. A., Floresco, S. B., Goto, Y., & Lodge, D. J. (2007). Regulation of firing of dopaminergic neurons and control of goal-directed behaviors. *Trends in Neurosciences*, *30*(5), 220–227.
Guo, N., Hwang, D.-R., Lo, E.-S., Huang, Y.-Y., Laruelle, M., & Abi-Dargham, A. (2003). Dopamine depletion and in vivo binding of PET D1 receptor radioligands: implications for imaging studies in schizophrenia. *Neuropsychopharmacology: Official Publication of the American College of Neuropsychopharmacology*, *28*(9), 1703–1711.
Guthrie, M., Myers, C. E., & Gluck, M. A. (2009). A neurocomputational model of tonic and phasic dopamine in action selection: a comparison with cognitive deficits in Parkinson's disease. *Behavioural Brain Research*, *200*(1), 48–59.
Haber, S. N. (2003). The primate basal ganglia: parallel and integrative networks. *Journal of Chemical Neuroanatomy*, *26*(4), 317–330.

Haber, S. N., Ryoo, H., Cox, C., & Lu, W. (1995). Subsets of midbrain dopaminergic neurons in monkeys are distinguished by different levels of mRNA for the dopamine transporter: comparison with the mRNA for the D2 receptor, tyrosine hydroxylase and calbindin immunoreactivity. *The Journal of Comparative Neurology*, *362*(3), 400–410.

Hall, H., Farde, L., & Sedvall, G. (1988). Human dopamine receptor subtypes--in vitro binding analysis using 3H-SCH 23390 and 3H-raclopride. *Journal of Neural Transmission*, *73*(1), 7–21.

Hamati, R., Ahrens, J., Shvetz, C., Holahan, M. R., & Tuominen, L. (2024). 65 years of research on dopamine's role in classical fear conditioning and extinction: A systematic review. *The European Journal of Neuroscience*, *59*(6), 1099–1140.

Hansen, H. G., Speyer, H., Starzer, M., Albert, N., Hjorthøj, C., Eplov, L. F., & Nordentoft, M. (2023). Clinical recovery among individuals with a first-episode schizophrenia an updated systematic review and meta-analysis. *Schizophrenia Bulletin*, *49*(2), 297–308.

Hietala, J., Syvälahti, E., Vuorio, K., Någren, K., Lehikoinen, P., Ruotsalainen, U., Räkköläinen, V., Lehtinen, V., & Wegelius, U. (1994). Striatal D2 dopamine receptor characteristics in neuroleptic-naive schizophrenic patients studied with positron emission tomography. *Archives of General Psychiatry*, *51*(2), 116–123.

Hilker, R., Helenius, D., Fagerlund, B., Skytthe, A., Christensen, K., Werge, T. M., Nordentoft, M., & Glenthøj, B. (2018). Heritability of schizophrenia and schizophrenia spectrum based on the nationwide Danish Twin Register. *Biological Psychiatry*, *83*(6), 492–498.

Hillman, E. M. C. (2014). Coupling mechanism and significance of the BOLD signal: a status report. *Annual Review of Neuroscience*, *37*(1), 161–181.

Holstege, J. C., Van Dijken, H., Buijs, R. M., Goedknegt, H., Gosens, T., & Bongers, C. M. (1996). Distribution of dopamine immunoreactivity in the rat, cat and monkey spinal cord. *The Journal of Comparative Neurology*, *376*(4), 631–652.

Howes, O. D., Bose, S. K., Turkheimer, F., Valli, I., Egerton, A., Valmaggia, L. R., Murray, R. M., & McGuire, P. (2011). Dopamine synthesis capacity before onset of psychosis: a prospective [18F]-DOPA PET imaging study. *The American Journal of Psychiatry*, *168*(12), 1311–1317.

Howes, O. D., Bukala, B. R., & Beck, K. (2024). Schizophrenia: from neurochemistry to circuits, symptoms and treatments. *Nature Reviews. Neurology*, *20*(1), 22–35.

Howes, O. D., & Kapur, S. (2009). The dopamine hypothesis of schizophrenia: version III--the final common pathway. *Schizophrenia Bulletin*, *35*(3), 549–562.

Howes, O. D., Williams, M., Ibrahim, K., Leung, G., Egerton, A., McGuire, P. K., & Turkheimer, F. (2013). Midbrain dopamine function in schizophrenia and depression: a post-mortem and positron emission tomographic imaging study. *Brain: A Journal of Neurology*, *136*(Pt 11), 3242–3251.

Huttunen, J., Heinimaa, M., Svirskis, T., Nyman, M., Kajander, J., Forsback, S., Solin, O., Ilonen, T., Korkeila, J., Ristkari, T., McGlashan, T., Salokangas, R. K. R., & Hietala, J. (2008). Striatal dopamine synthesis in first-degree relatives of patients with schizophrenia. *Biological Psychiatry*, *63*(1), 114–117.

Ichise, M., Liow, J.-S., Lu, J.-Q., Takano, A., Model, K., Toyama, H., Suhara, T., Suzuki, K., Innis, R. B., & Carson, R. E. (2003). Linearized reference tissue parametric imaging methods: application to [11C]DASB positron emission tomography studies of the serotonin transporter in human brain. *Journal of Cerebral Blood Flow and Metabolism: Official Journal of the International Society of Cerebral Blood Flow and Metabolism*, *23*(9), 1096–1112.

Inanaga, K., Inoue, K., Tachibana, H., Oshima, M., & Kotorii, T. (1972). Effect of L-dopa in schizophrenia. *Folia Psychiatrica et Neurologica Japonica*, *26*(2), 145–157.

Inanaga, K., Nakazawa, Y., Inoue, K., Tachibana, H., & Oshima, M. (1975). Double-blind controlled study of L-Dopa therapy in schizophrenia. *Folia Psychiatrica et Neurologica Japonica*, *29*(2), 123–143.

Innis, R. B., Cunningham, V. J., Delforge, J., Fujita, M., Gjedde, A., Gunn, R. N., Holden, J., Houle, S., Huang, S.-C., Ichise, M., Iida, H., Ito, H., Kimura, Y., Koeppe, R. A., Knudsen, G. M., Knuuti, J., Lammertsma, A. A., Laruelle, M., Logan, J., … Carson, R. E. (2007). Consensus nomenclature for in vivo imaging of reversibly binding radioligands. *Journal of Cerebral Blood Flow and Metabolism: Official Journal of the International Society of Cerebral Blood Flow and Metabolism*, *27*(9), 1533–1539.

Iyer, S. N., Boekestyn, L., Cassidy, C. M., King, S., Joober, R., & Malla, A. K. (2008). Signs and symptoms in the pre-psychotic phase: description and implications for diagnostic trajectories. *Psychological Medicine*, *38*(8), 1147–1156.

Izquierdo-Garcia, D., Hansen, A. E., Förster, S., Benoit, D., Schachoff, S., Fürst, S., Chen, K. T., Chonde, D. B., & Catana, C. (2014). An SPM8-based approach for attenuation correction combining segmentation and nonrigid template formation: application to simultaneous PET/MR brain imaging. *Journal of Nuclear Medicine: Official Publication, Society of Nuclear Medicine*, *55*(11), 1825–1830.

Janowsky, D. S., el-Yousel, M. K., Davis, J. M., & Sekerke, H. J. (1973). Provocation of schizophrenic symptoms by intravenous administration of methylphenidate. *Archives of General Psychiatry*, *28*(2), 185–191.

Jaskiw, G. E., & Popli, A. P. (2004). A meta-analysis of the response to chronic L-dopa in patients with schizophrenia: therapeutic and heuristic implications. *Psychopharmacology*, *171*(4), 365–374.

Jauhar, S., McCutcheon, R. A., Nour, M. M., Veronese, M., Rogdaki, M., Bonoldi, I., Azis, M., Whitehurst, T., Arumuham, A., Onwordi, E., Turkheimer, F., McGuire, P., Young, A. H., & Howes, O. D. (2025). Dopamine and mood in psychotic disorders: An 18F-DOPA PET study. *JAMA Psychiatry (Chicago, Ill.)*. https://doi.org/10.1001/jamapsychiatry.2025.1811

Jauhar, S., Nour, M. M., Veronese, M., Rogdaki, M., Bonoldi, I., Azis, M., Turkheimer, F., McGuire, P., Young, A. H., & Howes, O. D. (2017). A test of the transdiagnostic dopamine hypothesis of psychosis using positron emission tomographic imaging in bipolar affective disorder and schizophrenia. *JAMA Psychiatry (Chicago, Ill.)*, *74*(12), 1206–1213.

Jauhar, S., Veronese, M., Nour, M. M., Rogdaki, M., Hathway, P., Turkheimer, F. E., Stone, J., Egerton, A., McGuire, P., Kapur, S., & Howes, O. D. (2019). Determinants of treatment response in first-episode psychosis: an 18F-DOPA PET study. *Molecular Psychiatry*, *24*(10), 1502–1512.

Jongsma, H. E., Turner, C., Kirkbride, J. B., & Jones, P. B. (2019). International incidence of psychotic disorders, 2002–17: a systematic review and meta-analysis. *The Lancet. Public Health*, *4*(5), e229–e244.

Jo, Y. S., Heymann, G., & Zweifel, L. S. (2018). Dopamine neurons reflect the uncertainty in fear generalization. *Neuron*, *100*(4), 916–925.e3.

Kapur, S. (2003). Psychosis as a state of aberrant salience: a framework linking biology, phenomenology, and pharmacology in schizophrenia. *The American Journal of Psychiatry*, *160*(1), 13–23.

Kapur, S., Mizrahi, R., & Li, M. (2005). From dopamine to salience to psychosis--

linking biology, pharmacology and phenomenology of psychosis. *Schizophrenia Research*, *79*(1), 59–68.
Kawahata, I., Finkelstein, D. I., & Fukunaga, K. (2024). Dopamine D1–D5 receptors in brain nuclei: Implications for health and disease. *Receptors (Basel, Switzerland)*, *3*(2), 155–181.
Kay, S. R., Fiszbein, A., & Opler, L. A. (1987). The positive and negative syndrome scale (PANSS) for schizophrenia. *Schizophrenia Bulletin*, *13*(2), 261–276.
Kay, S. R., & Opler, L. A. (1985). L-dopa in the treatment of negative schizophrenic symptoms: a single-subject experimental study. *International Journal of Psychiatry in Medicine*, *15*(3), 293–298.
Kikuchi, T., Maeda, K., Suzuki, M., Hirose, T., Futamura, T., & McQuade, R. D. (2021). Discovery research and development history of the dopamine D2 receptor partial agonists, aripiprazole and brexpiprazole. *Neuropsychopharmacology Reports*, *41*(2), 134–143.
Kintscher, M., Kochubey, O., & Schneggenburger, R. (2023). A striatal circuit balances learned fear in the presence and absence of sensory cues. *eLife*, *12*. https://doi.org/10.7554/eLife.75703
Köhler, C., Hall, H., Ogren, S. O., & Gawell, L. (1985). Specific in vitro and in vivo binding of 3H-raclopride. A potent substituted benzamide drug with high affinity for dopamine D-2 receptors in the rat brain. *Biochemical Pharmacology*, *34*(13), 2251–2259.
Kravitz, A. V., & Kreitzer, A. C. (2012). Striatal mechanisms underlying movement, reinforcement, and punishment. *Physiology (Bethesda, Md.)*, *27*(3), 167–177.
Kumar, V., Ramesh, V., Manchegowda, S., Krishna Prasad, M., & Rao, N. (2025). Levodopa augmentation of antipsychotics for persistent negative symptoms in schizophrenia: An open-label study: An open-label study. *Journal of Clinical Psychopharmacology*, 10.1097/JCP.0000000000002084.
Kwak, S., & Jung, M. W. (2019). Distinct roles of striatal direct and indirect pathways in value-based decision making. *eLife*, *8*. https://doi.org/10.7554/eLife.46050
Laakso, A., Bergman, J., Haaparanta, M., Vilkman, H., Solin, O., Syvälahti, E., & Hietala, J. (2001). Decreased striatal dopamine transporter binding in vivo in chronic schizophrenia. *Schizophrenia Research*, *52*(1-2), 115–120.
Laakso, A., Vilkman, H., Alakare, B., Haaparanta, M., Bergman, J., Solin, O., Peurasaari, J., Räkköläinen, V., Syvälahti, E., & Hietala, J. (2000). Striatal dopamine transporter binding in neuroleptic-naive patients with schizophrenia studied with positron emission tomography. *The American Journal of Psychiatry*, *157*(2), 269–271.
Lalive, A. L., Munoz, M. B., Bellone, C., Slesinger, P. A., Lüscher, C., & Tan, K. R. (2014). Firing modes of dopamine neurons drive bidirectional GIRK channel plasticity. *The Journal of Neuroscience: The Official Journal of the Society for Neuroscience*, *34*(15), 5107–5114.
Laruelle, M. (2000). Imaging synaptic neurotransmission with in vivo binding competition techniques: a critical review. *Journal of Cerebral Blood Flow and Metabolism: Official Journal of the International Society of Cerebral Blood Flow and Metabolism*, *20*(3), 423–451.
Laruelle, M., Abi-Dargham, A., van Dyck, C. H., Gil, R., D'Souza, C. D., Erdos, J., McCance, E., Rosenblatt, W., Fingado, C., Zoghbi, S. S., Baldwin, R. M., Seibyl, J. P., Krystal, J. H., Charney, D. S., & Innis, R. B. (1996). Single photon emission computerized tomography imaging of amphetamine-induced dopamine release in drug-free schizophrenic subjects. *Proceedings of the National*

Academy of Sciences of the United States of America, *93*(17), 9235–9240.
Lavalaye, J., Linszen, D. H., Booij, J., Dingemans, P. M., Reneman, L., Habraken, J. B., Gersons, B. P., & van Royen, E. A. (2001). Dopamine transporter density in young patients with schizophrenia assessed with [123]FP-CIT SPECT. *Schizophrenia Research*, *47*(1), 59–67.
Li, H., & Jin, X. (2023). Multiple dynamic interactions from basal ganglia direct and indirect pathways mediate action selection. *eLife*, *12*(RP87644). https://doi.org/10.7554/eLife.87644
Lindström, L. H., Gefvert, O., Hagberg, G., Lundberg, T., Bergström, M., Hartvig, P., & Långström, B. (1999). Increased dopamine synthesis rate in medial prefrontal cortex and striatum in schizophrenia indicated by L-(beta-11C) DOPA and PET. *Biological Psychiatry*, *46*(5), 681–688.
Lindvall, O., Björklund, A., & Divac, I. (1978). Organization of catecholamine neurons projecting to the frontal cortex in the rat. *Brain Research*, *142*(1), 1–24.
Lissemore, J. I., Nagano-Saito, A., Smart, K., Gravel, P., Leyton, M., & Benkelfat, C. (2020). Dopaminergic plasticity in the bilateral hippocampus following threat reversal in humans. *Scientific Reports*, *10*(1), 7627.
Liu, C., Goel, P., & Kaeser, P. S. (2021). Spatial and temporal scales of dopamine transmission. *Nature Reviews. Neuroscience*, *22*(6), 345–358.
Logothetis, N. K., Pauls, J., Augath, M., Trinath, T., & Oeltermann, A. (2001). Neurophysiological investigation of the basis of the fMRI signal. *Nature*, *412*(6843), 150–157.
Loopuijt, L. D., & Sebens, J. B. (1990). Loss of dopamine receptors in the olfactory bulb of patients with Alzheimer's disease. *Brain Research*, *529*(1-2), 239–244.
Lu, S., Telu, S., Siméon, F. G., Cai, L., & Pike, V. W. (2024). Gas phase transformations in carbon-11 chemistry. *International Journal of Molecular Sciences*, *25*(2), 1167.
Magelund, G., Gerlach, J., & Casey, D. E. (1979). Neuroleptic-potentiating effect of alpha-methyl-p-tyrosine compared with haloperidol and placebo in a double-blind cross-over trial. *Acta Psychiatrica Scandinavica*, *60*(2), 185–189.
Maia, T. V., & Frank, M. J. (2017). An integrative perspective on the role of dopamine in schizophrenia. *Biological Psychiatry*, *81*(1), 52–66.
Marder, S. R., Davis, J. M., & Chouinard, G. (1997). The effects of risperidone on the five dimensions of schizophrenia derived by factor analysis: combined results of the North American trials. *J Clin Psychiatry*, *58*(12), 538–546.
Martel, J. C., & Gatti McArthur, S. (2020). Dopamine receptor subtypes, physiology and pharmacology: New ligands and concepts in schizophrenia. *Frontiers in Pharmacology*, *11*, 1003.
Martinot, J. L., Peron-Magnan, P., Huret, J. D., Mazoyer, B., Baron, J. C., Boulenger, J. P., Loc'h, C., Maziere, B., Caillard, V., & Loo, H. (1990). Striatal D2 dopaminergic receptors assessed with positron emission tomography and [76Br]bromospiperone in untreated schizophrenic patients. *The American Journal of Psychiatry*, *147*(1), 44–50.
Matheson, G. (2018). *Reliability, replicability and reproducibility in PET imaging* [Karolinska Institutet]. https://hdl.handle.net/10616/46523
McCutcheon, R. A., Abi-Dargham, A., & Howes, O. D. (2019). Schizophrenia, dopamine and the striatum: From biology to symptoms. *Trends in Neurosciences*, *42*(3), 205–220.
Meltzer, H. Y., & Stahl, S. M. (1976). The dopamine hypothesis of schizophrenia: a review. *Schizophrenia Bulletin*, *2*(1), 19–76.

Menegas, W., Babayan, B. M., Uchida, N., & Watabe-Uchida, M. (2017). Opposite initialization to novel cues in dopamine signaling in ventral and posterior striatum in mice. *eLife*, *6*. https://doi.org/10.7554/eLife.21886

Millard, S. J., Bearden, C. E., Karlsgodt, K. H., & Sharpe, M. J. (2022). The prediction-error hypothesis of schizophrenia: new data point to circuit-specific changes in dopamine activity. *Neuropsychopharmacology: Official Publication of the American College of Neuropsychopharmacology*, *47*(3), 628–640.

Mizrahi, R., Addington, J., Rusjan, P. M., Suridjan, I., Ng, A., Boileau, I., Pruessner, J. C., Remington, G., Houle, S., & Wilson, A. A. (2012). Increased stress-induced dopamine release in psychosis. *Biological Psychiatry*, *71*(6), 561–567.

Mohebi, A., Wei, W., Pelattini, L., Kim, K., & Berke, J. D. (2024). Dopamine transients follow a striatal gradient of reward time horizons. *Nature Neuroscience*, *27*(4), 737–746.

Moran, L. V., Skinner, J. P., Shinn, A. K., Nielsen, K., Rao, V., Taylor, S. T., Cohen, T. R., Erkol, C., Merchant, J., Mujica, C. A., Perlis, R. H., & Ongur, D. (2024). Risk of incident psychosis and mania with prescription amphetamines. *The American Journal of Psychiatry*, *181*(10), 901–909.

Moreno-Küstner, B., Martín, C., & Pastor, L. (2018). Prevalence of psychotic disorders and its association with methodological issues. A systematic review and meta-analyses. *PloS One*, *13*(4), e0195687.

Mourgues-Codern, C., Benrimoh, D., Gandhi, J., Farina, E. A., Vin, R., Zamorano, T., Parekh, D., Malla, A., Joober, R., Lepage, M., Iyer, S. N., Addington, J., Bearden, C. E., Cadenhead, K. S., Cornblatt, B., Keshavan, M., Stone, W. S., Mathalon, D. H., Perkins, D. O., … Powers, A. R. (2025). Emergence and dynamics of delusions and hallucinations across stages in early psychosis. *Biological Psychiatry*, *98*(9), 679–688.

Nasrallah, H. A., Donnelly, E. F., Bigelow, L. B., Rivera-Calimlim, L., Rogol, A., Potkin, S., Rauscher, F. P., & Wyatt, R. J. (1977). Inhibition of dopamine synthesis in chronic schizophrenia. Clinical ineffectiveness of metyrosine. *Archives of General Psychiatry*, *34*(6), 649–655.

Nordström, A. L., Farde, L., Eriksson, L., & Halldin, C. (1995). No elevated D2 dopamine receptors in neuroleptic-naive schizophrenic patients revealed by positron emission tomography and [11C]N-methylspiperone. *Psychiatry Research*, *61*(2), 67–83.

Osugo, M., Wall, M. B., Selvaggi, P., Zahid, U., Finelli, V., Chapman, G. E., Whitehurst, T., Onwordi, E. C., Statton, B., McCutcheon, R. A., Murray, R. M., Marques, T. R., Mehta, M. A., & Howes, O. D. (2025). Striatal dopamine D2/D3 receptor regulation of human reward processing and behaviour. *Nature Communications*, *16*(1), 1852.

Osugo, M., Whitehurst, T., Shatalina, E., Townsend, L., O'Brien, O., Mak, T. L. A., McCutcheon, R., & Howes, O. (2022). Dopamine partial agonists and prodopaminergic drugs for schizophrenia: Systematic review and meta-analysis of randomized controlled trials. *Neuroscience and Biobehavioral Reviews*, *135*(104568), 104568.

Overall, J. E., & Gorham, D. R. (1962). The brief psychiatric rating scale. *Psychological Reports*, *10*(3), 799–812.

Pedruzo, B., Aymerich, C., Martínez-Asensi, C., Yorca-Ruiz, A., Herrero, R. M., Díaz-Pons, A., Ortiz-García de la Foz, V., Radua, J., Alonso-Alconada, D., Salazar de Pablo, G., González-Torres, M. Á., Fusar-Poli, P., Catalán, A., & Ayesa-Arriola, R. (2025). Systematic Review and meta-analysis: Neurocognitive

alterations in offspring of individuals with schizophrenia or Bipolar Disorder compared to offspring of unaffected parents. *Journal of the American Academy of Child and Adolescent Psychiatry*. https://doi.org/10.1016/j.jaac.2025.07.008

Pérez, V., Catafau, A. M., Corripio, I., Martín, J. C., & Alvarez, E. (2003). Preliminary evidence of striatal D2 receptor density as a possible biological marker of prognosis in naive schizophrenic patients. *Progress in Neuro-Psychopharmacology & Biological Psychiatry*, *27*(5), 767–770.

Phillips, L. J., McGorry, P. D., Yung, A. R., McGlashan, T. H., Cornblatt, B., & Klosterkötter, J. (2005). Prepsychotic phase of schizophrenia and related disorders: recent progress and future opportunities. *The British Journal of Psychiatry. Supplement*, *48*(S48), s33–s44.

Pinto, S. R., & Uchida, N. (2023). Tonic dopamine and biases in value learning linked through a biologically inspired reinforcement learning model. In *bioRxivorg* (p. 2023.11.10.566580). https://doi.org/10.1101/2023.11.10.566580

Pogarell, O., Koch, W., Karch, S., Dehning, S., Müller, N., Tatsch, K., Poepperl, G., & Möller, H.-J. (2012). Dopaminergic neurotransmission in patients with schizophrenia in relation to positive and negative symptoms. *Pharmacopsychiatry*, *45 Suppl 1*(S 01), S36–S41.

Prescott, C. A., Kuhn, J. W., & Pedersen, N. L. (2007). Twin pair resemblance for psychiatric hospitalization in the Swedish Twin Registry: a 32-year follow-up study of 29,602 twin pairs. *Behavior Genetics*, *37*(4), 547–558.

Quarmley, M., Gur, R. C., Turetsky, B. I., Watters, A. J., Bilker, W. B., Elliott, M. A., Calkins, M. E., Kohler, C. G., Ruparel, K., Rupert, P., Gur, R. E., & Wolf, D. H. (2019). Reduced safety processing during aversive social conditioning in psychosis and clinical risk. *Neuropsychopharmacology: Official Publication of the American College of Neuropsychopharmacology*, *44*(13), 2247–2253.

Radhakrishnan, R., Guloksuz, S., Ten Have, M., de Graaf, R., van Dorsselaer, S., Gunther, N., Rauschenberg, C., Reininghaus, U., Pries, L.-K., Bak, M., & van Os, J. (2019). Interaction between environmental and familial affective risk impacts psychosis admixture in states of affective dysregulation. *Psychological Medicine*, *49*(11), 1879–1889.

Rao, N., Northoff, G., Tagore, A., Rusjan, P., Kenk, M., Wilson, A., Houle, S., Strafella, A., Remington, G., & Mizrahi, R. (2019). Impaired prefrontal cortical dopamine release in schizophrenia during a cognitive task: A [11C]FLB 457 positron emission tomography study. *Schizophrenia Bulletin*, *45*(3), 670–679.

Rijsdijk, F. V., Gottesman, I. I., McGuffin, P., & Cardno, A. G. (2011). Heritability estimates for psychotic symptom dimensions in twins with psychotic disorders. *American Journal of Medical Genetics. Part B, Neuropsychiatric Genetics: The Official Publication of the International Society of Psychiatric Genetics*, *156B*(1), 89–98.

Robinson, D. G., Woerner, M. G., McMeniman, M., Mendelowitz, A., & Bilder, R. M. (2004). Symptomatic and functional recovery from a first episode of schizophrenia or schizoaffective disorder. *The American Journal of Psychiatry*, *161*(3), 473–479.

Rogdaki, M., Devroye, C., Ciampoli, M., Veronese, M., Ashok, A. H., McCutcheon, R. A., Jauhar, S., Bonoldi, I., Gudbrandsen, M., Daly, E., van Amelsvoort, T., Van Den Bree, M., Owen, M. J., Turkheimer, F., Papaleo, F., & Howes, O. D. (2023). Striatal dopaminergic alterations in individuals with copy number variants at the 22q11.2 genetic locus and their implications for psychosis risk: a [18F]-DOPA PET study. *Molecular Psychiatry*, *28*(5), 1995–2006.

Sánchez-González, M. A., García-Cabezas, M. A., Rico, B., & Cavada, C. (2005). The primate thalamus is a key target for brain dopamine. *The Journal of Neuroscience: The Official Journal of the Society for Neuroscience*, *25*(26), 6076–6083.

Seeman, P., Ko, F., & Tallerico, T. (2005). Dopamine receptor contribution to the action of PCP, LSD and ketamine psychotomimetics. *Molecular Psychiatry*, *10*(9), 877–883.

Seeman, P., & Lee, T. (1974). The dopamine-releasing actions of neuroleptics and ethanol. *The Journal of Pharmacology and Experimental Therapeutics*, *190*(1), 131–140.

Shotbolt, P., Stokes, P. R., Owens, S. F., Toulopoulou, T., Picchioni, M. M., Bose, S. K., Murray, R. M., & Howes, O. D. (2011). Striatal dopamine synthesis capacity in twins discordant for schizophrenia. *Psychological Medicine*, *41*(11), 2331–2338.

Sisti, D., Rocchi, M. B. L., Siddi, S., Mura, T., Manca, S., Preti, A., & Petretto, D. R. (2012). Preoccupation and distress are relevant dimensions in delusional beliefs. *Comprehensive Psychiatry*, *53*(7), 1039–1043.

Slifstein, M., Kegeles, L. S., Xu, X., Thompson, J. L., Urban, N., Castrillon, J., Hackett, E., Bae, S.-A., Laruelle, M., & Abi-Dargham, A. (2010). Striatal and extrastriatal dopamine release measured with PET and [(18)F] fallypride. *Synapse (New York, N.Y.)*, *64*(5), 350–362.

Slifstein, M., van de Giessen, E., Van Snellenberg, J., Thompson, J. L., Narendran, R., Gil, R., Hackett, E., Girgis, R., Ojeil, N., Moore, H., D'Souza, D., Malison, R. T., Huang, Y., Lim, K., Nabulsi, N., Carson, R. E., Lieberman, J. A., & Abi-Dargham, A. (2015). Deficits in prefrontal cortical and extrastriatal dopamine release in schizophrenia: a positron emission tomographic functional magnetic resonance imaging study. *JAMA Psychiatry (Chicago, Ill.)*, *72*(4), 316–324.

Snyder, S. H. (1976). The dopamine hypothesis of schizophrenia: focus on the dopamine receptor. *The American Journal of Psychiatry*, *133*(2), 197–202.

Solmi, M., Seitidis, G., Mavridis, D., Correll, C. U., Dragioti, E., Guimond, S., Tuominen, L., Dargél, A., Carvalho, A. F., Fornaro, M., Maes, M., Monaco, F., Song, M., Il Shin, J., & Cortese, S. (2023). Incidence, prevalence, and global burden of schizophrenia - data, with critical appraisal, from the Global Burden of Disease (GBD) 2019. *Molecular Psychiatry*, *28*(12), 5319–5327.

So, S. H.-W., Peters, E. R., Swendsen, J., Garety, P. A., & Kapur, S. (2014). Changes in delusions in the early phase of antipsychotic treatment - an experience sampling study. *Psychiatry Research*, *215*(3), 568–573.

Sportelli, L., Eisenberg, D. P., Passiatore, R., D'Ambrosio, E., Antonucci, L. A., Bettina, J. S., Chen, Q., Goldman, A. L., Gregory, M. D., Griffiths, K., Hyde, T. M., Kleinman, J. E., Pardiñas, A. F., Parihar, M., Popolizio, T., Rampino, A., Shin, J. H., Veronese, M., Ulrich, W. S., … Pergola, G. (2024). Dopamine signaling enriched striatal gene set predicts striatal dopamine synthesis and physiological activity in vivo. *Nature Communications*, *15*(1), 3342.

Stewart, A. J., Patten, S. B., Fiest, K. M., Williamson, T. S., Wick, J. P., & Ronksley, P. E. (2022). 10-year trends in healthcare spending among patients with schizophrenia in Alberta, Canada. *Canadian Journal of Psychiatry. Revue Canadienne de Psychiatrie*, *67*(9), 723–733.

Suker, S., Mihov, Y., Wolf, A., Mueller, S. V., & Hasler, G. (2023). Behavioral response to catecholamine depletion in individuals with schizophrenia and healthy volunteers. *Schizophrenia Bulletin Open*, *4*(1), sgad023.

Sullivan, P. F., Kendler, K. S., & Neale, M. C. (2003). Schizophrenia as a complex trait: evidence from a meta-analysis of twin studies: Evidence from a meta-analysis of twin studies. *Archives of General Psychiatry*, *60*(12), 1187–1192.
Sulzer, D., Cassidy, C., Horga, G., Kang, U. J., Fahn, S., Casella, L., Pezzoli, G., Langley, J., Hu, X. P., Zucca, F. A., Isaias, I. U., & Zecca, L. (2018). Neuromelanin detection by magnetic resonance imaging (MRI) and its promise as a biomarker for Parkinson's disease. *NPJ Parkinson's Disease*, *4*(1), 11.
Tandon, R. (2011). Antipsychotics in the treatment of schizophrenia: an overview. *The Journal of Clinical Psychiatry*, *72 Suppl 1*, 4–8.
Taylor, M. J., Freeman, D., Lundström, S., Larsson, H., & Ronald, A. (2022). Heritability of psychotic experiences in adolescents and interaction with environmental risk. *JAMA Psychiatry (Chicago, Ill.)*, *79*(9), 889–897.
Trujillo, P., Aumann, M. A., & Claassen, D. O. (2023). Neuromelanin-sensitive MRI as a promising biomarker of catecholamine function. *Brain : A Journal of Neurology*. https://doi.org/10.1093/brain/awad300
Tseng, H.-H., Watts, J. J., Kiang, M., Suridjan, I., Wilson, A. A., Houle, S., Rusjan, P. M., & Mizrahi, R. (2018). Nigral stress-induced dopamine release in clinical high risk and antipsychotic-naïve schizophrenia. *Schizophrenia Bulletin*, *44*(3), 542–551.
Tsuang, M. T., Stone, W. S., & Faraone, S. V. (1999). Schizophrenia: a review of genetic studies. *Harvard Review of Psychiatry*, *7*(4), 185–207.
Tuominen, L., Romaniuk, L., Milad, M. R., Goff, D. C., Hall, J., & Holt, D. J. (2022). Impairment in acquisition of conditioned fear in schizophrenia. *Neuropsychopharmacology: Official Publication of the American College of Neuropsychopharmacology*, *47*(3), 681–686.
Turkington, T. G. (2001). Introduction to PET instrumentation. *Journal of Nuclear Medicine Technology*, *29*(1), 4–11.
Ueno, F., Iwata, Y., Nakajima, S., Caravaggio, F., Rubio, J. M., Horga, G., Cassidy, C. M., Torres-Carmona, E., de Luca, V., Tsugawa, S., Honda, S., Moriguchi, S., Noda, Y., Gerretsen, P., & Graff-Guerrero, A. (2022). Neuromelanin accumulation in patients with schizophrenia: A systematic review and meta-analysis. *Neuroscience and Biobehavioral Reviews*, *132*, 1205–1213.
Vano, L. J., McCutcheon, R. A., Rutigliano, G., Kaar, S. J., Finelli, V., Nordio, G., Wellby, G., Sedlacik, J., Statton, B., Rabiner, E. A., Ye, R., Veronese, M., Hopkins, S. C., Koblan, K. S., Everall, I. P., & Howes, O. D. (2024). Mesostriatal dopaminergic circuit dysfunction in schizophrenia: A multimodal neuromelanin-sensitive magnetic resonance imaging and [18F]-DOPA positron emission tomography study. *Biological Psychiatry*, *96*(8), 674–683.
Varrone, A., Sjöholm, N., Eriksson, L., Gulyás, B., Halldin, C., & Farde, L. (2009). Advancement in PET quantification using 3D-OP-OSEM point spread function reconstruction with the HRRT. *European Journal of Nuclear Medicine and Molecular Imaging*, *36*(10), 1639–1650.
Wålinder, J., Skott, A., Carlsson, A., & Roos, B. E. (1976). Potentiation by metyrosine of thioridazine effects in chronic schizophrenics. A long-term trial using double-blind crossover technique. *Archives of General Psychiatry*, *33*(4), 501–505.
Wengler, K., He, X., Abi-Dargham, A., & Horga, G. (2020). Reproducibility assessment of neuromelanin-sensitive magnetic resonance imaging protocols for region-of-interest and voxelwise analyses. *NeuroImage*, *208*(116457), 116457.

Wengler, K., Seth C. Baker, M. S., Anastasia Velikovskaya, B. A., Alissa Fogelson, B. A., Girgis, R. R., MSc, F. R.-M. M., Lee, S., de la Fuente-Sandoval, C., Mph, N. O. P., & Horga, G. (2024). Generalizability and Out-of-Sample Predictive Ability of Associations Between Neuromelanin-Sensitive Magnetic Resonance Imagingand Psychosis in Antipsychotic-Free Individuals. *JAMA Psychiatry (Chicago, Ill.)*, *81*(2), 198–208.

Wengler, K., Trujillo, P., Cassidy, C. M., & Horga, G. (2024). Neuromelanin-sensitive MRI for mechanistic research and biomarker development in psychiatry. *Neuropsychopharmacology: Official Publication of the American College of Neuropsychopharmacology*, *50*(1), 137–152.

Wieland, L., Fromm, S., Hetzer, S., Schlagenhauf, F., & Kaminski, J. (2021). Neuromelanin-sensitive magnetic resonance imaging in schizophrenia: A meta-analysis of case-control studies. *Frontiers in Psychiatry*, *12*, 770282.

Winkelman, N. W., Jr. (1954). Chlorpromazine in the treatment of neuropsychiatric disorders. *Journal of the American Medical Association*, *155*(1), 18–21.

Winton-Brown, T. T., Fusar-Poli, P., Ungless, M. A., & Howes, O. D. (2014). Dopaminergic basis of salience dysregulation in psychosis. *Trends in Neurosciences*, *37*(2), 85–94.

Wolkin, A., Duncan, E., Sanfilipo, M., Wieland, S., Cooper, T. B., & Rotrosen, J. (1994). Persistent psychosis after reduction in pre- and post-synaptic dopaminergic function. *Journal of Neural Transmission. General Section*, *95*(1), 49–61.

Wong, D. F., Wagner, H. N., Jr, Tune, L. E., Dannals, R. F., Pearlson, G. D., Links, J. M., Tamminga, C. A., Broussolle, E. P., Ravert, H. T., Wilson, A. A., Toung, J. K., Malat, J., Williams, J. A., O'Tuama, L. A., Snyder, S. H., Kuhar, M. J., & Gjedde, A. (1986). Positron emission tomography reveals elevated D2 dopamine receptors in drug-naive schizophrenics. *Science (New York, N.Y.)*, *234*(4783), 1558–1563.

Yaryura-Tobias, J. A., & Diamond, B. (1971). Levodopa-Nicotinic Acid Interaction in Psychiatric Patients. *Schizophrenia*. https://isom.ca/wp-content/uploads/2020/01/JOM_1971_03_3-4_05_Levodopa-Nicotinic_Acid_Interaction_in_Psychiatric-.pdf

Zahm, D. S., & Trimble, M. (2008). The dopaminergic projection system, basal forebrain macrosystems, and conditioned stimuli. *CNS Spectrums*, *13*(1), 32–40.

Zavos, H. M. S., Freeman, D., Haworth, C. M. A., McGuire, P., Plomin, R., Cardno, A. G., & Ronald, A. (2014). Consistent etiology of severe, frequent psychotic experiences and milder, less frequent manifestations: a twin study of specific psychotic experiences in adolescence: A twin study of specific psychotic experiences in adolescence. *JAMA Psychiatry (Chicago, Ill.)*, *71*(9), 1049–1057.

Zucca, F. A., Basso, E., Cupaioli, F. A., Ferrari, E., Sulzer, D., Casella, L., & Zecca, L. (2014). Neuromelanin of the human substantia nigra: an update. *Neurotoxicity Research*, *25*(1), 13–23.